ELEC 301 Projects Fall 2009

Collection Editor:
Rice University ELEC 301

ELEC 301 Projects Fall 2009

Collection Editor:
Rice University ELEC 301

Authors:

Anthony Austin
Jeffrey Bridge
Robert Brockman
Dan Calderon
Lei Cao
Grant Cathcart
Sharon Du
Catherine Elder
Jose Garcia
Gilberto Hernandez
Peter Hokanson
Seoyeon(Tara) Hong
Graham Houser
Chinwei Hu
Alysha Jeans
Stephen Jong
James Kohli
Stephen Kruzick
Kyle Li
Haiying Lu
Stamatios Mastrogiannis
Nicholas Newton
Norman Pai
Sam Soundar
Cynthia Sung
Matt Szalkowski
Brian Viel
Yilong Yao
Jeff Yeh
Aron Yu
Graham de Wit

Online:
< http://cnx.org/content/col11153/1.3/ >

C O N N E X I O N S

Rice University, Houston, Texas

Collection structure revised: December 26, 2009
PDF generated: April 21, 2011
For copyright and attribution information for the modules contained in this collection, see p. 154.

Table of Contents

Chapter 1

Digital Song Identification Using Frequency Analysis

1.1 Introduction[1]

Imagine sitting at a café (or "other" public venue) and you hear a song playing on the stereo. You decide that you really like it, but you don't know the name of the song. There's a solution for that. Software song identification has been a topic of interest for years. However, it is computationally difficult to tackle this problem using conventional algorithms. Frequency analysis provides for a fast and accurate solution to this problem, and we decided to use this analysis to come up with a fun project idea. The main purpose of our project was to be able to accurately match a noisy song segment with a song in our song library. The company Shazam was our main inspiration and we started out by studying how Shazam works.

1.2 The Fingerprint of a Song[2]

Just like how every individual has a unique fingerprint that can be used to distinguish one person from another, our algorithm creates a digital fingerprint for each song that can be used to distinguish two songs. The song's fingerprint consists of list of time-frequency pairs that uniquely represent all the significant peaks in the song's spectrogram. To assure accurate matching between two fingerprints, our algorithm needs to take into account the following issues when choosing peaks for the fingerprint:

- **Uniqueness** – The fingerprint of each song needs to be unique to that one song. Fingerprints of different songs need to be different enough to be easily distinguished by our scoring algorithm.
- **Sparseness** – The computational time of our matched filter depends on the amount of data in each song's fingerprint. Thus each fingerprint needs to sparse enough for fast results, but still contain enough information to provide accurate matches.
- **Noise Resistant** – Song data may contain large amounts of background noise. The fingerprinting algorithm must be able to differentiate between the signal and added noise, storing only the signal information in the fingerprint.

These criteria are all met by identifying major peaks in the song's spectrogram. The following section describes the fingerprinting algorithm in more detail.

[1] This content is available online at <http://cnx.org/content/m33185/1.2/>.
[2] This content is available online at <http://cnx.org/content/m33186/1.2/>.

1.3 The Fingerprint Finding Algorithm[3]

1.3.1 Filtering and Resampling

After the song data is imported, the signal is then resampled to 8000 samples per second in order to reduce the number of columns in the spectrogram. This will speed up later computations but still leaves enough resolution in the data for accurate results.

Then the data is high-pass filtered using a 30^{th} order filter with a cutoff frequency around 2KHz (half the bandwidth of the resampled signal). Filtering is used because the higher frequencies in songs are more unique to each individual song. The bass, however, tends to overshadow these frequencies, thus the filter is used make fingerprint include more high frequencies points. Testing has shown that the algorithm has a much easier time distinguishing songs after they are high-pass filtering.

1.3.2 The Spectrogram

The spectrogram of the signal is then taken in order to view the frequencies present in each time slice. The spectrogram below is from a 10 second noisy recording.

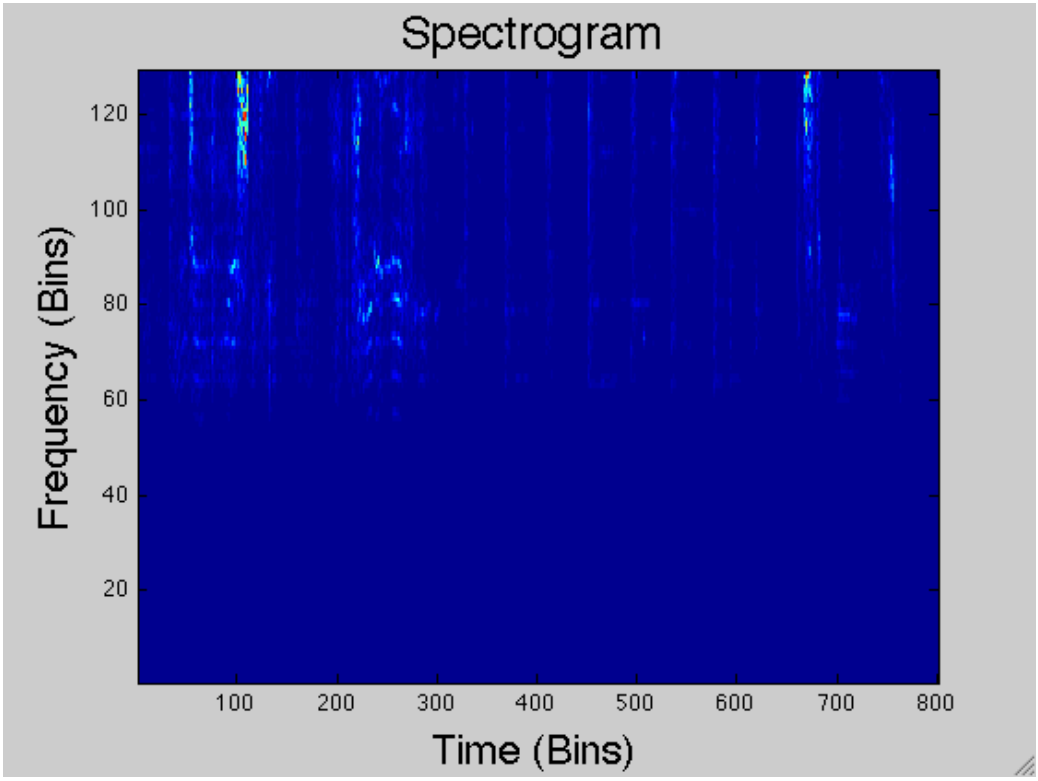

Figure 1.1: The effect of the low-pass filter is clearly visible in the spectrogram. However, local maxima in the low frequencies still exist and will still show up in the fingerprint.

[3]This content is available online at <http://cnx.org/content/m33188/1.4/>.

Each vertical time slice in the bin is then analyzed for prominent local maxima as described in the next section.

1.3.3 Finding the Local Maxima

In the first time slice, the five greatest local maxima are stored as points in the fingerprint. Then a threshold is created by convolving these five maxima with a Gaussian curve, creating a different value for the threshold at each frequency. An example threshold is shown in the figure below. The threshold is used to spread out the data stored in the fingerprint, since peaks that are close in time and frequency are stored as one point.

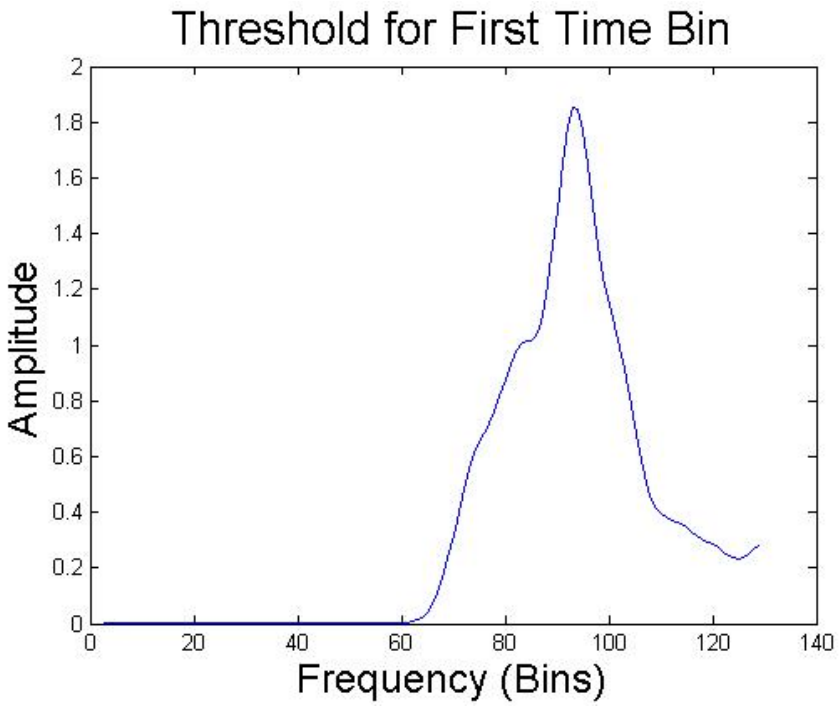

Figure 1.2: The initial threshold, formed by convolving the peaks in the first time slice with a Gaussian curve.

For each of the remaining time slices, up to five local maxima above the threshold are added to fingerprint. If there are more than five maxima, then the five greatest in amplitude are chosen. The threshold is then updated by adding new Gaussian curves centered at the frequencies of the newly found peaks. Finally the threshold is scaled down so that it decays exponentially over time. The following figure shows how the threshold changes over time.

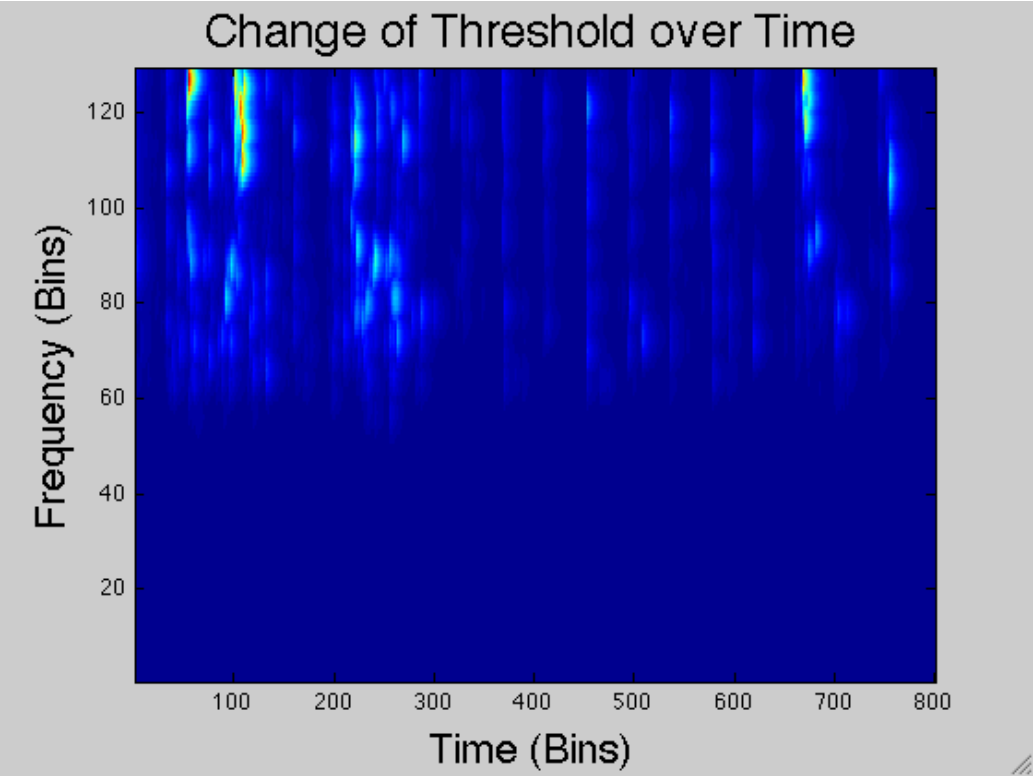

Figure 1.3: The threshold increases whenever a new peak is formed around that peak's frequency and decays exponentially over time.

The final list of the time and frequencies of the local maxima above the threshold are returned as the song's fingerprint.

1.4 The Resulting Fingerprint[4]

The following is the fingerprint of the sample signal from the examples above.

[4] This content is available online at <http://cnx.org/content/m33189/1.4/>.

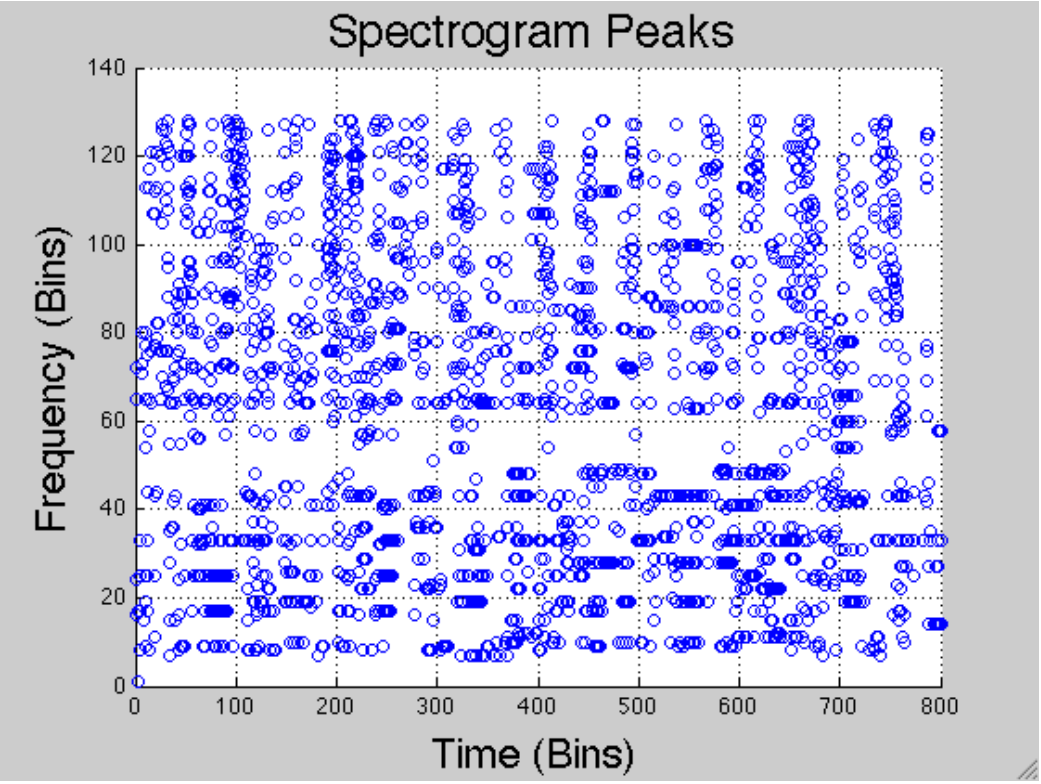

Figure 1.4: The fingerprint of the 10 second segment from the previous examples

From the graph, it is easy to see patterns and different notes in the song. Lets see how the algorithm addresses the three issues identified in the first paragraph:

- Uniqueness – The algorithm only stores the prominent peaks in the spectrogram. Different songs have a different pattern of peaks in frequency and time, thus each song will have a unique fingerprint.
- Sparseness – The algorithm only picks up at most five peaks per time slice. This limits the number of peaks in the resulting fingerprint. The threshold spreads out the positions of peaks so that the fingerprint is more representational of the data.
- Noise Resistant – Unless the background noise is loud enough to create peaks greater than the peaks present in the song, then very little noise will show up in the fingerprint. Also, a ten second segment has around 6000 data points, so a matched filter will be able to detect a match between two fingerprints, even with a reasonable amount of added noise.

The next section will detail the process used to compare the fingerprint of the song segment to the fingerprints of the songs in the library.

1.5 Matched Filter for Spectrogram Peaks[5]

In order to compare songs, we can generate match scores for them using a matched filter. We wanted a filter capable of taking the spectral peaks information generated by the fingerprint finding algorithm for two different songs and produce a single number that would tell us how much the two songs being compared look alike. We wanted this filter to be as insensitive as possible to noise and produce a score that is independent of the length of each recording.

Our approach to this was completely different from that used by the creators of Shazam, as we did not use Hash tables at all and did not combine the peaks into pairs limited by certain regions, as they did. In the end we still managed to get very good accuracy and decent performance by using a matched filter.

1.6 The Matched Filter Algorithm[6]

1.6.1 Preparation

Before filtering, we take the lists of spectral peaks that is the output of the landmarks generator algorithm and generate matrices that are the same size as the spectrograms, with the peaks replaced by 1's in their respective positions and all other points replaced by 0's. At some point during our project we had the idea of convolving this matrix with a Gaussian curve, in order to allow peaks to match somewhat if they were shifted only slightly. However, we later determined that even a very small Gaussian would worsen our noise resistance, so this idea was dropped. So basically now we have one map for each song that shows the position in time and frequency bins of all peaks. Next we normalize these matrices using their Frobenius norm. This ensures that the final score is normalized. Then we apply the matched filter which basically consists of flipping one of the matrices and convolving them, which is done by zero padding them both to the proper size and multiplying their 2D FFT's, for speed. The result is a cross correlation matrix, but we still need to extract a single number from it to be our match score.

1.6.2 Extracting Information from the Cross Correlation Matrix

Through much testing, we determined that the most accurate and noise-resistant measure of the match was simply taking the global maximum of the result. Other approaches that we tried, such as taking the trace of the X^TX or the sum of the global maxima for each row or column, had much more frequent mismatches. Taking just the global maximum of the whole matrix was simple and extremely effective.

When looking at test results, however, we saw that the score still had a certain dependency on the size of the segments being compared. Through more testing, we determined that this dependency looked approximately like a dependency on the square root of the ratio of the lower number of peaks by the higher number of peaks, when testing with a noiseless fragment of a larger song. This can be seen in this plot:

[5] This content is available online at <http://cnx.org/content/m33191/1.1/>.
[6] This content is available online at <http://cnx.org/content/m33193/1.3/>.

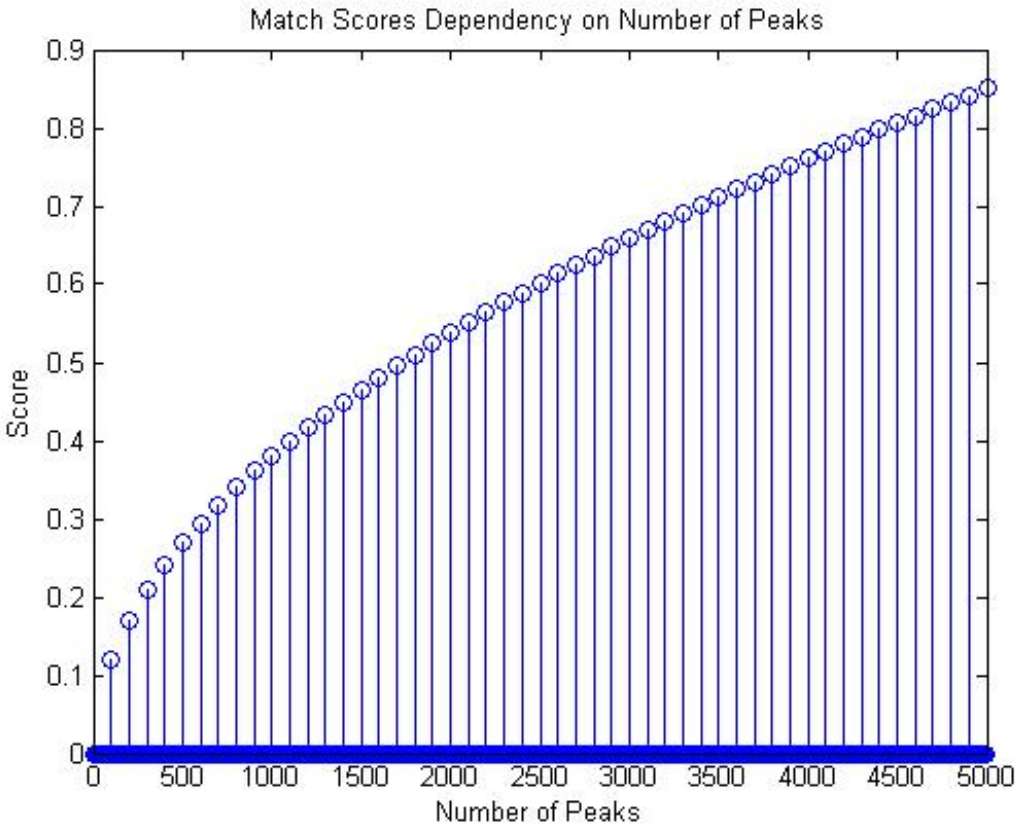

Figure 1.5: A plot showing the score of a song fragment that should perfectly match the song it was taken from, seen without correcting the square root dependency mentioned above

In the plot above, the original segment has 6915 peaks and the fragment was tested with between 100 and 5000 peaks, in intervals of 100. Since smaller sample sizes usually lead to having fewer peaks, we had to get rid of this dependency. To prevent the square root growth of the scores, the final score is multiplied by the inverse of this square root, yielding a match score that is approximately independent of sample size. This can be seen in the next stem plot, made with the same segments as the first:

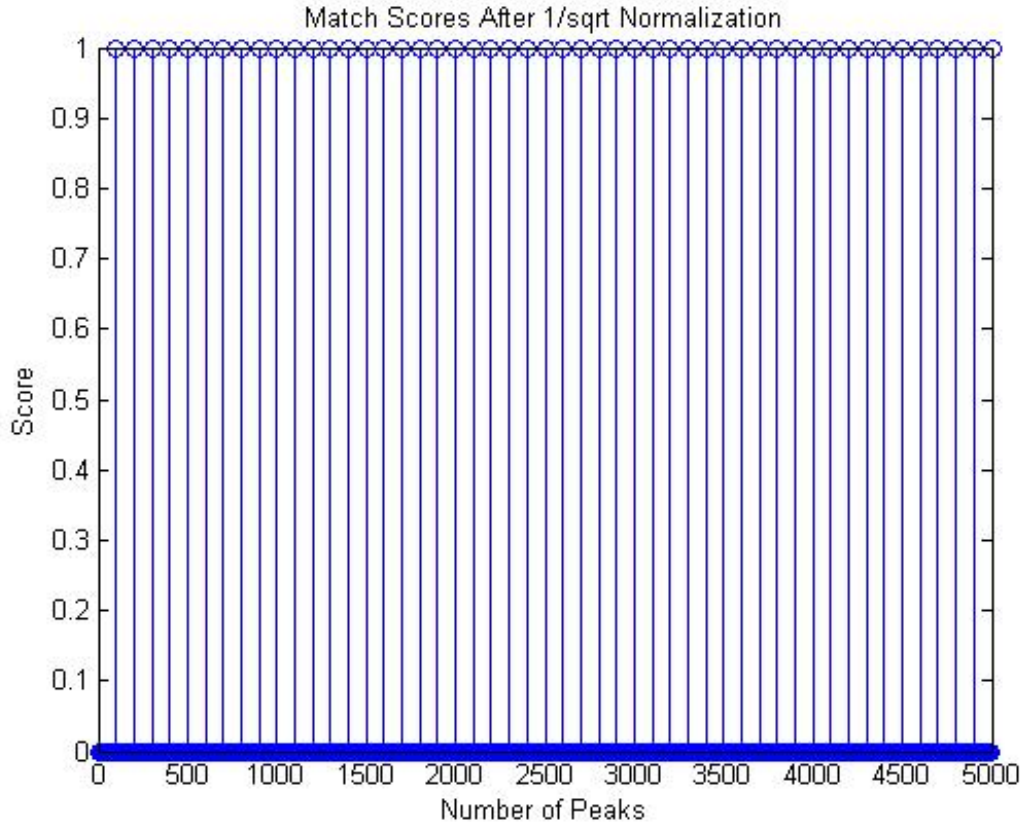

Figure 1.6: The same plot shown before, but with the square root dependency on number of peaks removed

So clearly this allows us to get better match scores with small song segments. After this process, we had a score that was approximately independent of segment size, normalized and could tell apart matches and mismatches, even with lots of noise. All that was left was to test it against different sets of data and set a threshold for distinguishing between matches and non-matches.

1.6.3 Setting a Threshold

The filter's behavior proved to be very consistent. Perfect matches (trying to match a segment with itself) always got scores of 1. Matching noiseless segments to the whole song usually yielded scores in the upper .8's or in the .9's, with a few rare exceptions that could have been caused by a bad choice of segment, such as a segment with a long period of silence, for example. Noisy segments usually gave us low scores such as in the .1's, but more importantly mismatches were even lower, in the .05's to .07's or so. This allowed us to set a threshold for determining when we have a match or not.

During our testing, we considered using a statistical approach to set the threshold. For example, if we wanted a 95% certainty that a song matched, we could require the highest match score to be greater than 1.66*[σ/sqrt(n)] + μ, where σ is the standard deviation, n is the sample size and μ is the mean. However, with our very small sample size, this threshold seemed to yield inaccurate results, so the simple threshold criterion of the highest match having to be at least 1.5 times the second highest in order to be considered a

match was used.

1.6.4 Similarities and Differences from Shazam's Approach

Even though we followed the ideas in the paper by Wang, we still had some significant differences from the approach used by Shazam. We followed the ideas they had for fingerprint creation, to a certain extent, however the company uses hash tables instead of matched filters to perform the comparison. While evidently faster than using a matched filter, hash tables are not covered in ELEC 301. Furthermore, when making a hash, Wang says they combine several points in an area with an anchor point and pair them up combinatorially. This allows the identification of a time offset to be used with the hash tables and makes the algorithm even faster and more robust. Perhaps investigating this would be an interesting extension of the project, if we had more time.

1.7 Results[7]

The final step in the project was to test the algorithm we had created so we went ahead and conducted a series of tests that would evaluate mostly correctness but also, to some extent, performance.

1.7.1 Testing

First, we wanted to test to make sure that our algorithm was working properly. To do this, we attempted to match short segments of the original song (i.e. "noiseless", actual copies of the library songs) of approximately ten seconds in length. The table below shows how these original clips matched. The titles from left to right are song segments, and titles running from top to bottom are library songs. We abbreviated them from the original, so they would fit in the matrix. The original names are "Stop this Train", by John Mayer, "Semi-Charmed Life", by Third Eye Blind, "I've got a Feeling" by Black Eyed Peas, "Love Like Rockets", by Angels and Airwaves, "Crash Into Me", by Dave Matthews Band and "Just Another Day in Paradise", by Phil Vassar.

	Noiseless Recordings					
	Train	Life	Feeling	Rockets	Crash	Paradise
Train	0.8685	0.0611	0.0876	0.0695	0.0886	0.0803
Life	0.0987	0.2914	0.0869	0.071	0.0725	0.0736
Feeling	0.1091	0.0679	0.9292	0.0695	0.0687	0.075
Rockets	0.0822	0.0691	0.0855	0.9488	0.0648	0.085
Crash	0.1256	0.0593	0.0967	0.0649	0.9031	0.0716
Paradise	0.1151	0.0722	0.096	0.0756	0.0777	0.9398

Figure 1.7: This matrix shows the match score results of the six noiseless recordings made from fragments of songs in the database, each of them compared to all songs in the database

[7] This content is available online at <http://cnx.org/content/m33194/1.3/>.

The clear matches with highest scores can be seen along the diagonal. Most of these are close to 1, and each match meets our criteria of being 1.5 times greater than the other scores (comparing horizontally.) This was a good test that we were able to use to modify our algorithm and try different techniques. Ultimately, the above results showed that our code was sufficient for our needs.

We then needed to see if our code actually worked with real world (noisy) song segments. Songs were recorded on an iPhone simultaneously with various types of noise as follows: Train- low volume talking, Life- loud recording (clipping), Crash- typing, Rockets- repeating computer error noise, Feeling- Gaussian noise (added in Matlab to wav file), and Paradise- very loud talking. There were two additional songs we used in this test to check for robustness and proper matching. One is a live version of Crash, which includes a lot of crowd noise but does not necessarily have all the identical features of the original Crash fingerprint. The other additional song, "Yellow", by Coldplay, is a song that is not in our library at all.

Noisy Recordings Using an iPhone

	Train	Life	Feeling	Rockets	Crash	Paradise	Crash (Live)	Yellow
Train	0.1385	0.0631	0.0705	0.0774	0.0892	0.0661	0.0598	0.0694
Life	0.0612	0.1269	0.0721	0.0842	0.0809	0.0646	0.0604	0.0666
Feeling	0.055	0.0623	0.3468	0.0867	0.0734	0.063	0.0586	0.0637
Rockets	0.0619	0.0764	0.0755	0.1759	0.0679	0.0764	0.058	0.066
Crash	0.0675	0.0631	0.0733	0.0741	0.1619	0.0669	0.0682	0.0711
Paradise	0.0675	0.0734	0.0738	0.0934	0.0837	0.1189	0.0622	0.0694

Figure 1.8: This matrix shows the match score results of the six noisy recordings made from fragments of songs in the database, plus a live version of a song in the database and another song entirely not in the database

Again, the clear matches are highlighted in yellow along the diagonal. The above results show that our algorithm can still accurately match the song segments in more realistic conditions. The graph below shows more interesting results.

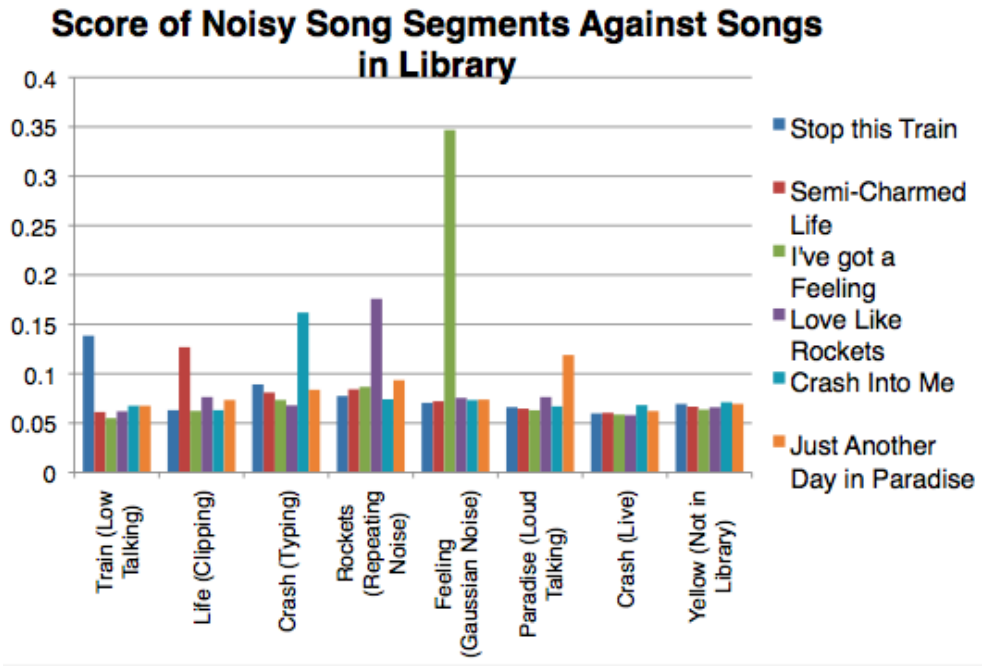

Figure 1.9: This plot is a visual representation of the results matrix seen above

1.7.2 Conclusions

As before, the matches in the first six songs (from left to right) are obvious, and Yellow does not show any clear correlation to any library song, as desired, but the live version of Crash presents an interesting question. Do we actually want this song to match? Since we wanted our fingerprinting method to be unique to each song and song segment, we decided it would be best to have a non-match in this scenario. However, if one observes closely, it can be seen that the closest match (though it is definitely not above the 1.5 mark) is, in fact, matching to the original Crash. This emerges as a small feature of our results. This small "match" says that although we may not match any songs in the library, we can tell you that this live version most resembles the original Crash version, which may be a desirable outcome if we were to market this project.

We were amazed that the final filter could perform so well. The idea of completely ignoring amplitude information in the filter came from the paper by Avery Li-Chun Wang, one of Shazam's developers. As he mentions, discarding amplitude information makes the algorithm more insensitive to equalization. However, this approach also makes it more noise resistant since, since what we do from there on basically consists of counting matching peaks versus non-matching peaks. Any leftover noise will count very little towards the final score, as the number of peaks per area in the spectrogram is limited by the thresholding algorithm and all peaks have the same magnitude in the filter.

1.8 About the Team[8]

1.8.1 Team Members

- Dante Soares is a Junior ECE student at Martel. He is specializing in Computer Engineering.
- Yilong Yao is a Junior ECE student at Sid Richardson. He is specializing in Computer Engineering.
- Curtis Thompson is a Junior ECE at Sid Richardson College. He is specializing in Signals and Systems.
- Shahzaib Shaheen is a Junior ECE at Sid Rich. He is specializing in Photonics.

1.8.2 Special Thanks

We would like to thank Eva Dyer for her help with the algorithm and her feedback on the poster presentation.

1.8.3 Sources

Dan, Ellis. "Robust Landmark-Based Audio Fingerprinting." Lab ROSA. Columbia University, 7 June 2006. Web. 6 Dec. 2009. <http://labrosa.ee.columbia.edu/>.

Dyer, Eva. Personal interview. 13 Nov. 2009.

Fiona, Harvey. "Name That Tune." Scientific American June 2003: 84-6. Print.

Wang, Avery Li-Chun. An Industrial-Strength Audio Search Algorithm. Bellingham: Society of Photo-Optical Instrumentation Engineers, 2003. Print. SPIE proceedings series.

[8] This content is available online at <http://cnx.org/content/m33196/1.2/>.

Chapter 2

A Matrix Completion Approach to Sensor Network Localization

2.1 Introduction[1]

2.1.1 Introduction

Sensor network localization refers to the problem of trying to reconstruct the shape of a network of sensors – that is, the positions of each sensor relative to all the others – from information about the pairwise distances between them. If all of the pairwise distances are known exactly, then the shape of the network may be recovered via a technique called *multidimensional scaling* (MDS) [10]. Of more practical interest is the case in which many – even most – of the distances are unknown and in which the known distance measurements have been corrupted with noise. Determining the shape of the network under these conditions is still an open problem. Over the years, researchers have come up with a variety of different approaches for tackling this problem, with some of the most recent ones being based on graph rigidty theory, such as those in [10] and [11]; however, for our project, we decided to examine this problem from a fundamentally different tack. Instead, we approach the problem using methods from the brand new field of *matrix completion*, which is concerned with "filling in the gaps" in a matrix for which not all of the entries may be known.

The remainder of this collection is divided as follows. In the next section, we provide an overview of the most recent work in matrix completion for those who may not be familiar with this very new field. After that, we discuss the procedures we used to conduct our investigation. Finally, we examine the results of our simulations and present our conclusions.

2.2 Matrix Completion: An Overview[2]

2.2.1 Overview of Matrix Completion

The fundamental question that the new and emerging field of matrix completion seeks to answer is this: Given a matrix with some of its entries missing, is it possible to determine what those entries should be? Answering this question has an enormous number of potential practical applications. To be more concrete, consider the problem of *collaborative filtering*, of which perhaps the most famous example is the *Netflix* problem [9]. The *Netflix* problem asks how one may be able to predict how an individual would rate movies he or she has not seen based on the ratings that individual has made in the past and on the ratings of other individuals stored in the database. This can be cast as a matrix completion problem in which each row of the matrix corresponds to a particular user, each column to a movie, and each entry a rating that the user

[1] This content is available online at <http://cnx.org/content/m33135/1.1/>.
[2] This content is available online at <http://cnx.org/content/m33136/1.1/>.

of that entry's row has given to the movie in that entry's column. Because there is a large number of users and movies and because each user has probably seen relatively few of the available movies, there are a large number of entries missing. The idea is to somehow fill in the missing entries and thereby determine how every user would rate every movie available. For more examples of potential uses of matrix completion, see the introduction of [2].

In general, matrix recovery is an impossible task because the unknown entries really could be anything; however, if one makes a few reasonable assumptions about the original matrix underlying the one being completed, then the matrix can indeed be reconstructed and often from a surprisingly low number of entries. More precisely, in their May, 2008 paper *Exact Matrix Completion via Convex Optimization*, matrix completion pioneers Emmanuel J. Candès and Benjamin Recht offer the following definitions [3]:

Definition: Let U be a subspace of $\mathbb{R}^n$ of dimension R, and let P_U be the operator that projects orthogonally onto U. The *coherence* $\mu(U)$ of U is defined by

$$\mu(U) = \frac{n}{r} \max_{1 \leq i \leq n} \| P_U e_i \|^2, \tag{2.1}$$

where e_i is the standard basis vector with a 1 in the i^{th} coordinate and all other coordinates are zero.

Definition: Let A be an m-by-n matrix of rank r with singular value decomposition $\sum_{k=1}^{r} \sigma_k u_k v_k^*$, and denote its column and row spaces by U and V, respectively. A is said to be (μ_0, μ_1)-*incoherent* if

1. There exists $\mu_0 > 0$ such that $max(\mu(U), \mu(V)) < \mu_0$.
2. There exists $\mu_1 > 0$ such that all entires of the m-by-n matrix $\sum_{k=1}^{r} u_k v_k^*$ are less than or equal to $\mu_1 \sqrt{\frac{r}{mn}}$ in magnitude.

Qualitatively, this definition means that the singular vectors of a (μ_0, μ_1)-incoherent matrix aren't too "spiky" and don't do anything "wild."

In the same paper, Candès and Recht go on to show that if A is an m-by-$n(\mu_0, \mu_1)$-incoherent matrix that has rank $r \ll N = max(m, n)$, then A can be recovered with high probability from a uniform sampling of M of its entries, where $M \geq O\left(N^{1.2} r log N\right)$[3]. This result was later strengthened to $M \geq O(N r max(r, log N))$ by Keshavan, Montanari, and Oh in [6]. These results, coupled with the fact that many matrices that one encounters in practice both satisfy the incoherence property and are of low rank means that matrix completion has some serious potential for use in practical applications.

Once one knows that matrix completion can be done, the next question is how to go about doing it. There are a variety of different matrix completion algorithms available. Candès et al. have developed a method that they call Singular Value Thresholding (SVT), which attempts to complete the matrix by solving the following optimization problem [1]: Find a matrix X of that minimizes $\| X \|_*$ subject to the condition that the entries of X be equal to those entries of the matrix A to be completed for which we know the value. Here, $\| X \|_*$ is the *nuclear norm* of X, defined to be the sum of the singular values of X. Keshavan, Montanari, and Oh offer an alternative algorithm, dubbed OptSpace, which is based on trimming the incomplete matrix to remove so-called "overrepresented" rows and columns whose values do not help reveal much about the unknown entries and then adjusting the trimmed matrix to minimize the error that is made at the entries whose values are known via a gradient descent procedure [6], [7]. There are other algorithms as well, and which algorithm to choose is really up to the user. For our work, we elected to use the OptSpace algorithm, since it just seems to produce better results.

2.3 Simulation Procedure[3]

2.3.1 Simulation Procedure

For our project, we applied these new matrix completion techniques to the sensor network localization problem. More explicitly, our idea was to take an incomplete matrix of distances between sensors and use

[3] This content is available online at <http://cnx.org/content/m33138/1.1/>.

the OptSpace algorithm mentioned previously to fill in the missing entries, whereupon the network may be reconstructed using multidimensional scaling methods. Because a matrix of Euclidean distances between random points is, in general, full rank, it cannot be completed directly; however, the matrix of the *squares* of the distances between the points has a fixed maximum rank depending on the dimension of the space in which the points are embedded. To see this, suppose that we are given N points $x_1, ..., x_n$ in $\mathbb{R}^n$, and let D_2 be the N-by-N matrix of their squared distances; that is, the ij-entry of D_2 is equal to $\| x_i - x_j \|^2$ for $i, j = 1, ..., n$. Denote the k^{th} coordinate of x_i by $x_i^{(k)}$. Because $\| x_i - x_j \|^2 = \| x_i \|^2 - 2 (x_i \bullet x_j) + \| x_j \|^2$ (where $\bullet$ denotes the usual dot product on $\mathbb{R}^n$), we have

$$D_2 = \begin{bmatrix} \| x_1 \|^2 & -2x_1^{(1)} & \cdots & -2x_1^{(n)} & 1 \\ \vdots & \vdots & & \vdots & \vdots \\ \| x_N \|^2 & -2x_N^{(1)} & \cdots & -2x_N^{(n)} & 1 \end{bmatrix} \cdot \begin{bmatrix} 1 & \cdots & 1 \\ x_1^{(1)} & \cdots & x_N^{(1)} \\ \vdots & & \vdots \\ x_1^{(n)} & \cdots & x_N^{(n)} \\ \| x_1 \|^2 & \cdots & \| x_N \|^2 \end{bmatrix}, \tag{2.2}$$

and so D_2 may be written as the product of a matrix with $n + 2$ columns and a matrix with $n + 2$ rows. The rank of D_2 may therefore not exceed $n + 2$. For our particular project, we restricted our attention to sensors embedded in a plane (in which case the rank of D_2 is at most 4 for any number of sensors N), but this property of the matrix D_2 offers a simple way to extend our work to higher dimensions.

To try out our ideas, we designed and executed several different MATLAB simulations, each of which proceded according to the following general outline:

1. Generate $N = 200$ uniformly distributed random points inside the unit square $[0, 1] \times [0, 1]$.
2. Form the matrix D of pairwise distances between the points. Add noise if necessary.
3. Form the matrix D_2 of the squares of the (possibly noisy) distances between the points.
4. Knock out pairs of distances in D_2 according one of two procedures (described below) to form the partially observed matrix R.
5. Complete the matrix R using OptSpace to get $\hat{D}_2$.
6. Form the matrix $\hat{D}$, which is the element-wise square-root of $\hat{D}_2$.
7. Compare the completed matrix $\hat{D}$ to the original D by measuring the relative Frobenius-norm error $e = \| \hat{D} - D \|_F / \| D \|_F$.
8. Repeat the above steps for 25 trials, and compute the average relative Frobenius-norm error at the end.

We used two different methods for determining which entries in the matrix to eliminate, which we call "random" and "realistic" knock-out, respectively. By random knock-out, we mean that distance pairs were selected at random to be knocked-out according to a fixed probability. In constrast, realistic knock-out involves removing all entries of the matrix that exceed a certain threshold distance. The idea is that in a realistic setting, sensors which are far apart from each other may not be able to construct an estimate of the distance between themselves.

To simulate noise in the trials that required it, we randomly generated values from zero-mean Gaussian distributions and added them to the entries in the matrix of distances. In order to understand what effect the noise amplitude would have on the results, we used five different values for the standard deviations of these distributions: 0.01, 0.05, 0.1, 0.2, and 0.5.

A copy of the MATLAB code we wrote for the simulations is available here[4] . The OptSpace code must be downloaded separately and may be found at the OptSpace website listed in this project's References module.

[4] http://cnx.org/content/m33138/latest/EXPT_CODE.zip

2.4 Results, Conclusions, and Future Work[5]

2.4.1 Results, Conclusions, and Future Work

2.4.1.1 Random Knock-Out Trials

The results from the simulations for the random knock-out runs are displayed in the figures below, which depict the average relative Frobenius-norm error over 25 trials versus fraction of unknown entries.

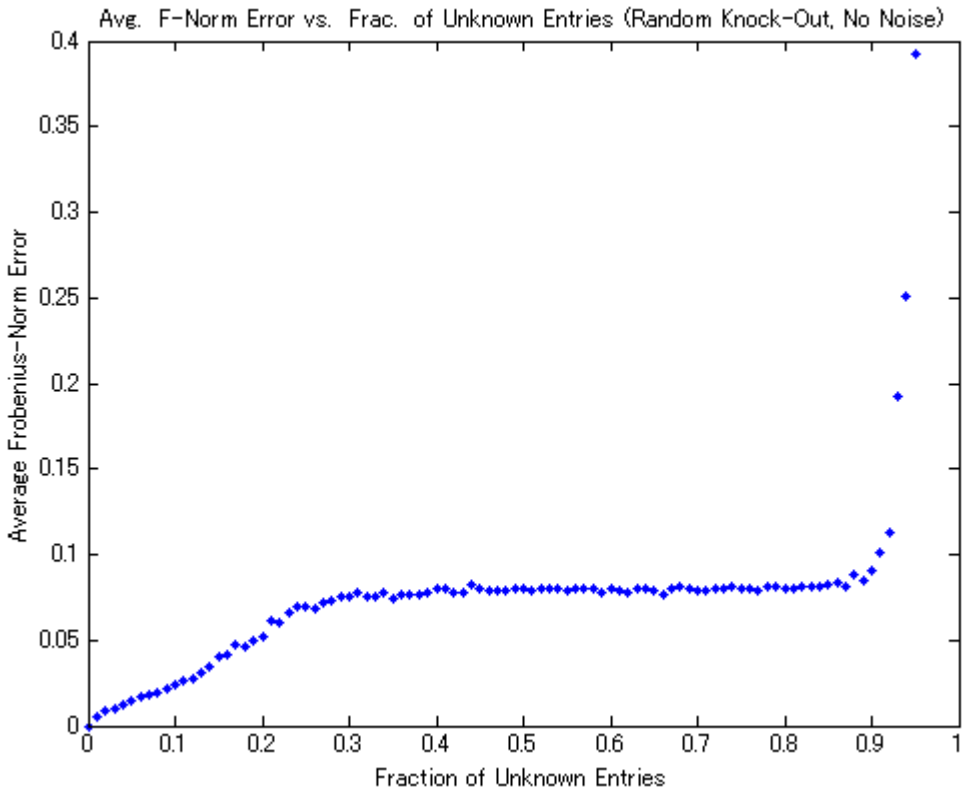

Figure 2.1: Simulation results for random knock-out trials with no noise.

[5]This content is available online at <http://cnx.org/content/m33141/1.1/>.

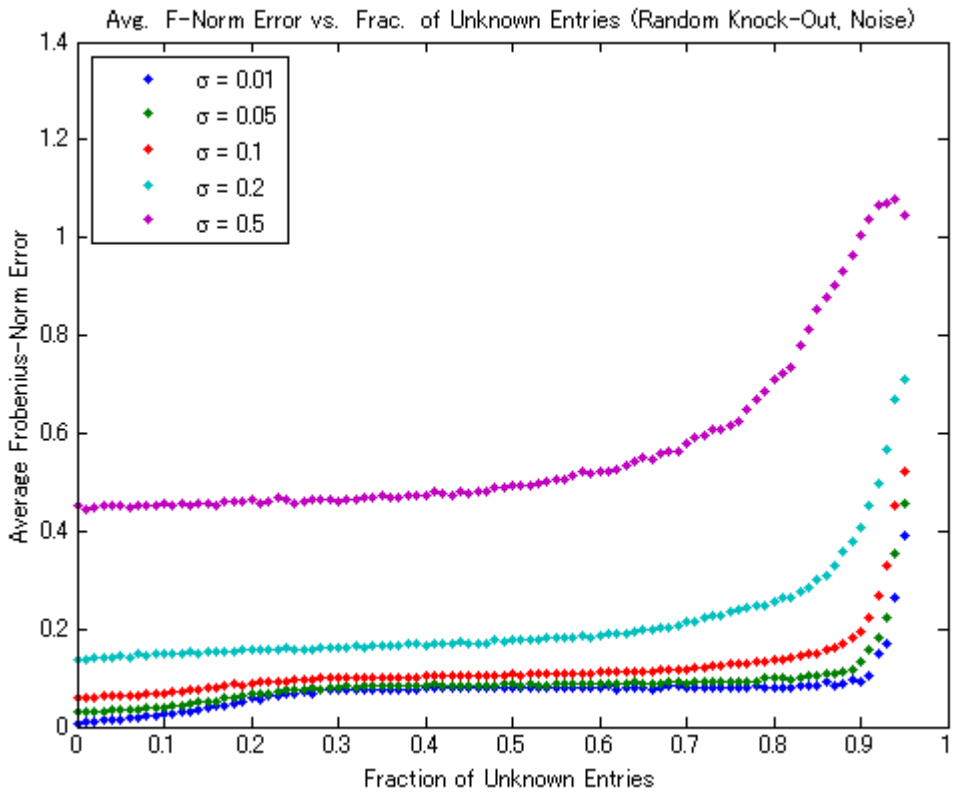

Figure 2.2: Simulation results for random knock-out trials with noise present.

As these two figures illustrate, the results for the random knock-out trials were quite good. As expected, as the fraction of unknown entries becomes large, the error eventually becomes severe, while for very low fractions of unknown entries, the error is extremely small. What is amazing is that for moderate fractions of unknown entries the algorithm still performs remarkably well, and its performance doesn't degrade much by the loss of a few more entries: the graphs are nearly flat over the range from 0.3 to 0.8! As the second figure shows (and as might be imagined), noise only makes the error worse; however, the plot also shows that the algorithm is reasonably robust to noise in that perturbations of the distance data by small amounts of noise don't become magnified into massive errors.

As an example, consider Figure 3 below, which displays the results of a typical no-noise random knock-out run with knock-out probability 0.5. On the left is a plot of the sparsity pattern for the incomplete matrix. A blue dot represents a known entry, while a blank space represents an unknown one. On the right is a plot of what the network looks like after being reconstructed using multidimensional scaling. Observe that the red circles for the network corresponding to the network generated by the completed matrix enclose the blue dots of the original network's structure quite well, indicating that the match is very good.

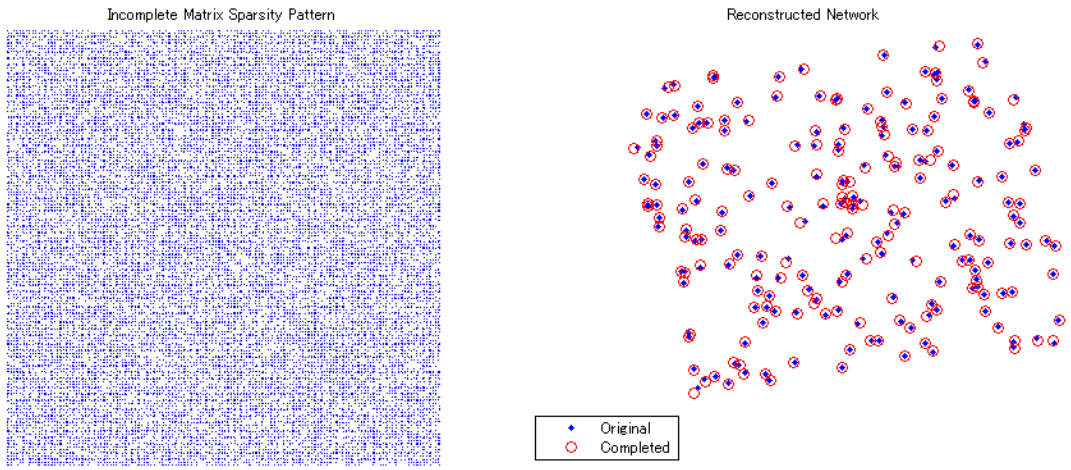

Figure 2.3: Results from a typical no-noise random knock-out trial with a knock-out probability of 0.5. Left: Sparsity pattern for the incomplete matrix. Right: Overlay figure demonstrating degree of agreement between the original network and the network generated from the completed matrix.

For an illustration of how the results look with noise, see Figure 4 below. This figure shows the results of a typical noise-present random knock-out run with knock-out probability of 0.5 and noise standard deviation 0.05. The agreement in the reconstructed network is not as good as it was for the no-noise case, but the points of the reconstructed network are "clustered" in the right locations, and some of the prominent features of the original network are present in the reconstructed one as well.

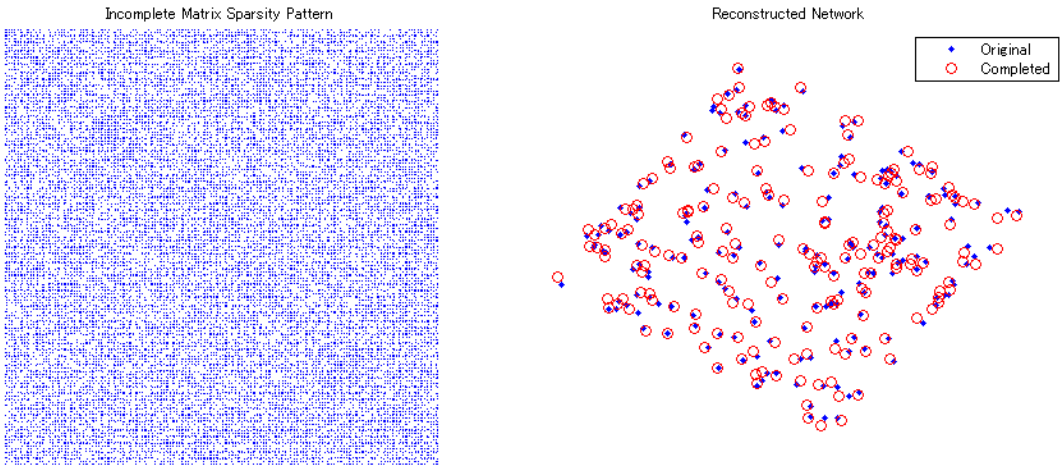

Figure 2.4: Results from a typical noise-present random knock-out trial with a knock-out probability of 0.5 and a noise standard deviation of 0.05. Left: Sparsity pattern for the incomplete matrix. Right: Overlay figure demonstrating degree of agreement between the original network and the network generated from the completed matrix.

2.4.1.2 Realistic Knock-Out Trials

The figures below, which show the results for the realistic knock-out trials, are similar to those above except that they plot the average relative Frobenius-norm error over 25 trials versus maximum radius as opposed to fraction of unknown entries.

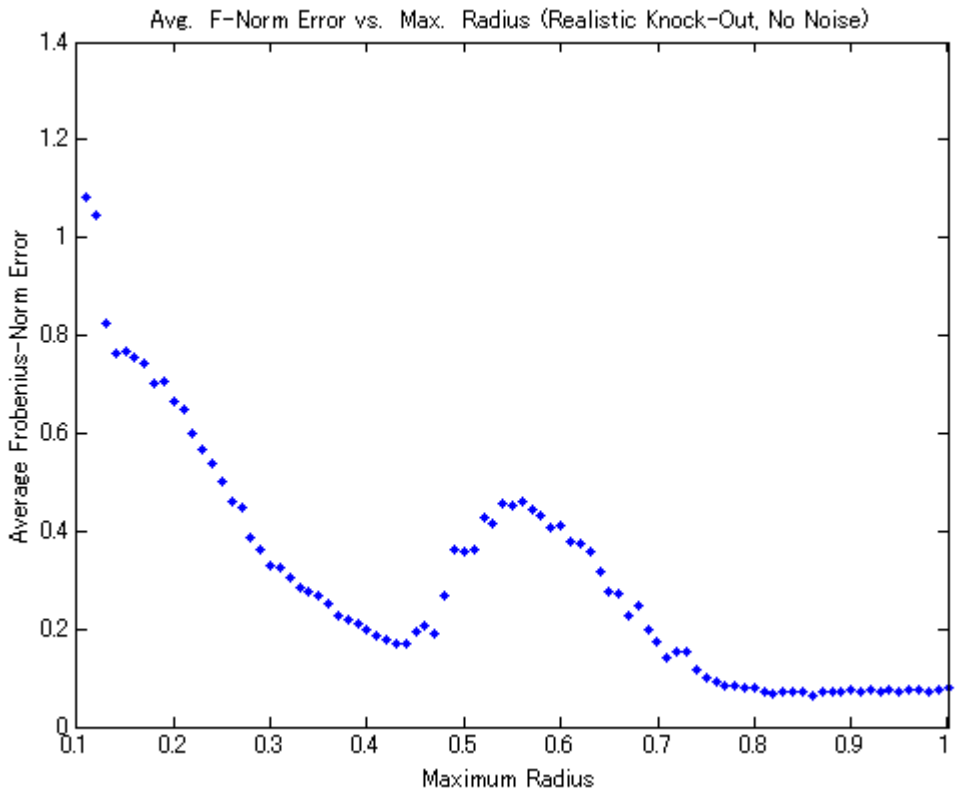

Figure 2.5: Simulation results for realistic knock-out trials without noise.

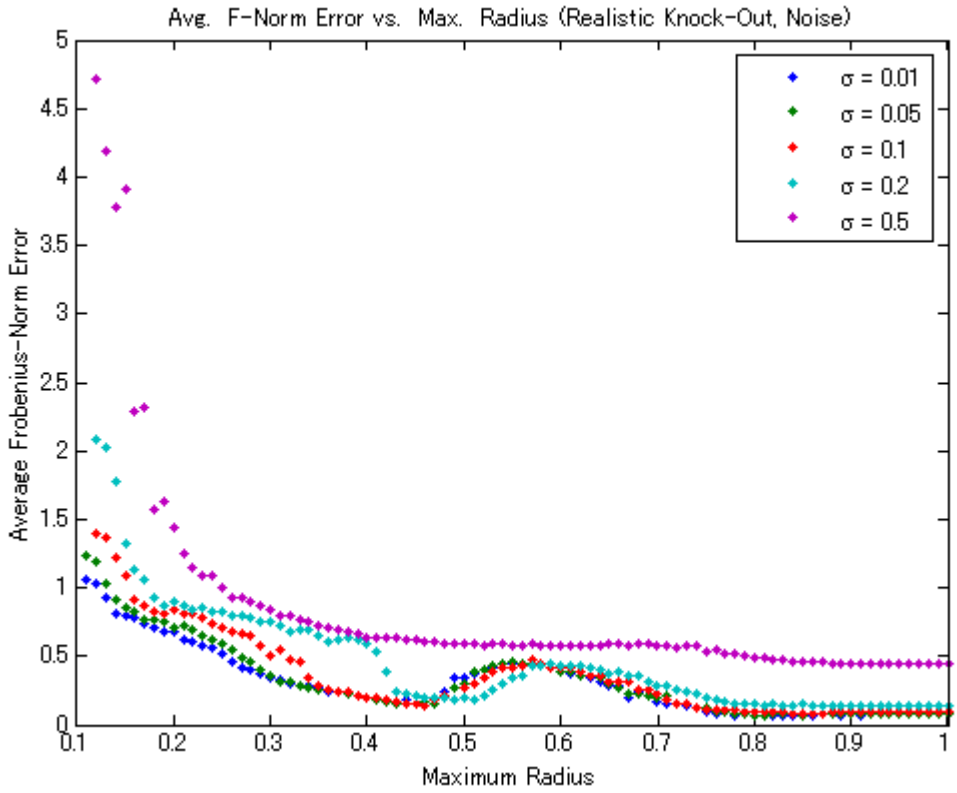

Figure 2.6: Simulation results for realistic knock-out trials with noise present.

The most salient feature of these graphs is the odd "hump" that appears from radius values of about 0.5 to 0.7, even in the no-noise case. Over this range, despite the fact that the radius is growing (meaning that more pairwise distances are known), the error in the completed matrix is actually becoming *worse* rather than better, which seems to contradict the excellent results discussed above for the random knock-out case. At the time of this writing, we are still unsure as to why this "hump" appears; however, we suspect that it may have something to do with the OptSpace algorithm itself because when we run the same experiment using the SVT algorithm of Candès, the hump does not appear, as the figure below shows. (Note that, nevertheless, OptSpace tends to produce less error than SVT, even over the offending range of radii.)

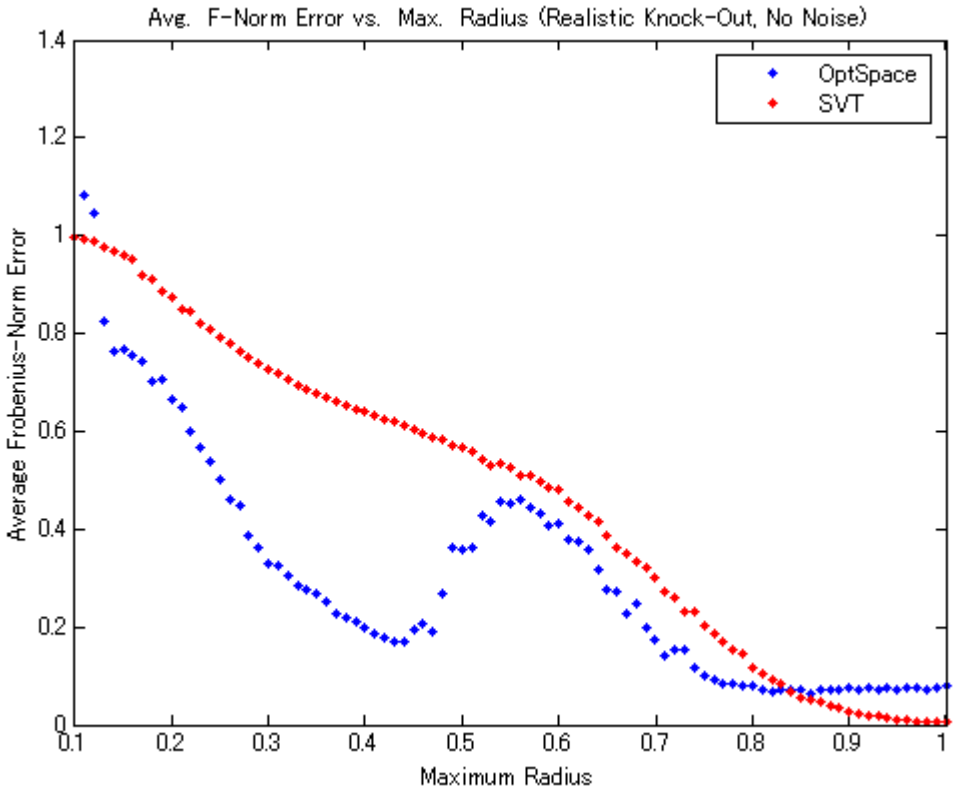

Figure 2.7: OptSpace performance vs. SVT performance for realistic entry knock-out without noise. SVT does not display a "hump," but OptSpace generally returns better error values.

Perhaps more important than the "hump," however, is the fact that the scales on the axes of the above graphs alone are enough to demonstrate that the performance of the method in the realistic knock-out case is decidedly worse than that for the random knock-out case. For example, consider the figure below, which shows the results of a typical no-noise, realistick knock-out trial with a maximum radius of 1. For this particular trial, over 97 percent of the pairs are known. The reconstructed network matches the original quite well near the "center" of the network, but at the edges, the match becomes much worse. This behavior is not exhibited at all by random knock-out trials for comparable fractions of unknown entries, as the picture at the bottom of the figure illustrates, which was generated from a non-noise random knock-out trial in which 90 percent of the pairs were known.

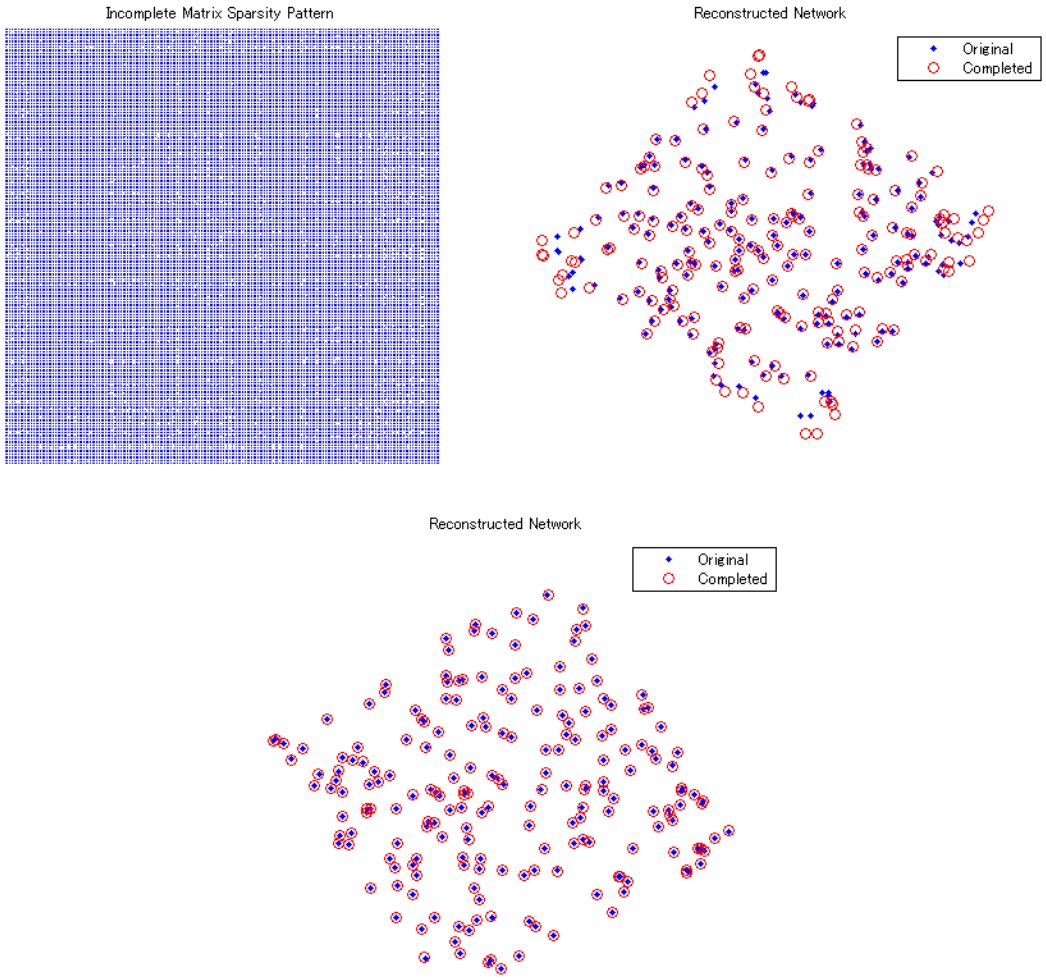

Figure 2.8: Results from a typical non-noise realistic knock-out trial with a maximum radius of 1. Top-Left: Sparsity pattern for the incomplete matrix. Top-Right: Overlay figure demonstrating degree of agreement between the original network and the network generated from the completed matrix. Bottom: Typical results from a non-noise random knock-out trial with knock out probability of 0.1 (90% of distance pairs are known).

Shrinking the radius only makes matters worse, as the next figure illustrates. The maximum radius here is $\sqrt{2}/2$. Around 77 percent of the distance pairs are known, and yet the match is terrible.

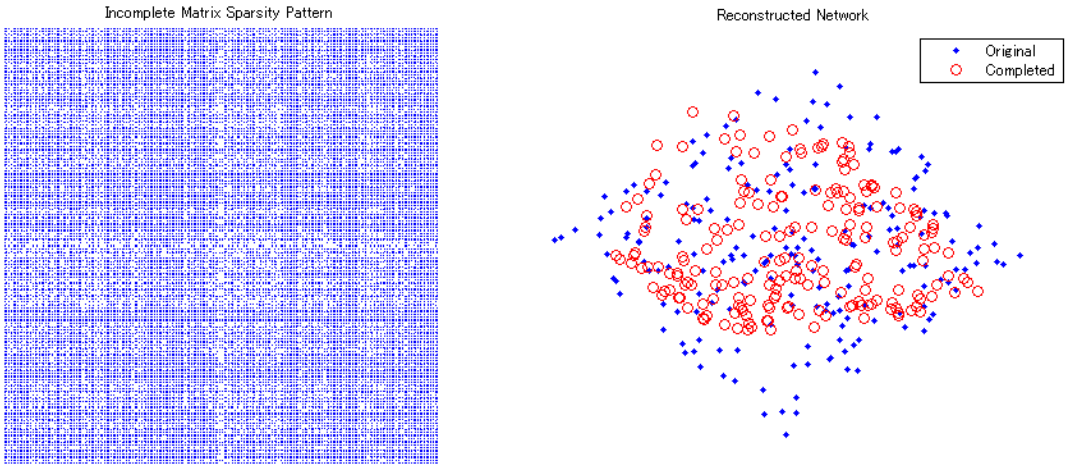

Figure 2.9: Results from a typical non-noise realistic knock-out trial with a maximum radius of $\sqrt{2}/2$. Left: Sparsity pattern for the incomplete matrix. Right: Overlay figure demonstrating degree of agreement between the original network and the network generated from the completed matrix.

Adding noise only makes the results even worse. At first glance, this behavior appears to be inexplicable; however examining the sparsity patterns of the incomplete matrices reveals an interesting fact: the entry knock-out in the realistic case is far from being "random!" The sparsity patterns for the realistic knock-out matrices reveal clear patterns of lines in their knocked-out entries that are not present in those for random knock-out cases. This unintended regularity of entry selection violates the assumption made in all of the matrix completion literature that the known entries are taken from a uniform sampling of the matrix, so it would seem that none of the theoretical results that have been derived apply in this case.

2.4.1.3 Conclusions

Our results show that matrix completion presents a viable means of approaching the sensor network localization problem under the assumption that the known pairs of distances come from a uniform sampling of the distance matrix. Under these conditions, matrix completion provides excellent network reconstruction and is fairly robust to noise. Unfortunately, its performance in the more realistic case in which distance information will be excluded or included based on a maximum possible distance over which two sensors can communicate leaves much to be desired.

2.4.1.4 Future Work

With more time on this project, we would like to have explored the following questions further:

- What is the true origin of the mysterious "hump?" If it really is due to OptSpace as the above seems to suggest, is there a way to modify the OptSpace algorithm to get it to go away?
- What is the fundamental reason that the realistic knock-out trials did not work? Is there a way to get them to work better? (Perhaps something like permuting the distance entries in the matrix around to make the sampling pattern apparently more random would do the trick. If the permutations are stored somewhere, they can be undone after the matrix is completed if necessary.)

- The experiment worked pretty well in two dimensions, at least for the random knock-out case. Will three dimensions show results that are any different?

2.5 Acknowledgments[6]

2.5.1 Acknowledgments

We would like to thank Mr. Andrew Waters for the invaluable support and guidance he provided us while we were working on this project as well as Prof. Baraniuk for suggesting such a fascinting project to us in the first place.

2.6 References[7]

2.6.1 References

In addition to the papers that are cited throughout the other modules in this collection, we made use of the following other resources when carrying out this project:

The OptSpace code written by Keshavan, Montanari, and Oh that was used for running the simulations carried out in this project was obtained from http://www.stanford.edu/~raghuram/optspace/code.html[8] . While the multidimensional scaling code used to generate the plots of the reconstructed networks was written entirely by us, we made use of the following book for information on how to go about writing it:

I. Borg and P. Groenen. *Modern Multidimensional Scaling: Theory and Applications*. New York: Springer, 1997. pg. 207-210, 261-267.

[6] This content is available online at <http://cnx.org/content/m33142/1.1/>.
[7] This content is available online at <http://cnx.org/content/m33146/1.1/>.
[8] http://www.stanford.edu/~raghuram/optspace/code.html

Chapter 3

Discrete Multi-Tone Communication Over Acoustic Channel

3.1 Introduction[1]

3.1.1 What is DMT and where is it used?

DMT is a form of Orthogonal Frequency Division Multiplexing. Effectively, information is coded and modulated by several different sub carriers. This is the same modulation scheme used in common DSL channels. Specifically, at frequencies above those reserved for speech, there exist several hundred channels of the equal bandwidth used to transmit data to and from the internet. This is very convenient for phone users, as these DMT channels can be easily filtered out using a simple low-pass filter, preventing any possible interference from connecting to the internet while talking on the phone.

3.1.2 Why transmit over an acoustic channel?

The acoustic channel, and the audible frequencies contained therein, was chosen as a test area for our DMT project simply because of its accessibility. No complex or expensive hardware is necessary to transmit over it, just a standard computer speaker and microphone setup.

3.1.3 What can DMT do for us?

As will be revealed in later modules, DMT modulation offers many features that protect our signal's information from being distorted by the channel. Specifically, by transmitting our information over several subcarriers at the same time instead of just one carrier, we can use the frequency response of the system to see which carriers are being attenuated and likewise increase the gain on those channels or get rid of them altogether. You will discover, as we did, how difficult that process turned out to be.

3.2 The Problem[2]

3.2.1 Creating a DSL Modem

Our goal is to use Discrete Multi-Tone modulation to transmit a text message over the audible range of frequencies in an acoustic channel. We are creating a DSL modem that transmits through the air.

[1] This content is available online at <http://cnx.org/content/m33147/1.1/>.
[2] This content is available online at <http://cnx.org/content/m33155/1.1/>.

To do this, we will observe the frequency characteristics of the channel, and use that information to equalize our received transmission in hope to preserve the maximum amount of content from the signal. As in any engineering problem, we are constantly striving to push the data-rate of our system, while minimizing the occurrence of errors. Here we go!

The Transmitter (Section 3.3)
The Channel (Section 3.4)
Receiver (Section 3.5)
Results and Conclusions (Section 3.6)

3.3 Transmitter[3]

3.3.1 Text to Binary Conversion

The first step is to convert our information into binary. We used the sentence "hello, this is our test message," repeated four times, as our text message. To get it into binary, we used standard ASCII text mapping.

hello = 01101000 01100101 01101100 01101100 01101111

3.3.2 Series to Parallel

The next step is converting this vector of zeros and ones into a matrix. The vector is simply broken up into blocks of length L, and each block is used to form column of the matrix.

3.3.3 Constellation Mapping

Now the fun begins. The primary method of modulation in DMT is by inverse Fourier Transform. Although it may seem counterintuitive to do so, by taking the inverse Fourier Transform of a vector or a matrix of vectors, it effectively treats each value as the Fourier coefficient of a sinusoid. Then, one could transmit this sum of sinusoids to a receiver that would in turn take the Fourier Transform (the inverse transform of the inverse transform, of course) and retrieve the original vectors.

But instead of taking the transform of our vectors of zeros and ones, we first convert bit streams of length B to specific complex numbers. We draw these complex numbers from a constellation map (a table of values spread out along the complex plane). See the figure below for an example of a 4 bit mapping.

[3]This content is available online at <http://cnx.org/content/m33148/1.1/>.

Constellation Mapping Table

Bit Sequence	Constellation Value	Bit Sequence	Constellation Value
0000	.354 + .354j	1000	1
0001	.707	1001	.707 + .707j
0010	.707j	1010	j
0011	-.354 + .354j	1011	-.707 + .707j
0100	-.707j	1100	-1
0101	.354 - .354j	1101	-.707 - .707j
0110	-.354 - .354j	1110	-j
0111	-.707	1111	.707 - .707j

Figure 3.1: This table shows which bit stream is mapped to which complex value.

3.3.4 Signal Mirroring and Inverse Fourier Transform

Why would we do that, you might ask. Doesn't converting binary numbers to complex ones just make things more complicated? Well, DMT utilizes the inverse Fourier Transform in order to attain its modulation. So taking the IFFT of a vector of complex numbers will result in a sum of sinusoids, which are great signals to be sending over any channel (they are the eigenfunctions of linear, time-invariant systems).

But before taking the inverse transform, the vectors/columns of the matrix must be mirrored and complex conjugated. The Inverse Fourier Transform of a conjugate symmetric signal results in a real signal. And since we can only transmit real signals in the real world, this is what we want.

3.3.5 Cyclic Prefix

If we were transmitting over an ideal wire system, we would be done at this point. We could simply send it over the line and start demodulating. But with most channels, especially our acoustic one, this is not the case. The channel's impulse response has non-zero duration, and will therefore cause inter-symbol interference in our output.

Intersymbol interference occurs during the convolution of the input and impulse response. Since the impulse response has more than a single value length, it will thus cause one block's information to bleed into the next one.

To prevent this, we added what is called a cyclic prefix to each block. As long as the length of the cyclic prefix is at least as long as the impulse response, it should prevent ISI. However, it has a secondary effect as well. We created the prefix by adding the last N values of each block (where N is the length of the response) to the beginning, preserving the order. Doing this effectively converts the linear convolution of the impulse response with the block sequence to circular convolution with each block separately, since there will now be the "wrap-around" effect. This will be handy later when we start characterizing the channel, since circular convolution in time is equivalent to multiplication of DFT's in frequency.

00010110011010001 => 010001000101100110100001

The first six bits in the second bit stream, 010001, is the cylcic prefix. Note that although these values are binary, they could essentially range from -1 to 1 since they sample the sinusoid sum that was formed after inverse Fourier Transforming.

Please see the block diagram below. It summarizes the entire transmission process covered above.

Transmission Block Diagram

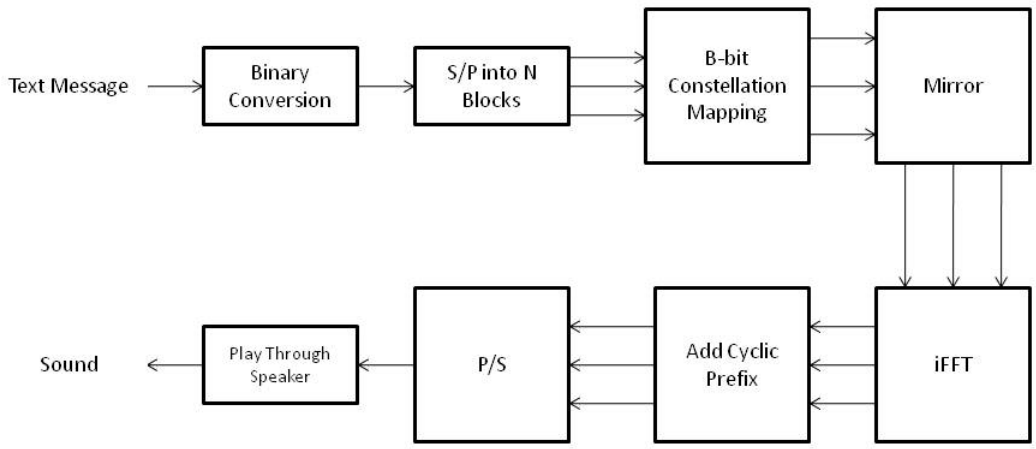

Figure 3.2: This diagram shows the all of the components and flow of our transmission system.

3.4 The Channel[4]

3.4.1 The Channel

To characterize the channel, we input an impulse by recording the tapping of the mic with our fingers. We then played that sound through the speaker and recorded the response with the mic. The signal is below, along with its spectrum.

Impulse Response of the Channel and its Spectrum

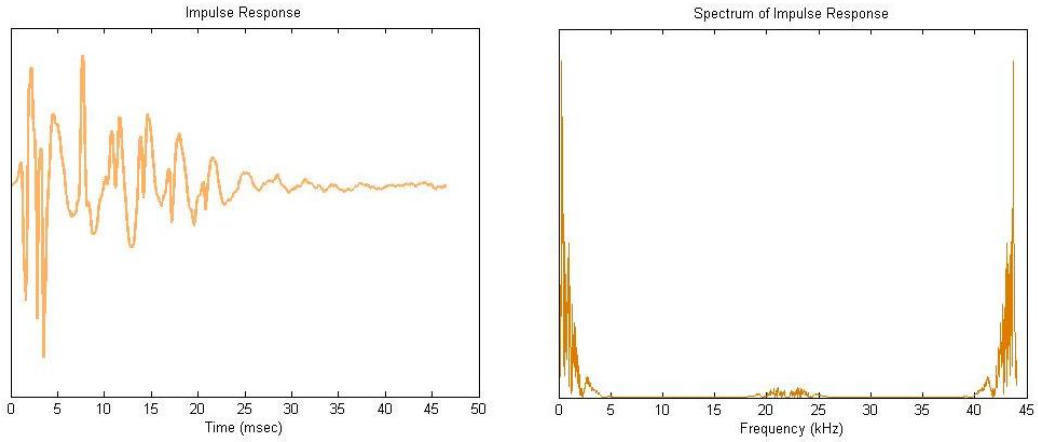

Figure 3.3: These graphs characterize the channel that we are transmitting through

We did this in preparation for the receiving end of the system to divide the received signal's FFT by the impulse response's FFT.

Below are plots of our transmitted and received signals, along with their spectrums. You will notice a great similarity between the signals in time, however a distinct difference in frequency. Unfortunately, this loss in frequency will translate to a loss of information.

[4]This content is available online at <http://cnx.org/content/m33144/1.1/>.

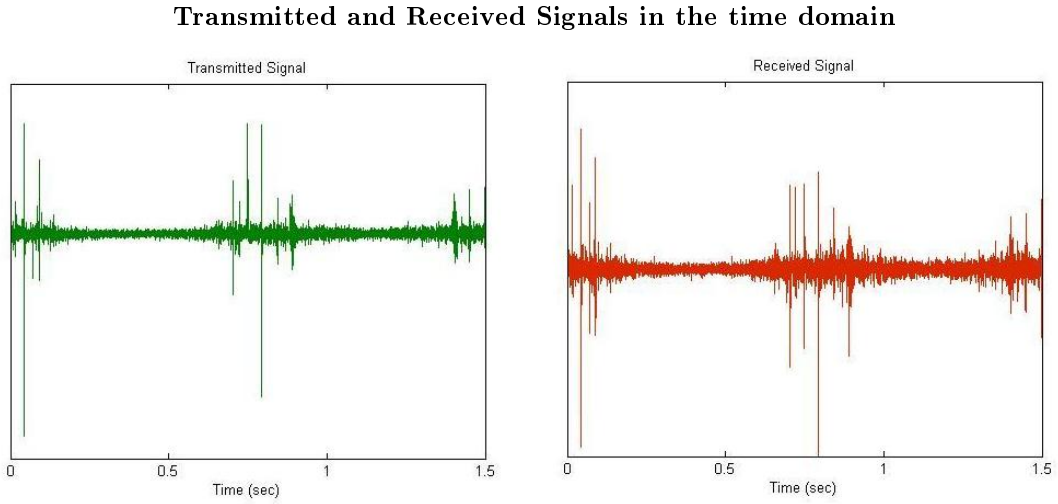

Figure 3.4: These are the signals in time that we transmitted (green) and that we received (red). As you can see they look very similar, and take it from us, they also sound similar.

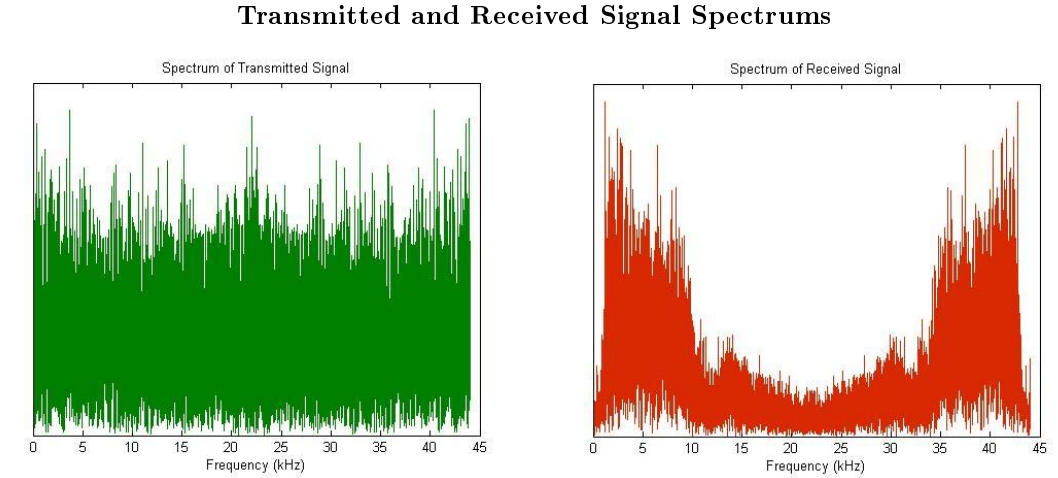

Figure 3.5: The green spectrum is of the signal we transmitted, and the red is the spectrum of the signal we received. We see a much bigger visual difference than we did in the time domain.

Above are plots for our transmitted and received signals. Here we used a block length of half the duration of the signal and sent it through the air at 44.1 kHz.

3.5 Receiver[5]

3.5.1 Decoding the Transmission

Since the receiver has full knowledge of all the steps taken to transmit, the reception process is the exact inverse of transmission. The only difference is the addition of the channel equalization described in the previous part. To get back the information we originally sent, we simply:

- Take the FFT of the reception and divide it by the FFT of the impulse response. Then iFFT it back.
- Remove the cyclic prefix
- Take the Fourier Transform
- Demirror the vector
- Approximate each received value to nearest point in constellation and map them back to the original bit sequences. See figure below for example in 4 bit approximation.
- Convert the binary series back to ascii letter equivalents.

Approximation of Constellation Map

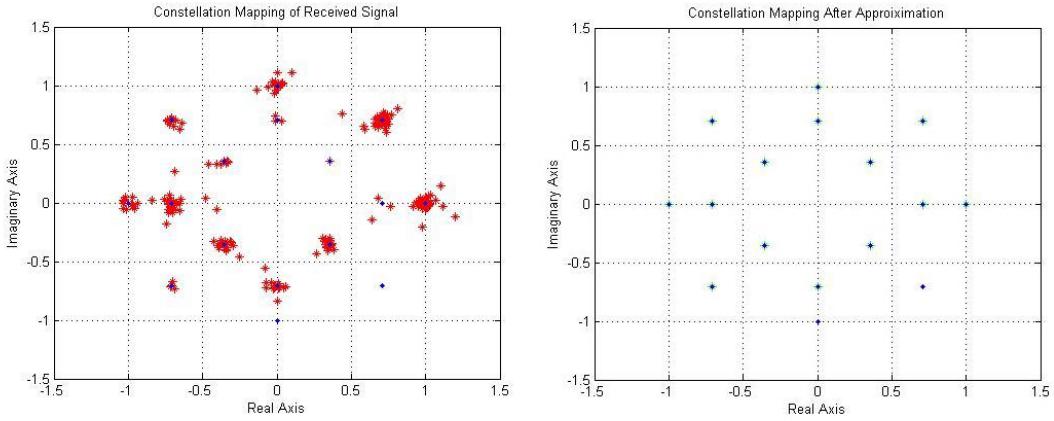

Figure 3.6: The map on the left was approximated to the one on the right with a 2.15% percent error.

Please see the block diagram below. It summarizes the reception process.

[5]This content is available online at <http://cnx.org/content/m33151/1.1/>.

Receive Block Diagram

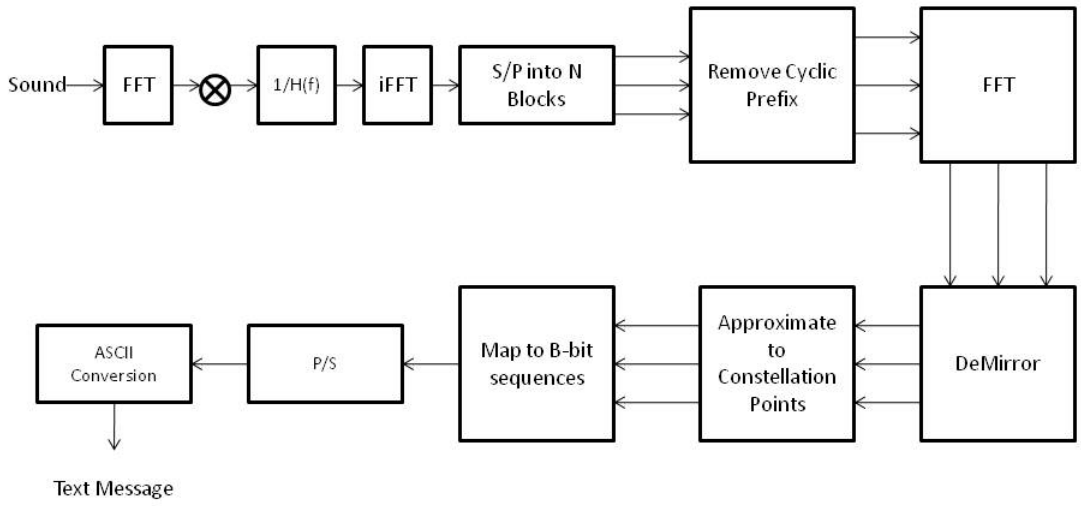

Figure 3.7: This diagram shows the all of the components and flow of our receiver system.

3.6 Results and Conclusions[6]

Results

Unfortunately, our microphone-speaker system was not successful in transmitting a text message. The measured transfer function seemed reasonable since it modeled a low-pass filter. But it was ineffective in equalizing our received signal. This is most likely because the channel added far too much noise, in addition to attenuating many of the frequencies beyond recovery.

Since we were unable to acquire the desired results on bit-rate maximization and error minimization in the acoustic channel, we created an artificial channel, using our observed frequency response plus Gaussian noise. Modeling this channel in Matlab produced notable results. See the figures below.

[6] This content is available online at <http://cnx.org/content/m33152/1.1/>.

Bit-rate vs Block Length (2 and 4 bit)

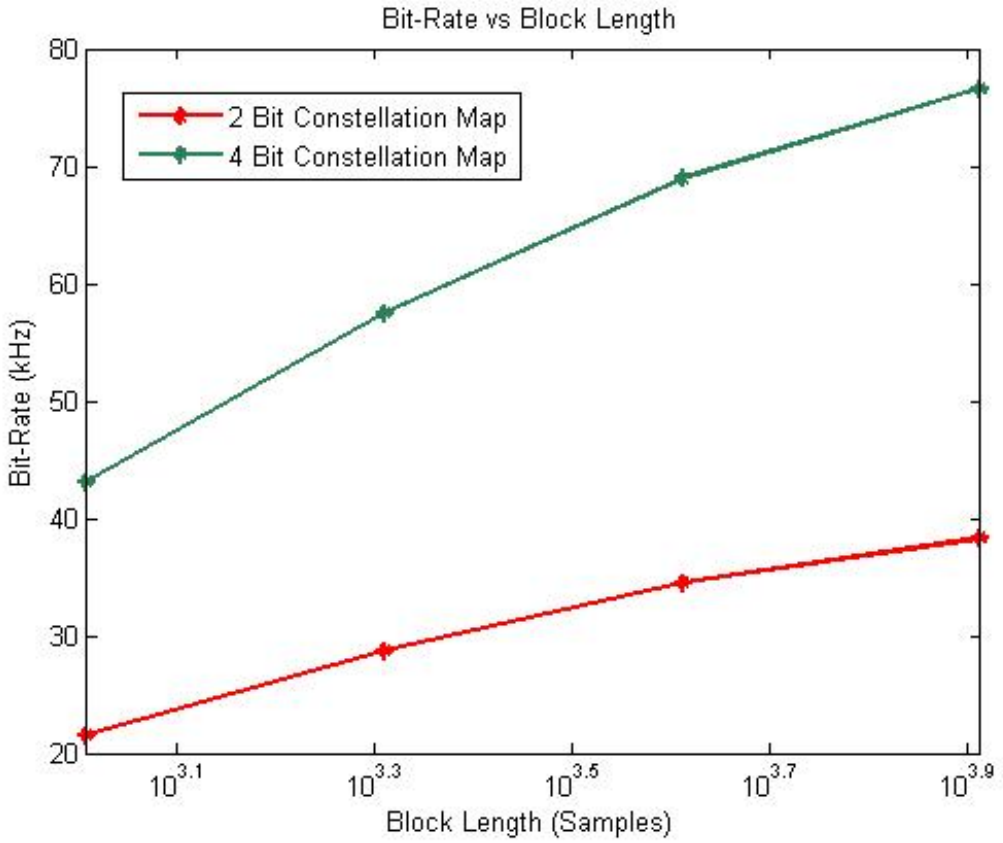

Figure 3.8: This graph illustrates the fact that data rate increases as we increase block length. It also shows that a 4-bit scheme has twice the data rate of a 2-bit scheme, as one would expect.

Percent Error vs Block Length (2 and 4 bit)

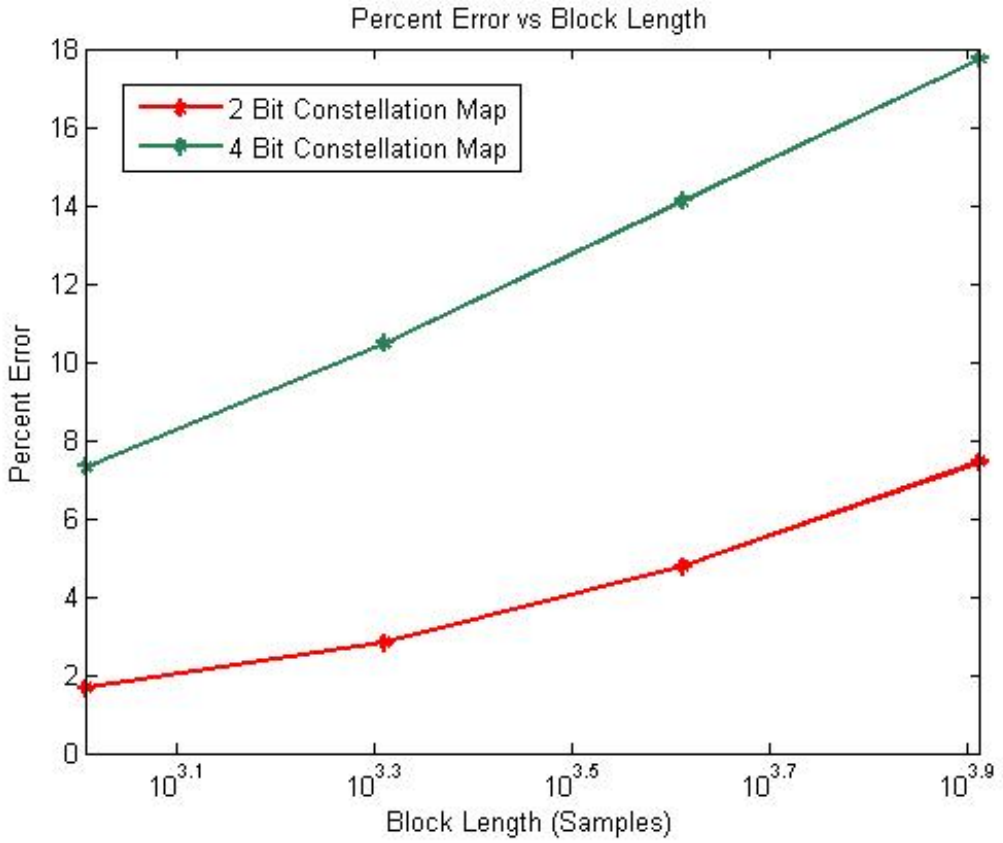

Figure 3.9: This graph illustrates the fact that as block length increases so will the amount of errors. Also we see that the 4-bit scheme has a much greater amount of errors than the 2-bit.

These figures indicate that both bit-rate and error-rate go up as block length increases. This makes sense since increasing the block length increases the number of channels (Taking the iFFT of a longer signal produces more unique sinusoids.). Squeezing more sinusoid carriers over the same bandlimited channel (0-22kHz) should result in more errors in demodulation, while transmitting more bits at the same time. It also makes sense that the 4 bit constellation mapping yielded higher bit-rates and error percentages since each sinusoid carries more information, yet can more easily be approximated to the wrong constellation point.

The next project dealing with Discrete Multi-Tone modulation in the acoustic channel should certainly involve a more professional recording system.

3.7 Our Gang[7]

3.7.1 Gang Members

Dangerous Brian Viel –Electrical and Computational Engineering
Soarin' Dylan Rumph – Electrical and Computational Engineering

3.8 Acknowledgements[8]

We would like to thank:
Jason Laska – Our project advisor for giving us moral support and steering us in the right direction.
Rich Baraniuk – Hell, he taught us all we know about DSP
2003 DMT Group (Travis White, Eric Garza, Chris Sramek) – We used much of their original matlab code as a start for our modulation.

[7] This content is available online at <http://cnx.org/content/m33153/1.1/>.
[8] This content is available online at <http://cnx.org/content/m33140/1.1/>.

Chapter 4

Language Recognition Using Vowel PMF Analysis

4.1 Meet the Team[1]

4.1.1 Language Recognition Using Vowel PMF Analysis

4.1.1.1 Meet the 4 Guys

Haiying Lu (hl6@) – Chinese boi from Mississippi. Likes sweet tea, fried chicken, and believes in true love. Dream occupation: Save the world with a law degree and lots of love.

Wharton Wang(wkw1@) –Culturally confused. 6'1 height complete waste. Fashion guru. Dream occupation: First Asian American President or win an Oscar, Grammy, & Tony.

Jason Xu (jax1@) – Hair never grows longer than one inch. Desires life to be like a musical. Diva. Dream occupation: Be the next Yao Ming or open his own gym.

Qian Zhang (qz1@) – Enjoys good tv shows and will critique your dance move. Campus celebrity. Dream occupation: Runway model or Pokemon Master.

[1] This content is available online at <http://cnx.org/content/m33133/1.2/>.

Figure 4.1

From L-R: Haiying Lu,Wharton Wang, Jason Xu, Qian Zhang

4.2 Introduction and some Background Information[2]

4.2.1 Introduction: Language Recognition Using Vowel PMF Analysis

In recent years, voice and sound recognition technology has become increasingly prevalent in general society. Early applications focused on security and privacy measures were utilized by a small portion of the total population. However, today virtually every person who owns a computer has access to such technology. There are programs which transcribe speech into text, identify different speakers, identify what song is being played, and accept audio signals as valuable input in general.

Our goal is to add language recognition to the growing list. The inspiration is from the multi-language background of all the group members and about 60% of the Rice students speak at least two languages fluently. Therefore, we think it will be interesting to develop a system which can "listen" to a speech sample and recognize the language it is using.

[2]This content is available online at <http://cnx.org/content/m33121/1.2/>.

4.2.2 Background: Formant Analysis of Vowel Sounds

Formants are broad peak envelopes found in the spectrum of sound. Vowel sounds are pronounced with an open vocal tract which creates a periodic resonance in air pressure. In contrast, consonant sounds require a closure of the tract at some point during pronunciation, making them devoid of the same type of resonance found in vowels. This results in easily identifiable differences between the two types of sounds in the frequency domain—one of the most evident being the emergence of clear formants in vowels.

Each vowel sound generally has 3 or 4 formants located at specific frequency ranges corresponding to how 'open', 'closed', 'front', 'back', or 'round' the sound is. These characteristics depend on how the lips, tongue, and jaw are used in pronunciation. Although there are 3 or 4 total formants for most vowel sounds, the first two formants are usually all that is required to distinguish between them.

For our purposes of finding PMFs of vowel sounds in different languages, we are only looking at 5 most basic vowel sounds so it is usually sufficient to check up to the first two formants to decide the vowel sound. In addition to a vowel sound's natural frequency, the speaker's pitch will also vary the position of the formant. Therefore, we only used male speech samples consistently so that we have a relatively consistent vowel distribution for every sample.

4.3 Our System Setup[3]

4.3.1 Our System Setup

We plan to use the probability mass function (PMF) of 5 different vowel sounds in 3 different languages to determine which language a speech sample is spoken in. However, before we can attempt to carry out that task, we require a means of counting the number of occurrences of the 5 different vowel sounds in any given speech sample to create the PMFs.

We chose English, Spanish and Japanese to analyze in this project. Spanish and Japanese both have simple vowel sounds. For example, 90% of Japanese speaking consists of the 5 basic vowel sounds in our database. Spanish is similar and English is a little more complicated in pronunciation but we can still find an approximate distribution with our system and database. The choice of these languages has a good representation of western and eastern language and they are all widely used languages.

Two important databases are crucial in order for the system to perform at this point. One is the formant's frequency of the 5 most basic vowel sounds (a, i, u, e, o). The other database we want to have is the reference PMF of the 3 languages we are using. If we believe that there is a certain pattern in the PMF of the vowel sound distribution in these languages, then statistically, if we have a large enough sample, the PMF should represent the population parameters. In our case, we decided to use a long speech sample of each language and use its vowel sound PMF as the reference data, which will be used later in the system to match smaller random speech samples.

[3]This content is available online at <http://cnx.org/content/m33115/1.1/>.

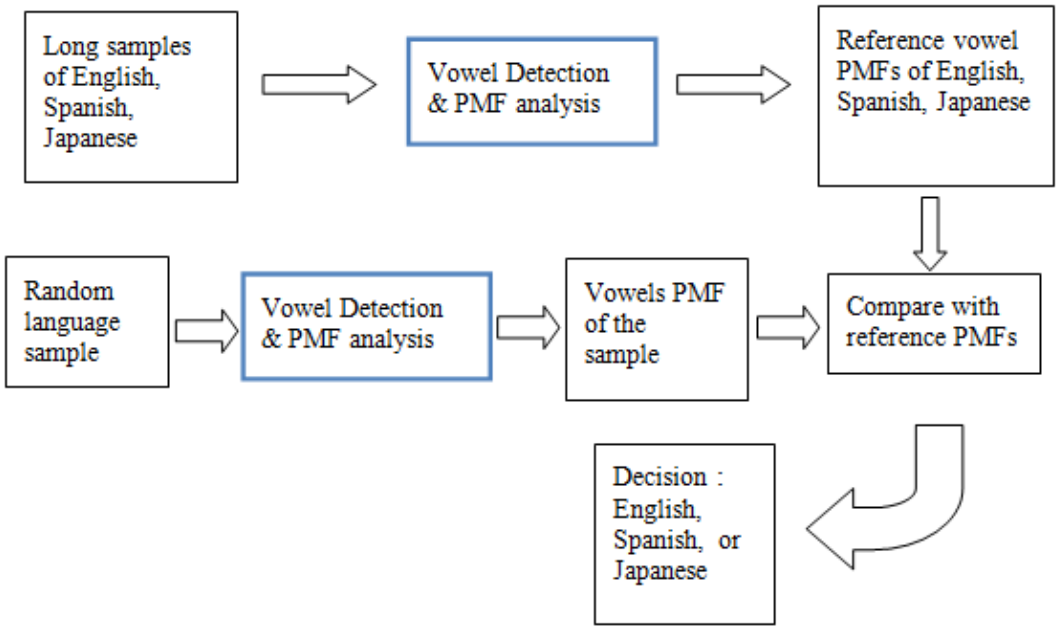

Figure 4.2

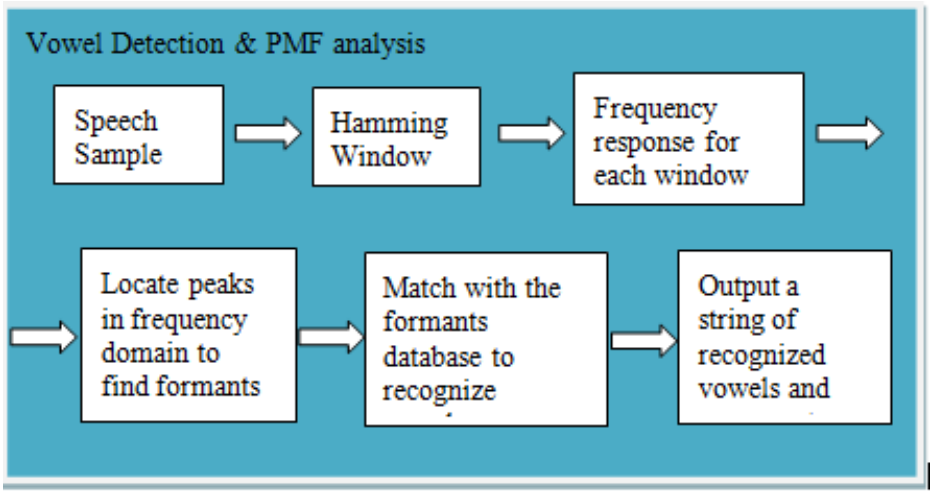

Figure 4.3

4.4 Behind the Scene: From Formants to PMFs[4]

4.4.1 Identifying Vowel Sounds in a Speech Sample

We exploit each vowel sound's unique formant distribution to identify every occurrence of certain vowel sounds in a sample of speech. This was done by:

Inputting a speech sample – Since human speech typically maxes out at frequencies of 4 kHz, we chose to sample at 8000 Hz. This enabled us to compile our PMF data much more quickly than if we had sampled at a higher standard of 44.1 kHz.

Windowing – A Hamming window is utilized to break our sample into separate chunks to be analyzed one at a time for the presence/absence of a vowel sound. Since the Hamming window slowly tapers towards zero at the edges, the spectrum will appear much smoother and less 'jagged' than it would have had we used a rectangular window.

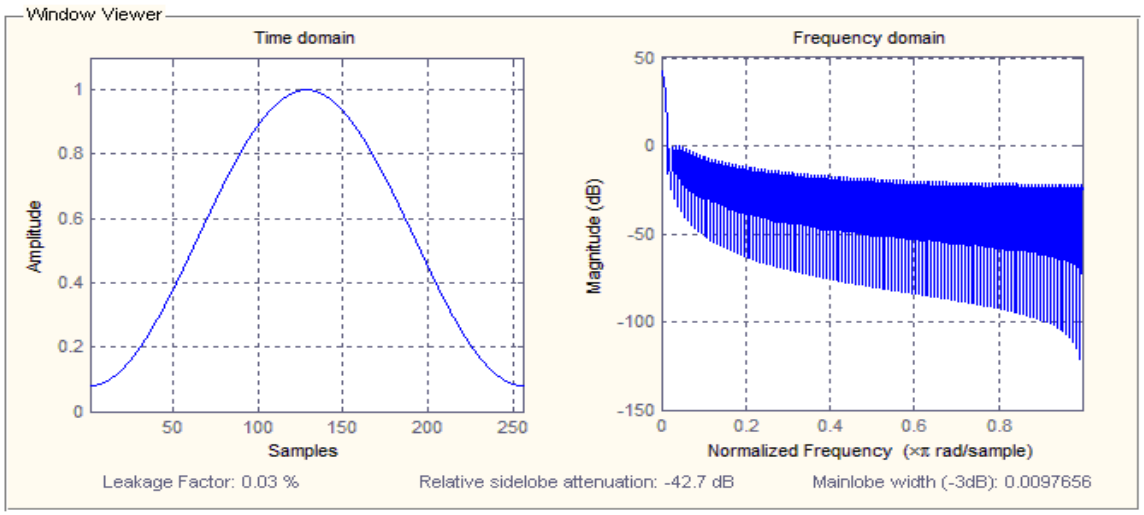

Figure 4.4

4.4.2 Frequency domain analysis of formants:

The code works as following:

Locate the peaks, decide the formant according to the frequencies of 3 or more consecutive high magnitude, set flags for the 5 vowel sound, go through the database to match, decide the vowel or consonant.

Look at each window and determine whether or not there is a vowel there; a string of a certain vowel sound (2 or more) will be treated as a 'vowel', otherwise "not a vowel". Then the system gives the output as a string of the five vowels: a, e, i, o, u and "C" if there is a consonant detected in between.

The plots below are generated by the code when we were building the formants data base using vowel sound samples.

[4]This content is available online at <http://cnx.org/content/m33134/1.3/>.

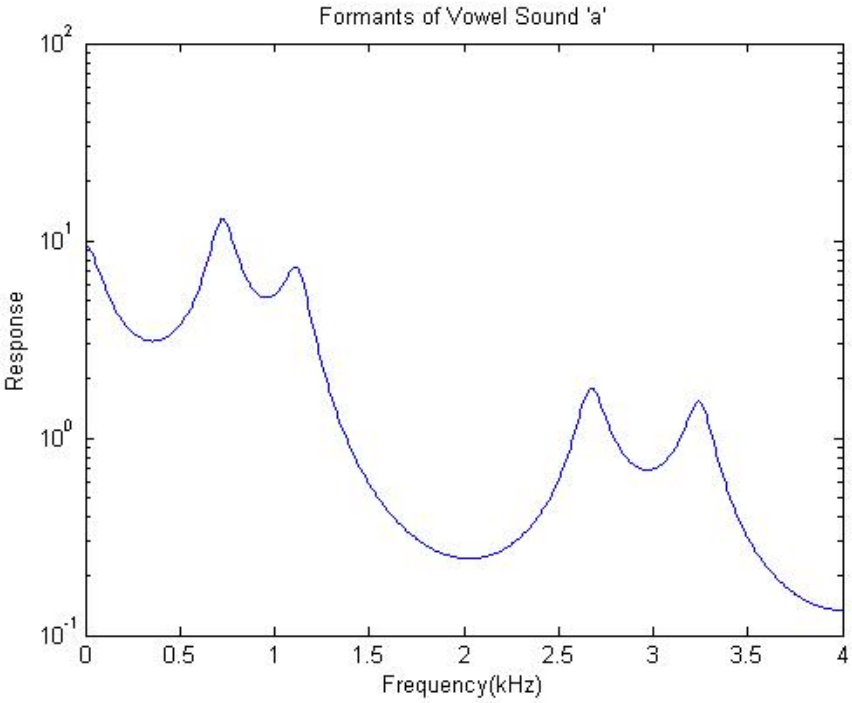
Formants of Vowel Sound 'a'
Response
Frequency(kHz)
10^2
10^1
10^0
10^-1
0
0.5
1
1.5
2
2.5
3
3.5
4

Figure 4.5

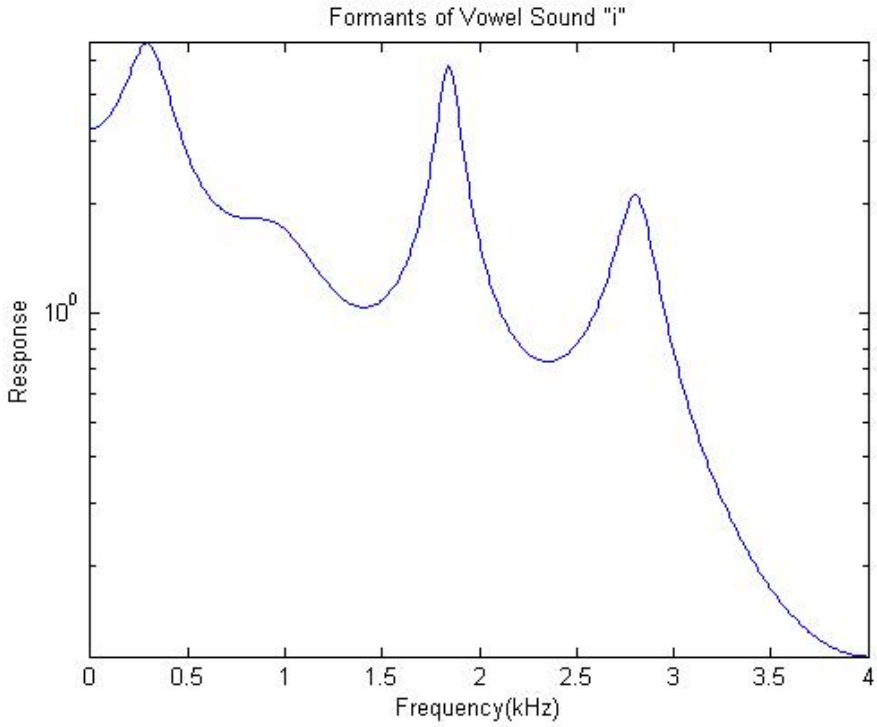
Formants of Vowel Sound "i"
Response
10^0
0
0.5
1
1.5
2
2.5
3
3.5
4
Frequency(kHz)

Figure 4.6

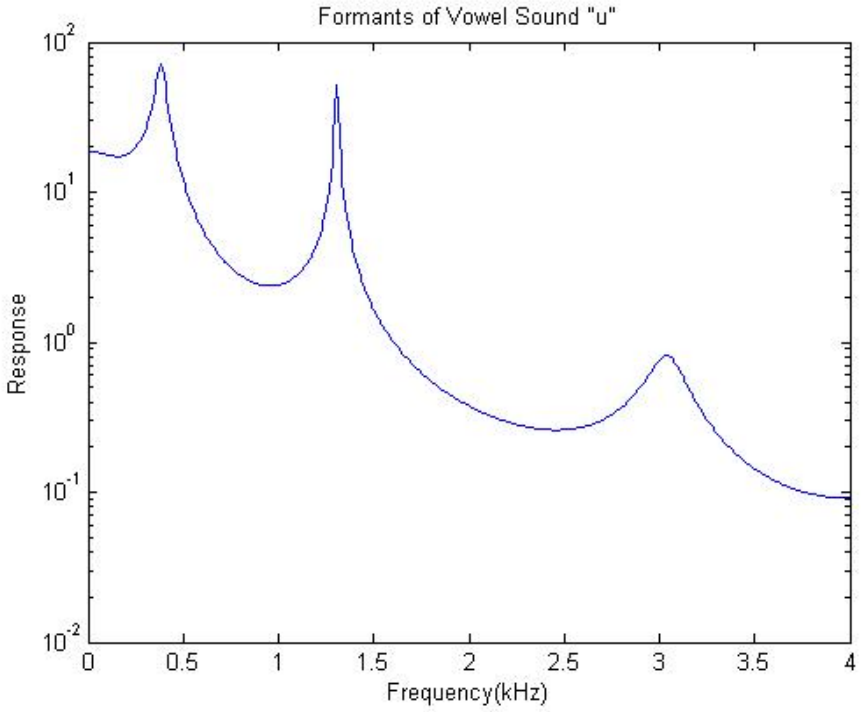
Formants of Vowel Sound "u"
Response
Frequency(kHz)
10^2
10^1
10^0
10^-1
10^-2
0
0.5
1
1.5
2
2.5
3
3.5
4

Figure 4.7

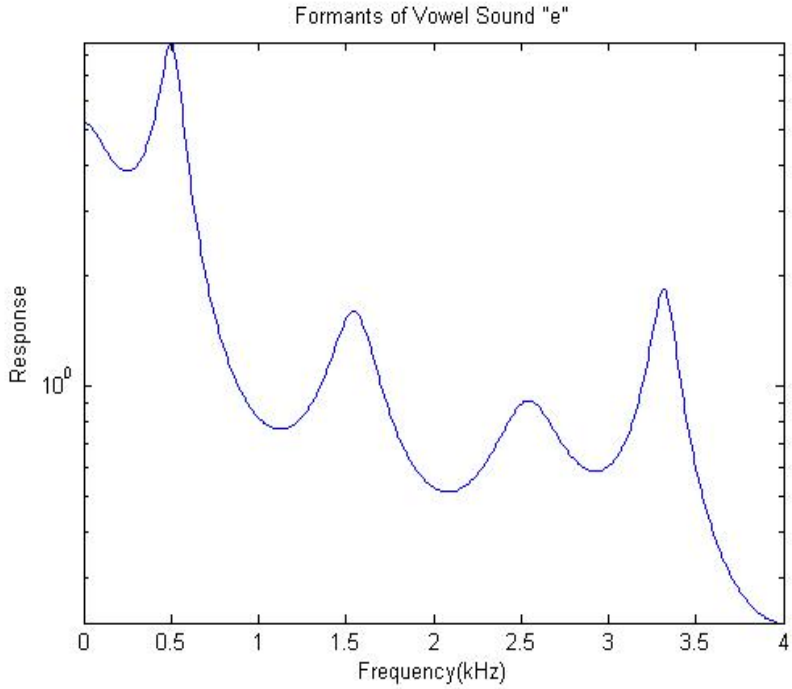
Formants of Vowel Sound "e"
Response
10^0
0
0.5
1
1.5
2
2.5
3
3.5
4
Frequency(kHz)

Figure 4.8

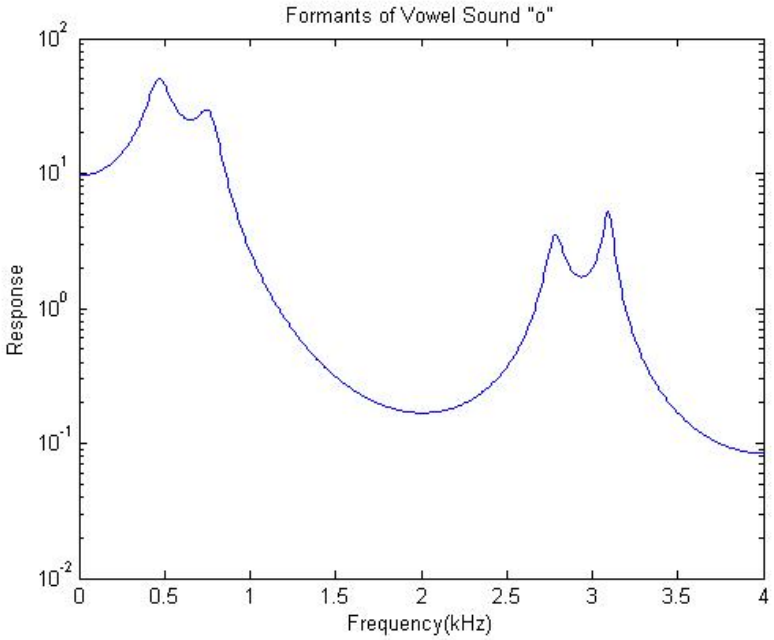

Figure 4.9

4.4.3 Creating Language PMFs

In order to create probability mass functions for the distribution of our 5 vowel sounds in different languages, we first gathered several speech samples of different languages. Since our code operates on .wav files sampled at 8000 kHz, we re-sampled all of our speech samples to meet these specifications. Using our code, we identified how often the 5 sounds occurred in all of the samples of one language, and then created a probability mass distribution function based off of that information.

```
function answer = langdetect(x)
%Transform the character string from formants.m to recognizable numerical
%values
x = double(x);
%Initiate count vector
count = zeros(5,1);
%Count the number of occurences for each vowel
for i=1:length(x)
if x(i) == 97
count(1) = count(1) + 1;
elseif x(i) == 101
count(2) = count(2) + 1;
elseif x(i) == 105
count(3) = count(3) + 1;
elseif x(i) == 111
count(4) = count(4) + 1;
```

```
elseif x(i) == 117
count(5) = count(5) + 1;
else
continue;
end
end
%Normalize
count = count/(sum(count));
%PMF Bank
JAP = [0.25 0.35 0.12 0.23 0.05];
SPA = [0.06 0.45 0.19 0.2 0.1];
ENG = [0.15 0.35 0.05 0.4 0.05];
%Finding the difference between the sample and the reference
japdiff = abs(count'-JAP);
spadiff = abs(count'-SPA);
engdiff = abs(count'-ENG);
%Put the sum of the differences into a vector
diff = [sum(japdiff), sum(spadiff), sum(engdiff)];
%Find the index and magnitude of the minimum difference
[Y,I] = min(diff);
%Check and output which language has the lowest absolute difference
if I == 1
answer = 'Japanese';
elseif I == 2
answer = 'Spanish';
else
answer = 'English';
end
```

4.5 Results[5]

4.5.1 Detection

For each language, we prepared five samples for detection. In essence, our code compares the pmfs of the sample with the reference pmfs in our database. The most straightforward method is to subtract the sample PMF vector from the 3 reference PMF vectors in the database and look at the sum of the difference from 5 vowels. The one with the smallest total error will be the output decision of the language.

	Reference PMFs				
	a	E	i	o	u
JAP	0.25	0.35	0.12	0.23	0.05
SPANISH	0.06	0.45	0.19	0.2	0.1
ENGLISH	0.15	0.35	0.5	0.4	0.5

Table 4.1: Reference pmfs compiled from sixty minute samples for each language

[5]This content is available online at <http://cnx.org/content/m33113/1.2/>.

4.5.2 Results

Japanese				
a	e	i	o	u
0.1866	0.4249	0.1593	0.2018	0.0273
0.2592	0.3723	0.1105	0.2020	0.0559
0.2606	0.3092	0.1238	0.2427	0.0635
0.2412	0.3496	0.1344	0.2092	0.0656
0.0816	0.3754	0.0727	0.3071	0.1632

Table 4.2: Pmfs generated from five five-minute Japanese samples

Spanish				
a	e	i	o	u
0.1008	0.4258	0.2145	0.1398	0.1192
0.0396	0.4578	0.1887	0.2559	0.0580
0.0506	0.454	0.1902	0.1979	0.1074
0.0682	0.4763	0.1630	0.2187	0.0738
0.0608	0.4053	0.2055	0.1929	0.1355

Table 4.3: Pmfs generated from five five-minute Spanish samples

English				
a	e	i	o	U
0.1580	0.3553	0.0769	0.3764	0.0335
0.1830	0.2468	0.1450	0.3021	0.1231
0.1798	0.4568	0.1023	0.2029	0.0582
0.1013	0.5023	0.0803	0.2587	0.0287
0.1670	0.3897	0.0598	0.3667	0.0168

Table 4.4: Pmfs generated from five five-minute English samples

Detection Results					
	Sample1	Sample2	Sample3	Sample4	Sample5
Japanese	Japanese	Japanese	Japanese	Japanese	English
Spanish	Spanish	Spanish	Spanish	Spanish	Spanish
English	English	Japanese	Japanese	Spanish	English

Table 4.5: Detection results of the five samples of each language

4.6 Conclusions[6]

4.6.1 Conclusions

After generating the PMFs from samples of each language, we notice that, for Japanese, the probability of the "u" sound is comparatively smaller than the other vowel sounds. This supports the fact that "u" sound is actually quite uncommon in the Japanese language. In addition, from our generated pmfs, it appears that detection for Japanese is fairly consistent, with only one sample missed. For Spanish, each of the five samples was detected correctly. However, for English, only two of the five samples were detected correctly. This result may suggest that English has greater variability in its vowel sounds than Spanish and Japanese. Therefore, five-minute samples are not enough for proper detection.

We conclude that our approach is inadequate for proper language detection. First, the PMFs of vowel sounds for different languages do not vary as much as we initially thought. Therefore, languages of similar origins (e.g. romantic languages) are difficult to differentiate apart. Second, our approach is extremely sample-size dependent, because it relies on the sample PMF to converge to the reference PMF. By the law of large numbers, our approach would only work with large sample sizes. In addition, there is no guarantee that our reference PMF is the expected PMF of the language. We compiled our reference PMF from sixty total minutes of samples, but the actual expected PMF may require much larger samples. Third, our method is quite tedious. Our samples require significant signal processing before it can be used in our system, including down-sampling, amplification, and noise removal. Also, each person speaks at different formant frequencies. Therefore, the vowel sound recognition system needs to be synced to each speaker. In conclusion, our language detection system is functional but severely limited.

4.6.2 Improvements

There's always room for improvement! As mentioned, a larger sample size would greatly improve the accuracy of our system. In addition, since what separate languages are not their vowels but consonants, I believe a consonant sound recognition system in complement with our vowel sound recognition system would drastically improve the applicability of our system. Finally, the detection process, especially the preparation of the speech samples, can be automated to lessen hardship on the tester.

4.6.3 Acknowledgements

We would like to extend our thanks to Professor Richard Baraniuk, Matthew Moravec, Daniel Williamson, and our mentor Stephen Schnelle.

[6] This content is available online at <http://cnx.org/content/m33127/1.3/>.

Chapter 5

A Flag Semaphore Computer Vision System

5.1 A Flag Semaphore Computer Vision System: Introduction[1]

5.1.1 A Flag Semaphore Recognition System

We seek to implement a computer vision system for classifying and interpreting flag semaphore systems, as recorded by something as simple and commonplace as a webcam. The classification is implemented in a MATLAB script that, taking an input video file in wmv format, produces a string of the message in semaphore in the video. This can optionally produce a marked-up video, showing the semaphores as they are recognized, overlaid with the video. Note that this can process video files faster than they can be played, and could be implemented in realtime with parallel capture methods.

We also seek to implement a related Internet Engineering Task Force protocol documented in `RFC 4824`. This documents transmitting IP datagrams over a link layer implemented in flag semaphore. We seek to bridge this link layer and a more standard Ethernet connection.

5.1.1.1 A Maritime Signaling System

Flag semaphore is a perhaps-archaic system for transmitting signals through a line of sight connections with different positions of colored flags. With one flag in each arm, and eight possible positions for each flag, there are 28 possible static signals with distinct positions for each flag, with an additional "attention" dynamic signal, and space, denoted with both flags down.

The traditional naval semaphore flags, as used in the system we have implemented are square, are square and are divided into two large red and yellow triangles across the diagonal. Because the flags are not rigid, they deform, making traditional matched filtering difficult, but the colorful design of the flags is helpful, because it allows us to use color tracking to determine the flags' positons.

[1] This content is available online at <http://cnx.org/content/m33092/1.2/>.

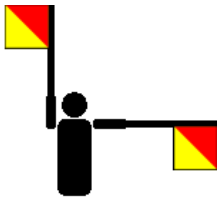

Figure 5.1: A diagram of signal "J" (courtesy of Wikipedia). This symbol is always used to begin transmission.

5.2 A Flag Semaphore Computer Vision System: Program Flow[2]

5.2.1 Program Computational Flow

This section describes the processes that the flag semaphore computer vision system we implemented undergoes in order to process input signals an produce output, separating the description into sections about the input, classification, and ouput. Refer to the flow chart in Figure 5.2 for an illustration and concise description.

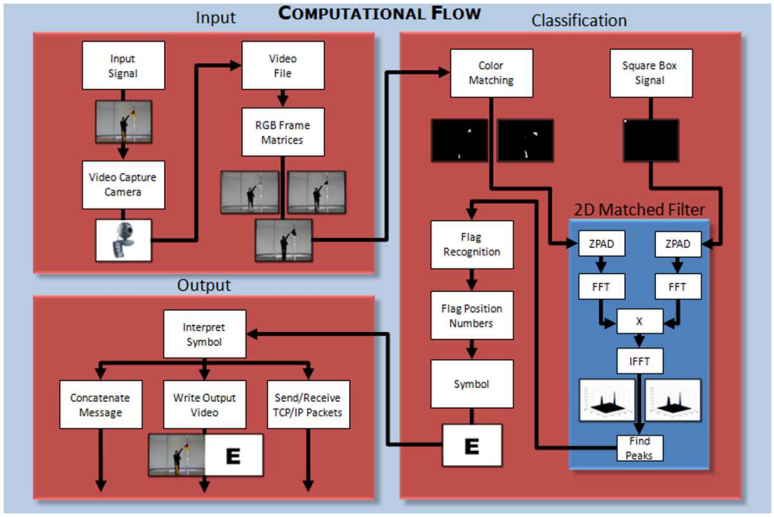

Figure 5.2: This flow chart illustrates the processes involved in the flag semaphore computer vision system from input signal to various outputs.

[2]This content is available online at <http://cnx.org/content/m33095/1.2/>.

5.2.2 Input

The flag semaphore computer vision and interpretation system we developed takes a prerecorded video file as input to a MATLAB function. The video signal should be produced with two semaphore signaling flags of the red and yellow triangle type. For best performance, the signaler should be near the center of the video frame images and as close to the camera as possible while ensureing that the vertical and horizontal signaling range fits within the images. The signaler may either signal facing the camera or signal facing away from the camera, and the proper adjustment will automatically be made by the program. Also, The upward direction of the camera must correspond to the upward direction of the signaler.

All signals should be formed through rapid motion to the desired flag positions. A signal is only guaranteed to register if it is held in place for at least the specified hold time (which defaults to 1 second). However, the framerate of the video file and the rate at which a person can signal limit the signaling rates compatible with this program to reasonable values. Increasing the hold time increases the accuracy of the output. Repeated characters should be formed by signaling a space between them. Please note that the "chip-chop" attention signal is not supported at this time. (It is an error in the RFC 4824 protocol.) Every signal must begin with the alphabetic character (J) on the first frame, which is used to determine the direction the signaler is facing and the pixel position of the signaler. This first character will not be displayed.

The video file itself should be in a wmv format, although other file types compatible with mmread may also function correctly. The file should be placed in the same directory as this file (FlagSemaphore.m) and the file name should be passed to the function in a string as the first arguement.

The second arguement, which is optional, supplies the desired time, in seconds, for which a signal must be held in order to be guarenteed to register. Increasing this parameter decreases the likelihood that a slow transition between two signals will be incorrectly registered as a signal, but decreases the best possible signaling rate. Thus, signal transitions should be fast and abrupt for this reason. The default hold time is one second.

5.2.3 Classification

The flag semaphore computer vision and interpretation system we developed, after extracting half of the hold time blocks of input video data as RGB matrices, classifies the signal as a flag semaphore symbol and then produces several forms of output. Because of the objects of interest in the image are two bright red and yellow flags, the classification problem suggests color tracking as a promising approach.

Hence, our classifier begins by performing color matching with the RGB matrix data of each frame in the half of the hold time interval in order to find the red regions and yellow regions in the image. Color matching is a somewhat difficult problem since the RGB regions corresponding to a given color are, in general, not convex and difficult to describe algorithmically. However, our rudimentary color matching algorithm was always sufficient to highlight the flag regions.

Because there are multiple flags in the image and there could be similarly colored objects nearby, we use a 2D matched filter with a small square box as the filtering signal implemented in the frequency domain for speed in order to discriminate between objects of the same color. A simple peak finding algorithm then finds the pixel locations of the red objects and the pixel locations of the red objects. Since our flags are red and yellow, we search for red objects near yellow objects and identify those as flags, with special case handling so that the cases in which less than two red objects or less than two yellow objects are found may still be correctly identified using saved data from the previous flag locations. This produces results that are highly resistant to noise contamination unless the noisy objects are colored with large patches of both red and yellow.

Each of the flag positions are then placed in one of eight angular regions about an estimate of the center of the signaler corresponding to the eight flag positions used to form flag semaphore signals. If the flags remain in the same angular region for the vast majority of the frames considered, the flags are not in motion and a symbol is registered according to which angular regions contain the flags. Otherwise, the flags are taken to be in transition. Thereafter, the output symbol is interpreted in the context of the sequence of previous symbols to produce a character or to toggle between letters and numbers.

5.2.4 Output

Several other inputs can optionally be supplied to specify other options. The print flag is the second argument and determines whether the interpreted message will be displayed on the MATLAB prompt. The third argument is the play flag which specifies whether the video will be played in a MATLAB figure window. The fourth argument is the transceiver flag which determines whether the program will attempt to send and receive TCP/IP packets (currently ignored). The final two arguments determine whether an output video file will be produced and specify the name of the output file. For information on how to form packets of TCP/IP data, refer to the RFC 4824 documentation[3] .

For example, the following would store a the message interpreted from the video file example1.wmv into the string message1 without printing to the MATLAB prompt, playing the video file, attempting to transmit and recieve packets, or writing an output video file.

```
message1=FlagSemaphore('example1.wmv');
```

This, on the other hand, would store a the message interpreted from the video file example2.wmv into the string message2 while printing to the MATLAB prompt but not playing the video file, attempting to transmit and recieve packets, or writing an output video file.

```
message2=FlagSemaphore('example2.wmv',1,1,0,0,0,'');
```

This, example would store a the message interpreted from the video file example3.wmv into the string message3 while playing the video file but not printing to the MATLAB prompt, attempting to transmit and recieve packets, or writing an output video file.

```
message3=FlagSemaphore('example3.wmv',1,0,1,0,0,'');
```

This, example would store a the message interpreted from the video file example4.wmv into the string message4 while attempting to transmit and recieve packets but not playing the video file, printing to the MATLAB prompt, or writing an output video file. Note that this option is not yet implemented and will be ignored.

```
message4=FlagSemaphore('example4.wmv',1,0,0,1,0,'');
```

This, example would store a the message interpreted from the video file example5.wmv into the string message5 while writing an output video file but not playing the video file, printing to the MATLAB prompt, or attempting to transmit and receive packets.

```
message5=FlagSemaphore('example5.wmv',1,0,0,0,1,'exampleoutput5.wmv');
```

Some example flag semaphore signal input video files and output video files can be found in the demonstrations section. Links to the full source code can be found in the additional resources section.

5.3 A Flag Semaphore Computer Vision System: Program Assessment[4]

5.3.1 Program Approach Advantages

The approach taken to the implementation of our flag semaphore computer vision classification and interpretation system described in the program flow module provides several important benefits.

Due to the use of the Fast Fourier Transform to implement the matched filter in the frequency domain, the program runs sufficiently fast that it could be used for real time video processing with the aid of additional parallel video capture software, such as that which can be found in the MATLAB Data Acquisition

[3] http://tools.ietf.org/html/rfc4824

[4] This content is available online at <http://cnx.org/content/m33098/1.2/>.

Toolbox. When additional speed is desired, we note that the program remains highly accurate, even with a downsampling factor of three in both spacial dimensions.

Furthermore, the program demonstrates robustness when presented data contaminated with noise in the form of extraneous red or yellow objects as a result of the use of both the red and yellow region data when attempting to identify the flags. Detailed special case handling prevents video frames in which one or more complete color region of a flag is occluded from ruining the color tracking.

Although it is difficult to get a good estimate of the accuracy of the classifier, limited testing, which can be seen on the demonstrations page, suggests that the results are quite accurate. Additionally, the program provides for variable accuracy by increasing or decreasing the signal hold time parameter This boosts accuracy by reducing the likelihood that a transition between symbols will be classified as a symbol but decreases the maximum possible signaling rate due to increased required pause time at each symbol. Hence this option represents a tradeoff, the optimal value of which will be different for different signalers.

5.3.2 Program Approach Disadvantages

Although sufficiently effective for the test videos, the color matching and peak detection algorithms used are not perfect. A full treatment of color matching would be somewhat difficult as RGB regions corresponding to a given color are, in general, not convex and thus difficult to describe. The solutions used are ad hoc solutions that we developed for the problems of color matching and peak detection, so there likely exist superior algorithms to perform those tasks.

Also, the program models the signaler arms as rotating about a single point, but there is width between human shoulders. While this problem was effectively overcome with empirical adjustment of the size of the angular regions by observation of signaler habits, it remains a weakness of the model.

Occasionally incorrect signaling due to signaler error makes it difficult to get a good estimate of the accuracy of the classifier, but the program works well for some hold time for every test signal video recorded.

5.4 A Flag Semaphore Computer Vision System: Demonstration[5]

5.4.1 Example Video Input and Output

In the testing of the recognition system, several basic signals were recorded. These tested things like recognizing the position of the sender from the first semaphore "J". This is essential to properly recognize all eight positions of the flags, each of which occurs in our test signals. We also test the letters to numbers state transition.

Example 5.1

Example Input Video: ELEC 301

This media object is a Flash object. Please view or download it at
<http://www.youtube.com/v/uU3_7cNT_7U&hl=en_US&fs=1&>

Figure 5.3: A sample signal that spells out the course number ELEC 301, which includes both letters and numbers.

[5]This content is available online at <http://cnx.org/content/m33100/1.2/>.

Example Output Video: ELEC 301

This media object is a Flash object. Please view or download it at
<http://www.youtube.com/v/5EeiXKrKwC8&hl=en_US&fs=1&>

Figure 5.4: The output of the the filter for the signal "ELEC 301 " above. Notice the blank output for the control codes for letters (the first) and numbers. This file is output directly from the MATLAB code.

Example 5.2

Example Input Video: ABCDEFG

This media object is a Flash object. Please view or download it at
<http://www.youtube.com/v/IbJ2fDOtUVs&hl=en_US&fs=1&>

Figure 5.5: A simple alphabetic test case of the flag semaphore recognition system. Note some of the patterns formed in the standard semaphore alphabet.

Example Output Video: ABCDEFG

This media object is a Flash object. Please view or download it at
<http://www.youtube.com/v/EC-3Ql_983c&hl=en_US&fs=1&>

Figure 5.6: The output of the recognition system for the signal "ABCDEFG". Note that the system correctly differentiates between the signals, even when little motion is involved.

Example 5.3

Example Input Video: WRC

This media object is a Flash object. Please view or download it at
<http://www.youtube.com/v/KgqXqYYVEpI&hl=en_US&fs=1&>

Figure 5.7: A short test signal "WRC". This was our first test case, and performs well.

Example Output Video: WRC

This media object is a Flash object. Please view or download it at
<http://www.youtube.com/v/LB4jJqiV0-A&hl=en_US&fs=1&>

Figure 5.8: The system correctly handles this three-letter signal.

5.5 A Flag Semaphore Computer Vision System: TCP/IP[6]

5.5.1 A Link-Level Layer for IP Transmissions

The idea of using flag semaphore to transmit Internet Protocol packets is suggested in `RFC 4824`[4]. This presents a link-layer protocol, suitable for encapsulating and transmitting IP packets, analogous to the Ethernet protocol frequently used for wire transmissions between machines, described by `RFC 894`[5] and other Internet Engineering Task Force (ITEF) standards.

This protocol was presented as a Request For Comments on April first, 2007. To our knowledge, no working implementation of this protocol has been implemented, although several errata in the original publication have been identified. A similar protocol, `RFC 1149`, which transfers IP datagrams over avian carriers, was successfully tested in 2001 by a Linux User Group in Bergen, Norway[8], more than ten years after the original specification was published.

Having implemented a flag semaphore recognition system, it seems reasonable to attempt to use it to implement the protocol described in `RFC 4824`. It even seems reasonable to attempt to write a IP-SFS to Ethernet bridge, but technical limitations prevented the completion of the bridge functionality. A complete receiver and transmitter framework exists, although the handling of states is incomplete.

5.5.1.1 IP-SFS Channel Design in Summary

The suggested channel protocol uses 25 of the alphabetic symbols in the standard semaphore alphabet. The first 16 characters are reserved for data transmission, and the remaining 9 are used for channel control codes.

The interface is half-duplex, in that an interface may be either idle, transmitting, or receiving. The idle state is characterized by occasional `KAL` keep-alive signals, and either interface can initiate a state change from idle to transmitting by sending a `RTT` signal.

5.5.1.2 Decoding IP-SFS Packets

In an incoming IP-SFS character stream, as with the one created by our MATLAB interface. We can use an internal state machine, which encodes frames as strings between `FST` and `FEN` signals, with characters deleted by the appropriate `FUN` or `SUN` undo signals. Note that this reception is received asynchronously, in a separate instance if `IpSfssRx`, so that decoding bottlenecks will not affect our semaphore receiver.

Once an entire packet is received, and control signals are stripped out, it is possible to condense our semaphore sequence to a byte array, as each signal represents a 4-bit *nibble*. A small amount of byte manipulation shifts each pair of semaphores into a single byte. Note that the number of semaphores received must be even.

The first two and last two bytes of each IP-SFS frame are header and footer data – the header defines one of five possible encapsulated protocols with support for compressed or uncompressed IPv4 or IPv6, and

[6] This content is available online at <http://cnx.org/content/m33094/1.2/>.

an optional cyclic redundancy check method – CRC CCITT 16, a standard polynomial redundancy check that is easy to implement. The last two bytes of the frame are the checksum of the frame so far.

The `IpSfssFrame` class can be constructed using a string – such a sequence of data semaphores. This will throw an exception in case of error, or create an instance of the frame. Errors are thrown for format violations or CRC failures. The object allows us to return the encapsulated packet as a byte array.

5.5.1.3 Sending IP-SFS Packets

The system also supports the propagation of IP datagrams. An `IpSfssFrame` can also be instantiated with a raw IP packet with any of the standard options, including compression and verifying checksums.

An asynchronous transmitter, `IpSfssTx`, can be instantiated. Running this in a separate thread allows semaphores to be queued, without the function blocking for completion. This is especially important because there is a (configurable) minimum display time for each signal. A Swing-based GUI can display these signals on the screen.

5.5.1.4 IP-SFS to Ethernet Bridge

The original goal was to produce an IP-SFS to Ethernet bridge, such that IP packets transmitted as the payload of SFS frames could be placed onto the outgoing queue of a running machine with a network connection.

Such "raw sockets" does not natively exist on Windows, although the WinPcap project offers link-layer access. The link-layer access, however, requires proper Ethernet headers on outgoing packets, which could likely be fabricated with additional time spent on the project.

The Java `libpcap` interface also offers methods to dump incoming packets to a file. This makes network sniffing possible, but does not allow packets to be read in real time.

5.5.1.5 Future Expansion

Because of time and scope constraints, the IP-SFS to Ethernet bridge was not satisfactorily completed. In the future, expanding this to full functionality would be quite an interesting project.

It should also be noted that much of the `IpSfssFrame` functionality was written in haste, and while it was tested on reasonable cases, more automated unit testing on this and other classes in the Java IP-SFS framework would be ideal.

The internal state of the transceiver is also partially incomplete. It does not respect the state (transmitting, receiving, idle), of the connection, nor does it acknowledge packet receptions with `ACK` signals (or `NAK` on errors), because the receiver and transmitter are not sufficiently connected.

5.6 A Flag Semaphore Computer Vision System: Future Work[7]

5.6.1 Real Time Video Processing

The flag semaphore computer vision and interpretation program that our group has a reasonably fast runtime due to the use of a matched filter implemented in the frequency domain and the accuracy of the program under spatial downsampling. In fact, the program runs in considerably less time than the duration of input video file provided that the program is not also attempting to write an output video file, clocking approximately 15 seconds for an approximately 20 second video. Consequently, this video processing could be performed in real time with the aid of video capture software operating in parallel, such as is provided in the MATLAB Data Acquisition Toolbox. However, due to a lack of funds, this was not implemented and left as a possible future addition that would require very little modification to our existing code.

[7] This content is available online at <http://cnx.org/content/m33103/1.2/>.

5.6.2 Identification of all Symbols

While we could successfully identify all of the static symbols in the flag semaphore symbol set, we left the "chip-chop" attention symbol unidentified as it is not used under the RFC 4828 TCP/IP standard and its exclusion greatly simplified the code. However, any future modifications may wish to support its identification for completeness.

5.6.3 TCP/IP Transceiver Implementation

Because of time and scope constraints, the IP-SFS to Ethernet bridge was not satisfactorily completed. In the future, expanding this to full functionality would be quite an interesting project. It should also be noted that much of the `IpSfssFrame` functionality was written in haste, and while it was tested on reasonable cases, more automated unit testing on this and other classes in the Java IP-SFS framework would be ideal. The internal state of the transceiver is also partially incomplete. It does not respect the state (transmitting, receiving, idle), of the connection, nor does it acknowledge packet receptions with `ACK` signals (or `NAK` on errors), because the receiver and transmitter are not sufficiently connected.

5.6.4 Miscellaneous

Other possible future expansions and modifications of our program could include improvements in the color matching and peak detection algorithms used to determine the positions of the flags. Although the current versions function correctly with a high degree of accuracy, they are ad hoc solutions that we developed to the problems of color matching and peak detection, so there may exist superior algorithms to perform those tasks. Further optimization of code for improved speed performance is desirable in order to perform both real time processing and real time video output writing to make the program more useful even if it is impractical.

5.7 A Flag Semaphore Computer Vision System: Acknowledgements[8]

5.7.1 Acknowledgements

The authors would now like to acknowledge some of the other people who have contributed to the success of this project. First, we thank Chinmay Hegde and Dr. Rich Baraniuk for mentoring our project group and instructing our ELEC 301 class, respectively. We also appreciate Dr. Alan Cox for providing us with information on the use of raw TCP sockets. Finally, we send our thanks to Micah Richert who published a program enabling our old version of MATLAB to read and write from wmv files and to the jNetPcap and WinPcap developers for their efforts.

5.8 A Flag Semaphore Computer Vision System: Additional Resources[9]

5.8.1 Semaphore Related Resources

- A section[10] of the 1913 Royal Navy Handbook of Signaling is available from the World War I Document Archive.[11]
- RFC 4824[12] documents sending IP datagrams over flag semaphore.

[8] This content is available online at <http://cnx.org/content/m33106/1.2/>.
[9] This content is available online at <http://cnx.org/content/m33107/1.2/>.
[10] http://www.gwpda.org/naval/s0900000.htm
[11] http://gwpda.org/
[12] http://tools.ietf.org/html/rfc4824

5.8.2 Project Resources

- The SourceForge[13] project page for our project is available: A Flag Semaphore Computer Vision System.[14]
- The videos[15] for the project are available on YouTube.

5.9 A Flag Semaphore Computer Vision System: Conclusions[16]

5.9.1 Conclusions

Over the course of the past month, our project group successfully implemented a computer vision system for the interpretation of flag semaphore signals. The approach taken has yielded accurate results that are robust under noise contamination and can withstand substantial spacial downsampling. However, weaknesses in color matching and peak detection along with several missing desirable features leaves room for future improvement. Notably, the program would be capable of processing video input in real time with the aid of parallel video capture software with few additional changes to the code. Also, significant progress toward fully implementing a TCP/IP packet transceiver using the RFC 4824 standard was made. Our limited testing results suggest that the program yields results that are of reasonably high accuracy, with a tradeoff between accuracy and signaling rate. Hence, we conclude with the primary demonstration of our projects success in the output video below that signals the class name "ELEC 301".

Example Output Video: ELEC 301

This media object is a Flash object. Please view or download it at
<http://www.youtube.com/v/5EeiXKrKwC8&hl=en_US&fs=1&>

Figure 5.9: The output of the the filter for the signal "ELEC 301 " above. Notice the blank output for the control codes for letters (the first) and numbers. This file is output directly from the MATLAB code.

[13] http://sf.net
[14] http://sourceforge.net/projects/flagsemaphore/
[15] http://www.youtube.com/user/smkruzick
[16] This content is available online at <http://cnx.org/content/m33109/1.2/>.

Chapter 6

License Plate Extraction

6.1 Prelude[1]

6.1.1 Purpose

To develop an algorithm for extraction of license plate numbers from still photos of stationary cars.

6.1.2 Methods

We divided this project into two sections- Image Processing and Support Vector Machine (SVM) Training:

- We take picture of a still car (from either front or back), compress and crop out to speed up the process, localize the plate position and extract the letters into individual binary matrices.
- We take each of the matrix generated in the previous process and use the SVM algorithm to distinguish which letter exactly it is.

6.1.3 Applications

This algorithm can be integrated to the related vehicle identification applications such as:

1. Parking lot registration
2. Traffic violation tracking
3. Vehicle surveillance

6.2 Image Processing - License Plate Localization and Letters Extraction[2]

The general method we used for extracting the license plate letters out of a picture was:

[1] This content is available online at <http://cnx.org/content/m33154/1.2/>.
[2] This content is available online at <http://cnx.org/content/m33156/1.2/>.

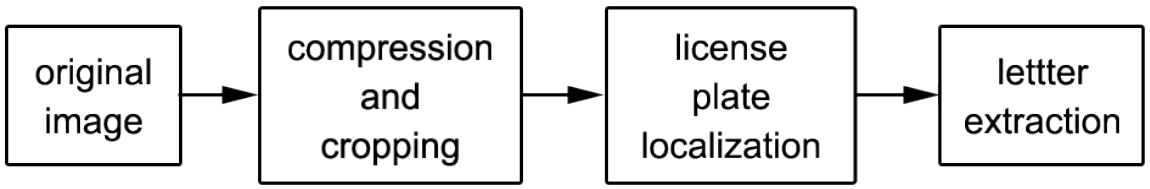

Figure 6.1: Overall method for finding license plate letters/numbers.

1. **Compression and Cropping:** decreases the size of the photo and and blacks out areas that definitely do not contain license plate.
2. **License Plate Localization:** determines the location of the plate in the photo
3. **Letter Extraction:** searches within the plate for the plate letters/numbers and copies them out of the photo.

Following is an explanation of the individual sections. Included are also images showing the effects of each section on the following picture:

Figure 6.2: Original image.

6.2.1 Compression and Cropping

In order to decrease image processing time, we first compress all pictures to a standard size and black out all areas that are definitely not license plates. The size we chose was 640px by 480px, the smallest size at which we could still reasonably read the license plates.

To determine which areas were definitely not license plates, we realized that the typical Texas plate contained red, blue, and white as major colors. Therefore, we focused on these two colors, making our cropping algorithm:

1. Separate the JPEG picture into its three layers of red, green, and blue.
2. Consider the area around a blue pixel, and black it out if the density of red is lower than a certain threshold value.

Figure 6.3: Compressed and cropped image (Note the black areas around the right and bottom of the photo).

6.2.2 License Plate Localization

Once we determined which areas possibly contained license plates, we looked in those areas for the plates themselves. We determined that most plates contain dark letters on light backgrounds and so looked for areas of high contrast.

Our final algorithm looked as follows:

1. Turn the cropped photo into black-and-white for easier differentiation between dark and light spots.
2. Filter the image to remove noise (single-pixel white spots).
3. Locate the license plate position by scanning the photo vertically. We expect a row running through the license plate row to have a maximum number of individual dark spots, or "clusters." Therefore, we find and store the two rows in the image with that contain the most clusters.
4. To find the horizontal position of the plate, scan the picture horizontally by moving a square window from left to right and counting the number of clusters inside. The final position of the license plate is square that contains the greatest number of clusters. If any two squares contain the same number of clusters, the two are merged together.

Figure 6.4: Close-up of the license plate as determined by the algorithm.

6.2.3 Letter Extraction

To find the letters on a license plate, we first determined some identifying characteristics:

1. Usually, and always on Texas plates, the letters of the plate are dark on a light background.
2. The letters are uniform in height
3. The letters all occur in approximately the same area.
4. There are usually between 3 and 7 letters on a plate.

These characteristics give us the form for our letter extracting algorithm.

1. From the plate-locating algorithm, we have a small 200px by 200px image that contains the car's license plate.
2. We convert the image into grayscale for easier processing.
3. We locate all the dark (low intensity) spots in the picture that are surrounded by light (high intensity) spots. We determine the separation between these dark spots and give each individual spot a label.
4. Compare the sizes of the spots and look for about six that have the same height. These six spots are the letters on the plate.
5. Save the pixels that make up the letters into their individual matrices.

We tried this algorithm and found that it worked for all images for which the plate-locating algorithm returned an image containing the entire plate.

Figure 6.5: Letters extracted from the photo.

6.3 SVM Train[3]

6.3.1 The Math and Algorithm

For digit recognition, we use Support Vector Machine (SVM) as a learning machine to perform multi-class classification.

The way SVM works is to map vectors into an N-dimensional space and use an (N-1)-dimensional hyperplane as a decision plane to classify data. The task of SVM modeling is to find the optimal hyperplane that separates different class membership.

Example 6.1
Let's take a look at a simple schematic example where every object either belongs to GREEN or RED.

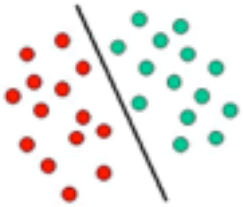

Figure 6.6: Picture from: Chih-Chung Chang and Chih-Jen Lin, LIBSVM : a library for support vector machines, 2001.

SVM finds the line defining the boundary between the two types. Then, it can classify a new object by looking at on which side of the line it falls.

However, it is unlikely that we can always have a linear dividing boundary. Rather than fitting nonlinear curves to the data, we can map each object into a different space via a kernel function where a linear dividing hyperplane is feasible.

[3]This content is available online at <http://cnx.org/content/m33159/1.2/>.

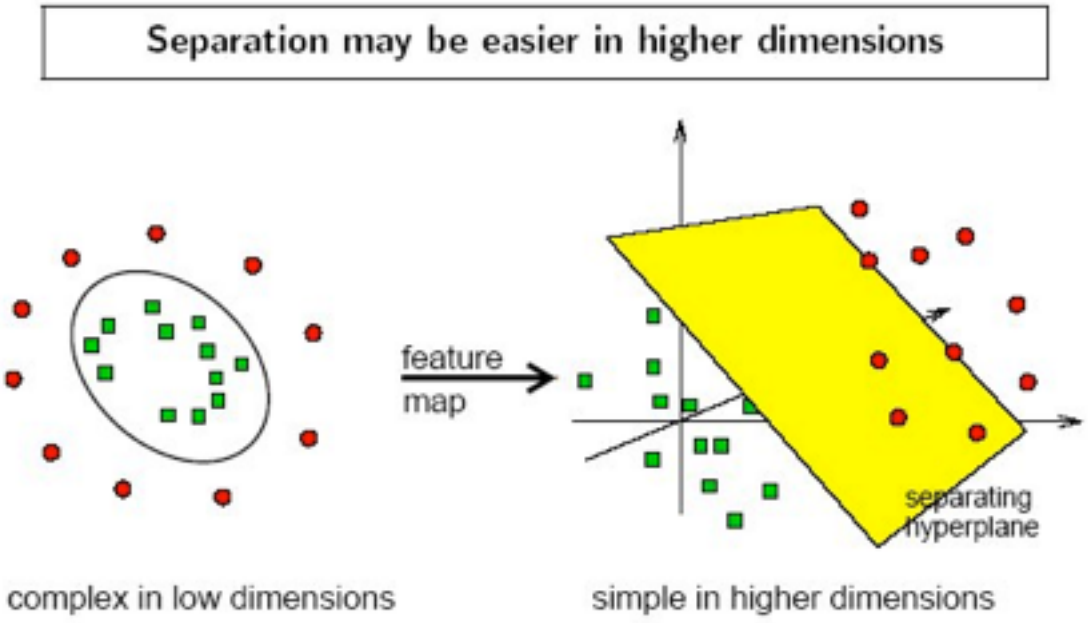

Figure 6.7: Hyperplane classifying the two cases (Picture from: Chih-Chung Chang and Chih-Jen Lin, LIBSVM : a library for support vector machines, 2001.)

The concept of the kernel mapping function is so powerful that SVM can perform separation with very complex boundaries. The kernel function we use in this project is radial basis function (RBF).

6.3.1.1 SVM Working Principles

- Vectorize each instance into an array of features (attributes).
- Model with training data to find optimal dividing hyperplane with maximal margin.
- Use SVM to map all the objects into a different space via a kernel function (see Figure 3 for examples).
- Classify new object according to its position with respect to hyperplane.
- Errors in training are allowed while the goal of training is to maximize the margin and minimize errors. Namely, find the solution to optimization problem in Figure 4, where x is the attribute, y is the object label, ξ is the error and ϕ is the mapping function.

- linear: $K(\mathbf{x}_i, \mathbf{x}_j) = \mathbf{x}_i^T \mathbf{x}_j$.
- polynomial: $K(\mathbf{x}_i, \mathbf{x}_j) = (\gamma \mathbf{x}_i{}^T \mathbf{x}_j + r)^d$, $\gamma > 0$.
- radial basis function (RBF): $K(\mathbf{x}_i, \mathbf{x}_j) = \exp(-\gamma \|\mathbf{x}_i - \mathbf{x}_j\|^2)$, $\gamma > 0$.
- sigmoid: $K(\mathbf{x}_i, \mathbf{x}_j) = \tanh(\gamma \mathbf{x}_i{}^T \mathbf{x}_j + r)$.

Figure 6.8: A few examples on the kernel functions; for our case we choose the radial basis function (RBF)

$$\begin{aligned} \min_{\mathbf{w},b,\boldsymbol{\xi}} \quad & \frac{1}{2}\mathbf{w}^T\mathbf{w} + C\sum_{i=1}^{l}\xi_i \\ \text{subject to} \quad & y_i(\mathbf{w}^T\phi(\mathbf{x}_i) + b) \geq 1 - \xi_i, \\ & \xi_i \geq 0. \end{aligned}$$

Figure 6.9: Find a hyperplane with the maximized margin space to split the two classes. (Equation from: Chih-Chung Chang and Chih-Jen Lin, LIBSVM : a library for support vector machines, 2001.)

6.3.2 Methods and Running Routines

1. Collect the matrices obtained from the Image Processing section and label each of the instances.
2. Select a reasonable amount as the training set, and the rest as the testing set, with a balanced choice for each of the instances.
3. Feed the training set into the SVM-train process to generate a model. This calculation takes time, but it only needs to be done once.
4. Now we're ready to make predictions to a given license plate! An input of labeled data will give us the accuracy of this algorithm; an unlabeled instance can also be fed in to see the prediction.

NOTE: The SVM library we used is available at: http://www.csie.ntu.edu.tw/∼cjlin/libsvm

6.4 Conclusions[4]

6.4.1 Results

We were able to successfully locate the license plate in about 70% of our sample pictures, and of the characters we extracted, we were able to recognize them with about 72.7% accuracy (619 sets of training data).

6.4.2 Future Improvements

6.4.2.1 Compression and Cropping

Since we were targeting Texas plates, which only have red, blue, and white colors, we were able to black out many parts of the images by wiping out all green regions. In the future, however, we would like to be able to recognize plates not from Texas that might have green components. Therefore, we should find a criteria for finding the plates other than color.

6.4.2.2 Letter Recognition

Acquiring State Pattern and Convention Attributes
In many license plates, it is difficult to tell the difference between a zero and an O, even for a human. Therefore, for the purposes of this project, zeros and Os were considered the same. However, in many states, it is actually possible to tell the difference because the license plate has a set pattern (e.g., 2 letters, 2 numbers, 2 letters). In the future, we could identify what state the plate comes from and then make use of this knowledge to get more accuracy in letter recognition.
Multi-class Support Vector Machine
In addition, one of the characteristics of SVM is that is solves a two-class problem. In order to get around this, for our project, we used a one-against-the-rest approach. This meant that we basically used the SVM machine to answer the question, "Is this a __?" 35 (A-Z, 1-9) times for each unknown letter/digit. In the future, we will want to look at more efficient and accurate methods. One of the possible improvement can be found in the work by T.-K. Huang, R. C. Weng, and C.-J. Lin. Generalized Bradley-Terry Models and Multi-class Probability Estimates. Journal of Machine Learning Research[5]
Automated Training Set Generation and Extraction Efficiency
Finally, currently, any digit that we feed into the SVM will register as something; we have no way of telling whether the image is in fact a letter/digit. In the future, we would like to train the machine to be able to tell characters from non-characters. This will allow less rigorous (and time-consuming) computation in the image-processing section and give our algorithm greater flexibility.

6.4.3 References

Chih-Chung Chang and Chih-Jen Lin, LIBSVM : a library for support vector machines, 2001. Software available at http://www.csie.ntu.edu.tw/∼cjlin/libsvm[6]

6.4.4 Special Thanks

Thanks to:

- Dr. Aswin Sankaranarayanan, our mentor
- Dr. Richard Baraniuk, the ELEC 301 instructor
- Dr. Fatih Porikli (MERL), for providing us with a license plate dataset
- Drew Bryant and Brian Bue for technical advising

[4] This content is available online at <http://cnx.org/content/m33160/1.3/>.
[5] http://www.csie.ntu.edu.tw/∼cjlin/libsvmtools/#9
[6] http://www.csie.ntu.edu.tw/∼cjlin/libsvm

Chapter 7

An evaluation of several ECG analysis Algorithms for a low-cost portable ECG detector

7.1 Introduction[1]

Introduction

Measuring vital signs is a crucial part of health care in hospitals across the world. However, these systems are often extremely expensive, and can often only be given to patients already in intensive care. Upon entering the Emergency ward, however, a patient often needs to wait before receiving direct medical attention, since it is important for health care professionals to prioritize to whom they direct attention. If a low-cost system of constant monitoring of vital signs existed, the emergency wards could potentially provide simple vital sign monitoring for every patient that entered the hospital, assisting in resource management and providing better tools with which to evaluate patients [1]. We aim in this module to discuss the basic physiology behind the ECG trace, provide an overview of the primary signal processing methods used to develop a heart rate calculator, and describe a test bed that can be used to test an algorithm, with some demo results. We will end with a discussion on the possibilities these algorithms provide for implementation of a real-time heart rate monitor.

The most important vital sign that can be monitored is the heart rate. Many physiological conditions can be diagnosed by analyzing heart rate abnormality, and abnormal heart rate has been shown to be a leading indicator for heart attack[2]. The primary conditions that are diagnosed are bradycardia and tachycardia. Bradycardia is known as the slowing of the heart rate; for adults, below 60 bpm. Tachycardia is the abnormal quickening of the heart; for adults, above 100 bpm.

Tachycardia has been shown to indicate greater oxygen demand for the heart, and eventually, can lead to a heart attack. More specifically, the case of ventricular tachycardia

is known to be a potentially life-threatening condition that can lead to sudden death if not immediately detected and treated.

Bradycardia also takes on different forms. Sinus bradycardia is a particularly slow heartrate that is associated with heart diseases. It is also possible for sinus bradycardia not to indicate any medical condition whatsoever, such as a patient's good fitness. An alternate form of bradycardia known as Sick sinus syndrome is caused by complications with the sinoatrial node, which naturally monitors the heart. Heart block is the most serious complication, as it can arise suddenly and lead to sudden cardiac arrest or other medical emergency [3].

[1] This content is available online at <http://cnx.org/content/m33167/1.3/>.

The primary action that needs to be taken in order to monitor these potentially life-threatening conditions is to take an ECG (electrocardiogram) recording of the signal. The Electrocardiogram has been extensively researched in the literature, and is relied upon and accepted by many medical professionals as the best way to measure and diagnose abnormal rhythms of the heart. An ECG machine works by measuring the electrical activity of the heart over time using electrodes placed at key places of the body. The electric potential between two electrodes is termed a lead, and averages are taken of different leads around the body to determine the overall electrical activity through different axes of the body. The current gold standard is the 12-lead ECG.

Even though the standard ECG is relied upon as the primary means of diagnosing abnormal rhythms, to actually glean this information off of the reading of the trace paper requires a great deal of training and specialization. Unless the trained specialist is present to continuously evaluate every patient's

ECG recording, in an emergency situation a medical complication may go unnoticed.

7.2 How ECG Signals Are Analyzed[2]

How ECG Signals Are Analyzed :

Methods have been developed to analyze the heart rate automatically, by reading the ECG signal trace and performing certain types of signal processing in order to extract the heart rate information. In analyzing the ECG, the most important parameter to focus on is the QRS complex. The ECG signal is split up in the literature into different waves, each with its own nomenclature.

Figure 7.1

[2]This content is available online at <http://cnx.org/content/m33166/1.2/>.

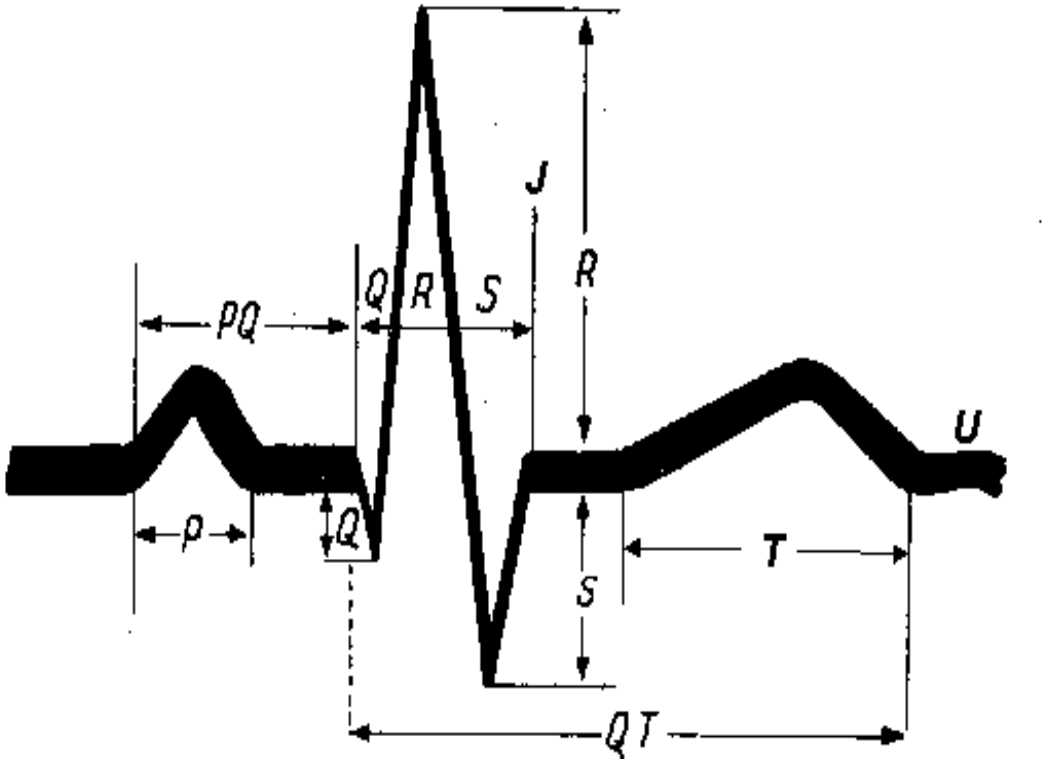

Figure 7.2

The QRS complex stands for the key portion of the ECG wave that involves the depolarization of the right and left ventricles. The QRS complex thus contains the peak of the pulse, and indicates that a heartbeat has occurred.

QRS detection is the most important parameter in the determination of heart rate variability []. Although not every QRS complex contains three separate Q, R and S waves, any conventional combination of these can be considered a QRS complex. However, in order to understand the ECG reading and analyze it, it is necessary to label each part of the complex. Once they are identified, they can be employed to characterize heartbeats.

Once the QRS has been detected, the location of the QRS in time can be annotated as a beat, and a sequence of beat annotation over time can be charted. A heart rate algorithm that takes the sequence of beat annotations, measures the time difference between beats to calculate a heart rate at every moment in time can then analyze this sequence of beat annotations.

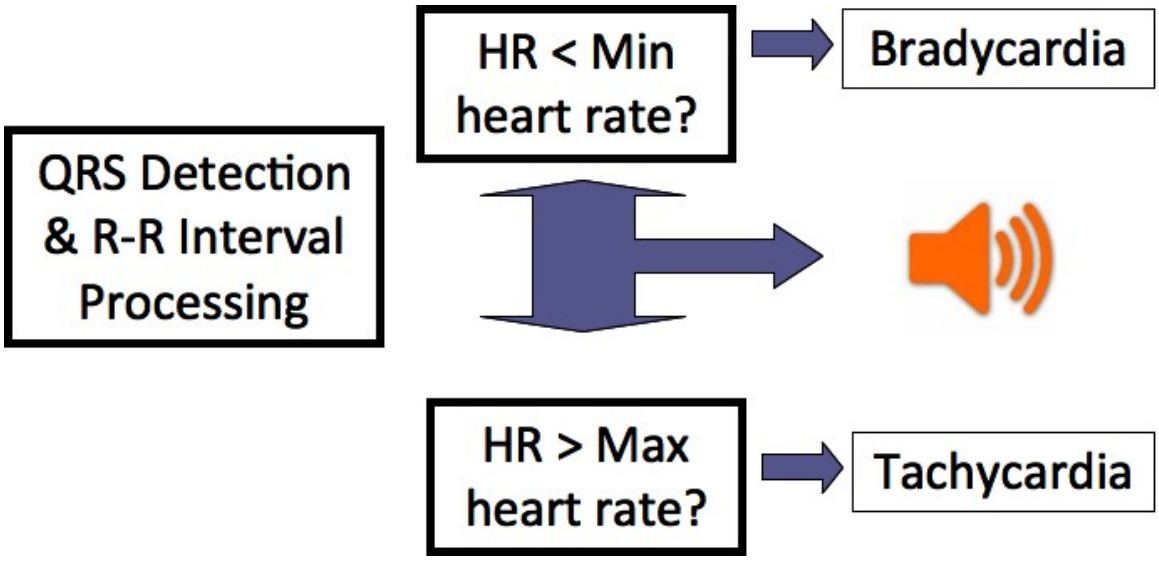

Figure 7.3

Now, with the necessary heart rate information extracted, basic thresholds can be put on a heart rate variability system in order to determine if the patient has exited a normal state. If the heart rate is below 60 bpm or above 100 bpm for a normal adult, an alarm can be raised to alert the medical personnel that the patient requires particular attention.

7.3 Algorithms[3]

There are a range of available algorithms for QRS detection, based on various methods such as peak detection, slope transform analysis, and length transform analysis. Most of these algorithms involve the use of adaptive filters, and others use non-adaptive filters. Adaptive filters are preferred when it comes to heart rate analysis, largely because ECG signals are non-linear. For this reason, it is necessary to periodically analyze the output and modify the filter parameters accordingly.

We aim in this project to give a brief overview of the existing literature and algorithms, and compare the robustness of two leading QRS detection algorithms in accurately detecting heartbeats.

Algorithms for ECG Analysis

There is an extensive library of QRS detection algorithms available in the medical literature, since QRS detectors are the most important signal processing algorithm involved in ECG analysis. We will here analyze three primary algorithm methods: Peak Detections, Slope transform analysis, and length transform analysis.

Particular Peak Detection Algorithm

The peak detection algorithm that we chose to analyze specifically looks at a 160ms window, splits the window into three segments, and finds if the maximum value is contained within the center segment; if so, a beat is annotated. If no beat is detected for longer than 200ms, the threshold is updated using an adaptive filter that functions according to the rate described below:

[3]This content is available online at <http://cnx.org/content/m33164/1.2/>.

$$\frac{last\ beat\ amplitude - current\ peak\ amplitude}{2} \cdot \frac{72}{60}$$

Figure 7.4

We were unable to generate a working peak detection algorithm in order to insert it into the algorithm tester; however, an in-depth review of the literature indicated that it was overall less accurate than the other two algorithms.

SQRS

The slope-detection algorithm that we chose uses a Finite Impulse response filter with the following filter mask:

[1 4 6 4 1 −1 −4 −6 −4 −1];

This filter mask corresponds to the basic shape of a QRS wave. After low-pass filtering to eliminate any remaining noise, this QRS "template" is convolved with the actual signal; the output of the convolution thus provides information about the places in which the signal best matches the QRS shape, wherein the peaks of the convolution correspond to the best matches.

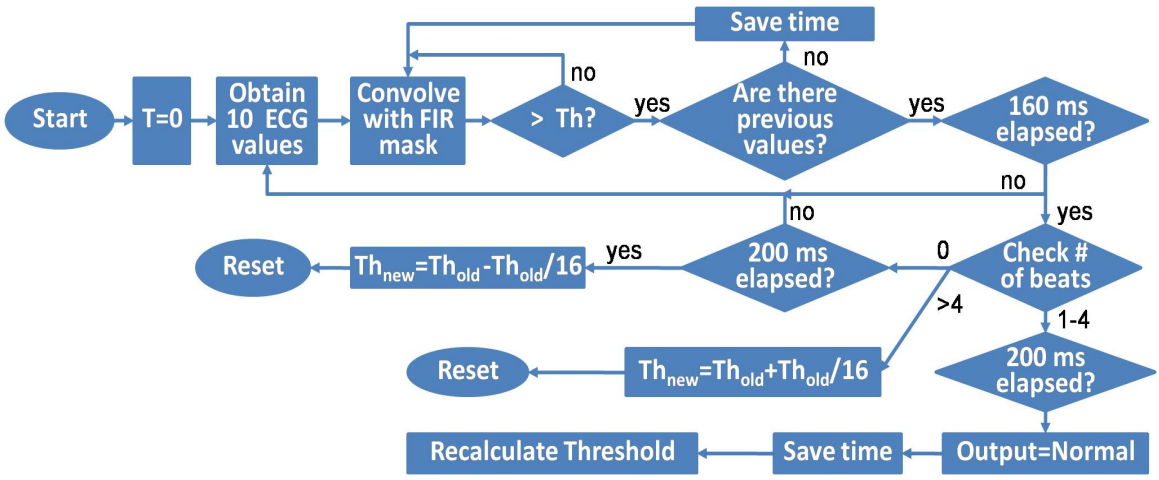

Figure 7.5

The algorithm incorporates an adaptive threshold that updates at every beat annotation, after 2 seconds without a beat annotation, or if the signal proves too noisy and contains too many physiologically impossible false positive detections. This is one of the two algorithms we investigated and tested. The algorithm is described by the following flow chart:

WQRS:

Finally, the second filter that we are investigating and testing is based on what is called the WQRS algorithm. This algorithm is different from the SQRS algorithm in the information it extracts from the raw ECG signal and the manner in which it does so. The main step in this algorithm that makes it different from the SQRS algorithm is that this takes a *length transform* of the ECG signal. This is a transformation

that essentially serves to convert the erratic ECG signal into another signal from which it is easier to analyze and extract useful information. When applied to a potential QRS complex, the length transform can tell us how wide the distance from Q to S is, and where the onset and the end of the complex are located in time. The length transformation also introduces a non-linear scaling factor into the mix, which scales different parts of the signal differently. This results in areas that we are interested in, i.e. the QRS complex being accentuated, and the areas that we do not require, such as noise and the P and T waves, being suppressed. Thus, we are able to obtain the information necessary to determine the heart rate whilst not letting noise interfere.

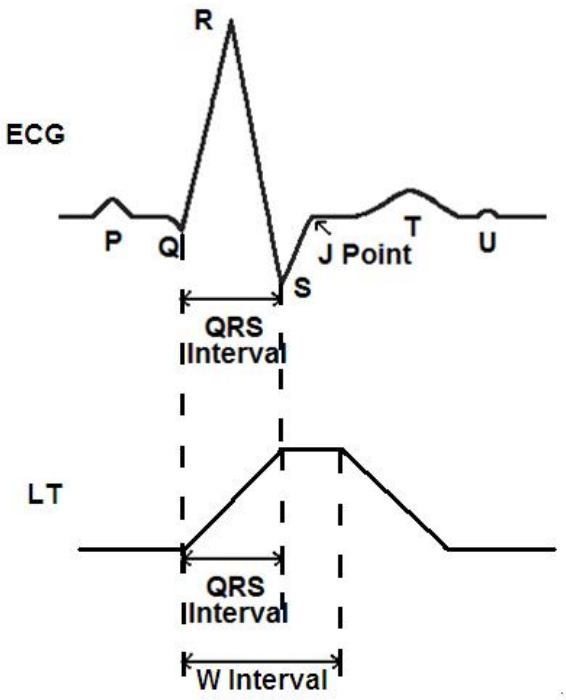

Figure 7.6

The first step in the algorithm is to low pass filter the signal in order to eliminate noise. Following this, the length transform is applied and a threshold value of the algorithm is set as three times the mean value of the length transform of the first set of data points. After 10 seconds have elapsed, the threshold value is readjusted to be one-third the threshold base value. Following this, the threshold base value is periodically adjusted.

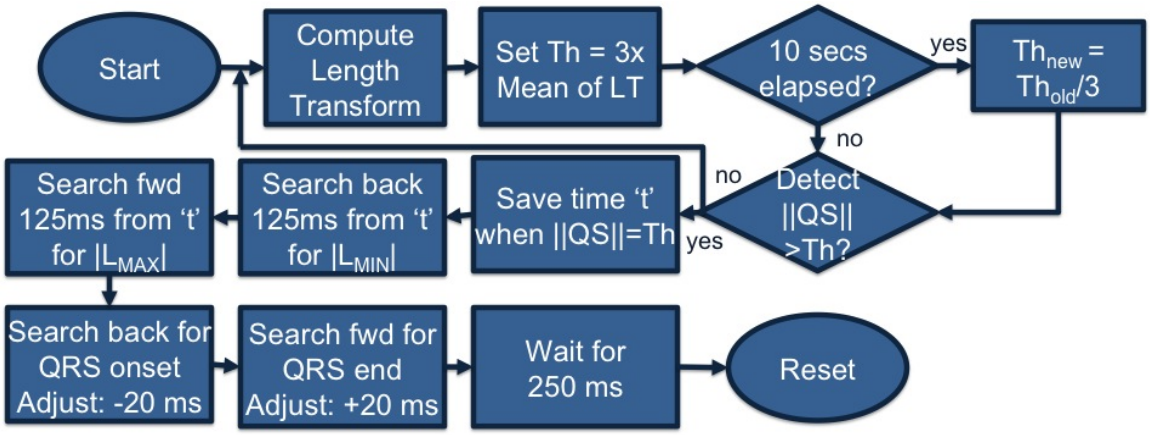

Figure 7.7

Once the algorithm detects a potential QRS complex in which the length of QS has just exceeded the threshold, the time 't' the event occurred is saved. Then we travel backward for 125 ms to the minimum value of the length L_{min} and forward for 125 ms from 't' to obtain the maximum value L_{max}, where L is the magnitude of the length transform. Next, we again travel backward to recover where the QRS onset is located in time and forward to recover where the end is located in time. The onset and end times are added with -20ms and +20ms respectively, in order to provide for potential losses caused by the threshold. This adjustment is based on statistical observations of typical heart rates and ECG signals. Finally, the algorithm waits for 250ms before proceeding to check for another QRS complex in order to avoid detecting the same beat again by mistake.

7.4 Testing[4]

Test-bed

A test bed can be setup using C. The data set used for testing in this module was a subset of the MIT-BIH Noise Stress test available online at www.physionet.org[5] . To evaluate sensitivity to noise, one can read different noise level recordings; here, we analyze three in particular from the Physionet Noise Stress Test tool, selecting 3 different Signal to Noise Ratios (SNR): 24 dB, 18 dB, and 0 dB.

First, download all of the compilers and specialized libraries for gathering ECG data, initialize storage spaces, processing signals stored in a certain format, formatting outputs for consistency and re-use in other algorithms, etc. This is all contained in the WFDB library toolkit. Then, download a specific heart rate file of your choice from the Physionet database and run one of the C programs containing one of the available algorithms under the physiological signal processing header. These algorithms are designed to output a Physionet-compatible annotation file. This annotation file can then be processed manually by running the instantaneous heart rate algorithm (ihr). Using this setup also allows one to save the output of the algorithm as a regular annotation file. This ensures that in the future, the setup could be used to read annotation files and save them directly onto a memory storage unit for processing elsewhere.

The test here constructed consists of running each one of the three algorithms on 3 different data files from the noise stress test. The annotations are compared to reference annotations available on the Physionet-website. Using Physionet's *"bxb"* program, one can compare the annotations beat by beat. The bxb program

[4]This content is available online at <http://cnx.org/content/m33168/1.2/>.
[5]http://www.ncbi.nlm.nih.gov/pmc/articles/PMC1560458/www.physionet.org

outputs the two key parameters of interest in the analysis of heart beat detection: Sensitivity and Positive Predictivity.

Sensitivity (Se) = TP/(TP+MB)

Positive Predictivity (+P) = TP/(TP+FP)

TP: number of true positive detections.

MB: number of false negatives or missed beats

FP: number of false positives; the system detected a beat where the reference annotation showed no beat.

Results

Table 1

	Noisy Signal with 0dB SNR		Noisy Signal with 18dB SNR		Noisy Signal with 24dB SNR		Non-Noisy Signal	
	SQRS	WQRS	SQRS	WQRS	SQRS	WQRS	SQRS	WQRS
QRS Sensitivity:	54.91%	99.53%	92.80%	100.00%	97.70%	100.00%	96.55%	99.97%
QRS Positive Predictivity:	77.75%	57.68%	95.18%	98.46%	98.63%	99.64%	99.76%	99.27%

Table 7.1

As can be seen from Table 1, the WQRS algorithm is overall more robust and tolerant to noise than the SQRS algorithm, particularly in the Sensitivity ratio. To note, however, is the situation that occurs to WQRS at 0dB noise, wherein the SQRS actually obtains a better Positive Predictivity ratio. This indicates that the WQRS formula is particularly adept at correctly noting beats and rarely misses beats, but is less capable of avoiding false positives at high noise levels. However, the WQRS also suppresses information in the ECG signal that we do not need i.e. the P and T waves which also lends to the filters effectiveness. Given that the overall spread from the other noise levels favors WQRS more, it seems best to side with WQRS for most applications.

7.5 Conclusion[6]

Conclusion

We have thus shown in this module an overview of the large body of established research in signal processing from which to draw from in developing a functional QRS detector and heart rate analyzer. The open-source community has developed a robust set of algorithms from which to streamline algorithm testing and implementation. We have conclusively demonstrated that the algorithms developed are capable of noise tolerance to an acceptable medical standard, with high sensitivity ratio and high Positive Predictivity ratio.

In particular, we found the WQRS algorithm was the most consistently noise-tolerant, and most accurate at all noise levels, and we recommend its use in implementation trials.

Given the open-source nature of the programs here analyzed, the reader is encouraged to download the toolkit and run the programs themselves to verify the conclusions of this module.

Having completed this testing, it is clear that this capable testbed available from the MIT Physiotoolkit database would allow a team to implement readily the software onto a processing program for real-time.

The particular steps that a team needs to take in order to implement this algorithm are to modify it for real-time signal analysis by attaching a set of electrodes to the patient, creating a set of analog filters to

[6] This content is available online at <http://cnx.org/content/m33165/1.2/>.

remove noise, and programming a data buffer from which to read in analog voltage signals from electrodes and separate them into discrete components that an Analog to Digital Converter can sample and read into a digital processor. These are topics out of the scope of this module.

Chapter 8

Sparse Signal Recovery in the Presence of Noise

8.1 Introduction[1]

8.1.1 Introduction

As we progress into the era of information overload, it becomes increasingly important to find ways to extract information efficiently from data sets. One of the key concerns in signal processing is the accurate decoding and interpretation of an input in a minimal period of time. In the distant past, the information theorists' objective primarily involved reducing the signal elements to be processed. Now, with a multitude of extraction options, we are also concerned about the computation time required to interpret each element.

In this project, we investigate a few methods by which we can "accurately" reconstruct an arbitrarily complex signal using a minimum number of iterations. The input signals we probe are deemed **sparse** – that is, they are constructed using a number of basis vectors that is small relative to the length of the signal. This generally means that the signals consist mostly of zero values, with spikes at a few selected positions. We compare the signal-to-noise ratios achieved by our recovery methods after specified numbers of iterations upon a variety of input signals, and deduce a few conclusions about the most efficient and most feasible recovery methods.

8.2 Theory[2]

8.2.1 Theory

8.2.1.1 Motivation

In theory, we should never have to 'recover' a signal – it should merely pass from one location to another, undisturbed. However, all real-world signals pass through the infamous "channel" – a path between the transmitter and the receiver that includes a variety of hazards, including **attenuation**, **phase shift**, and, perhaps most insidiously, **noise**. Nonetheless, we depend upon precise signal transmission daily – in our watches, computer networks, and advanced defense systems. Therefore, the field of signal processing concerns itself not only with the deployment of a signal, but also with its recovery in the most efficient and most accurate manner.

[1] This content is available online at <http://cnx.org/content/m33082/1.2/>.
[2] This content is available online at <http://cnx.org/content/m33087/1.2/>.

8.2.1.2 Types of Noise

Noise takes many forms. The various 'colors' of noise are used to refer to the different power spectral density curves that types of noise exhibit. For example, the power density of pink noise falls off at 10dB per decade. The power density spectrum of pink noise is flat in logarithmic space. The most common type of noise, however, is **white noise**. White noise exhibits a flat power density spectrum in linear space. In many physical process (and in this report), we deal primarily with Additive White Gaussian Noise – abbreviated **AWGN**. As a reminder, the Gaussian distribution has the following PDF (Probability Density Function):

$$\frac{1}{\sqrt{2\pi\sigma^2}} \exp\left(-\frac{(x-\mu)^2}{2\sigma^2}\right)$$

Figure 8.1

μ is the mean; $\sigma^2 \geq 0$ is the variance.

8.2.1.3 Sparse Signals

An additional constraint we imposed upon our input signals was that they were required to be **sparse**. A signal that is sparse in a given basis can be reconstructed using a small number of the basis vectors in that basis. In the standard basis for R^n, for example, the signal (1,0,0,0,...,0) would be as sparse as possible – it requires only the basis vector e_1 for reconstruction (in fact, e_1 is the signal!). By assuming that the original signals are sparse, we are able to employ novel recovery methods and minimize computation time.

8.2.1.4 Typical Reconstruction Approaches

We have a number of choices for the recovery of sparse signals. As a first idea, we could "**optimally select**" the samples we use for our calculations from the signal. However, this is a complicated and not always fruitful process.

Another approach is **Orthogonal Matching Pursuit (OMP)**. OMP essentially involves projecting a length-n signal into the space determined by the span of a k-component "nearly orthonormal" basis (a random array of 1/sqrt(n) and (-1)/sqrt(n) values). Such a projection is termed a **Random Fourier Projection**. Entries in the projection that do not reach a certain threshold are assigned a value of zero. This computation is iterated and the result obtained is an approximation of the original sparse signal. Unfortunately, OMP itself can be fairly complicated, as the optimal basis is often a wavelet basis. Wavelets are frequency "packets" - that is, localized in both time and frequency; in contrast, the Fourier transform is only localized in frequency.

8.2.1.5 Signal Reconstruction: Our Method

The fundamental principle for our method of signal analysis is determining where the signal is not, rather than finding where it is. This information is stored in a **mask** that, when multiplied with the **running average** of the signal, will provide the current approximation of the signal. This mask is built up by determining whether a given value in the signal is above a threshold, which is determined by the standard deviation of the noise; if so, the value is most likely a signal element. This process is repeated until the signal expected is approximately equal to a signal stored in a library on the device. While this operation is naturally more noticeable at each iteration with sparse signals, even for non-sparse signals the only limiting

factor is the **minimum value** of the signal. For reasons of application, the primary limiting factor is the number of samples required to recover the signal. This is because the raw mathematical operations take fractions of a second to a few seconds to execute (which is more than enough for conventional applications). The signal itself may be transmitted for a very short period; the requisite **number of samples** must be garnered before transmission halts. Further, given an arbitrary amount of computation time, our algorithm can reconstruct a sparse signal contaminated with *any* level of AWGN – there is no mathematical limit on the recovery process. This is an impressive and surprising feat.

8.3 Implementation[3]

8.3.1 Implementation

Our implementation of the system was based around a controller program, which accepts the password to be transmitted, and then simulate the transmission and reconstruction. The program then returns whether or not the password received is the same as that which activated the system. In the final application, the controller is called repeatedly until the system is activated; it returns immediately after a non-match, and continues in sequence after the first element is matched.

For each of the passwords element's iterations in the controller the following algorithm is used. The threshold is set to [the minimum value of the ideal signal minus three times the standard deviation of the base noise] (in our case one), and the mask is initialized to all ones. Then we prime the noise to reach either that standard deviation or less by priming the running total with a series of samples, the exact number of which is determined by the standard deviation of the noise. Then we execute the following function until either it runs a set number of times, or succeeds. Then the program compares the reconstructed signal after the iteration with the ideal signals, and returns if there is a reasonable match.

This function does the following four times: it samples the signal, updates the running total, and counts whether the maximum imaginary or real part of the Fourier transform of the signal is greater than the threshold. If at least two of the four cycles result in a value greater than the threshold, the mask's value at that point is set to the previous value of the mask; otherwise, the mask's value is set to zero. This allows a degree of leniency (which is useful in an inherently probabilistic method) and drastically reduces the probability of failure, albeit at the expense of increasing processing time.

The priming of the noise either reduces it to a standard deviation of two and a half, or three, based on the standard deviation of the noise. The method which is selected will result in fewer net samples required than the alternative method: although processing the information can take large quantities of samples, preprocessing requires sd^2/(2.5^2) or sd^2/(3^2) samples; hence, a larger denominator can cut off incredible quantities of samples. The reason why these values in particular were selected is that experimentally we determined that at 2.5 standard deviations, most signals required only one additional sample to become fully reconstructed, while at 3 standard deviations, they took a couple dozen to a few hundred, and a maximum of a few thousand additional samples, but it appeared to terminate the vast majority of the time as shown in Figure 1 and Figure 2.

[3]This content is available online at <http://cnx.org/content/m33081/1.2/>.

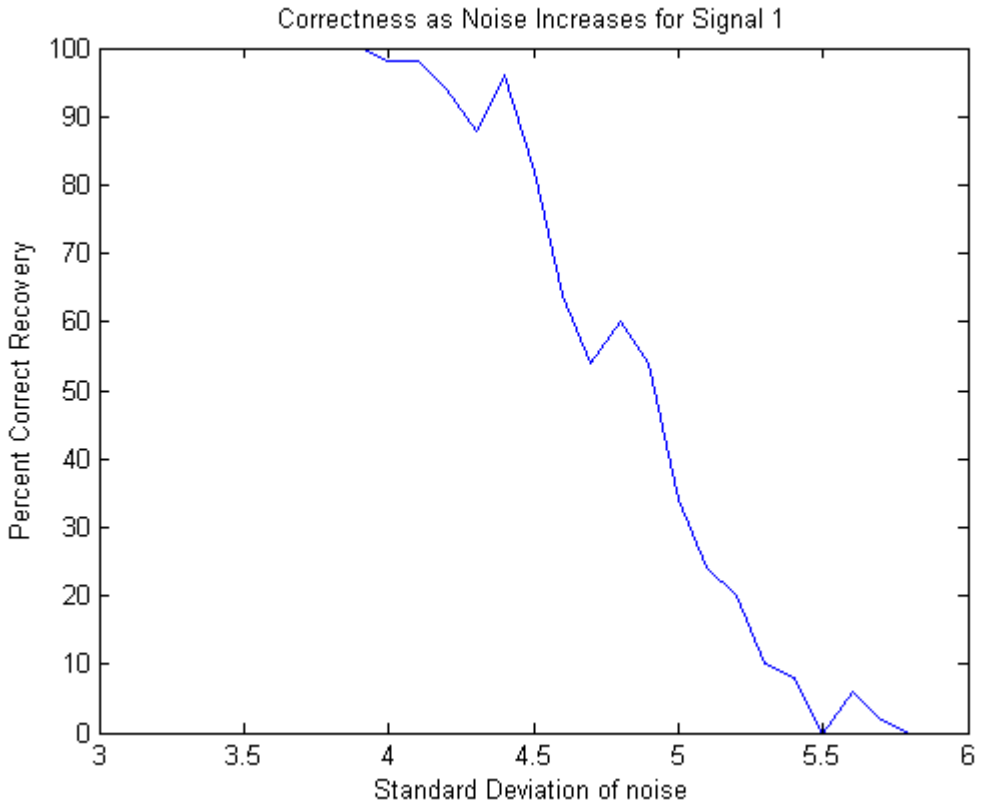

Figure 8.2

The success of a simple signal as a function of the standard deviation of the noise for a single cycle of a sinusoid with no priming(50 repetitions at each point).

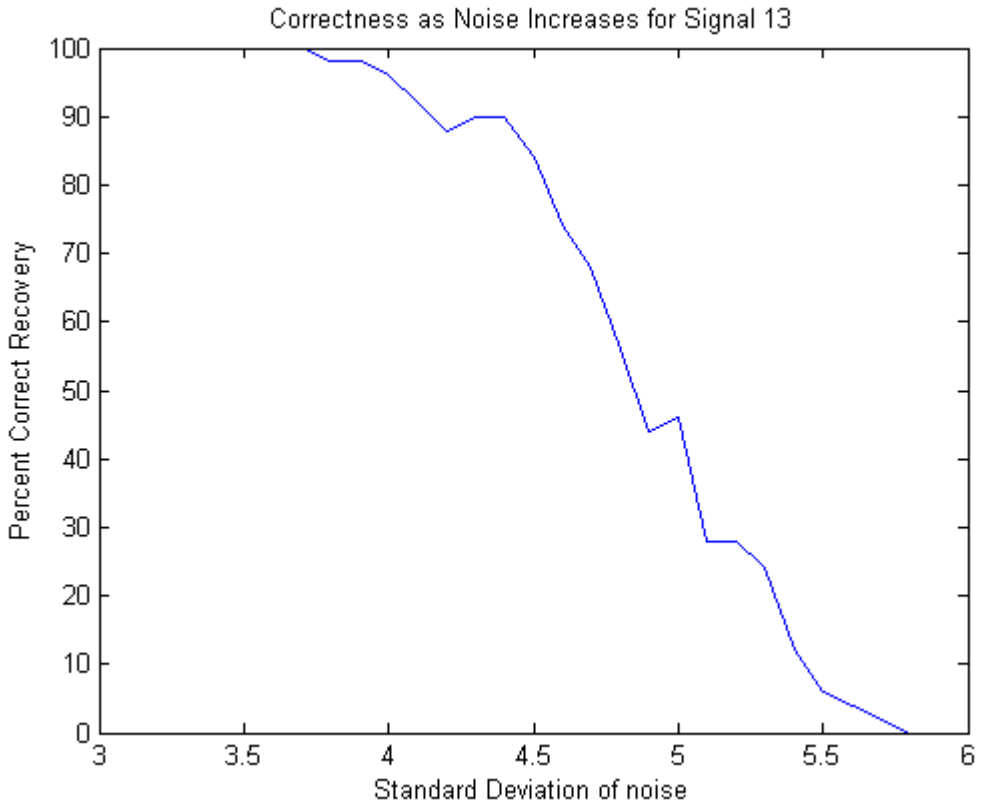

Figure 8.3

The success of a sum of a frequency one sine wave, a frequency four sine wave, and a frequency 20 cosine wave as a function of the standard deviation of the noise with no priming(50 repetitions at each point).

The priming is a necessity, since without it, the probability of success decreases rapidly as the standard deviation increases, but with it the probability of success, while not one, remains constantly above 99%. This is because after priming the effective standard deviation is always three or less, making the original signal consistently recoverable.

8.3.2 Timing Analysis

All of the initializitions before the priming, assignations etc. require O(1) operations. The priming itself requires O(sd^2) operations. The post priming processing, requires O(library size) operations since although the fft is O(N*logN), N is bounded and therefore even if the sd wasn't bounded to minimize the computation it still would always be less than a constant value. The only variable processing part is the comparisons with the library, which is O(libsize*N*logN) with N being bounded, simplifying to O(libsize). This means that the algorithm itself is O(sd^2)+O(libsize)=O(sd^2) since libsize will tend to be small. This is supported by experimental results as shown in Figure 1 and Figure 2.

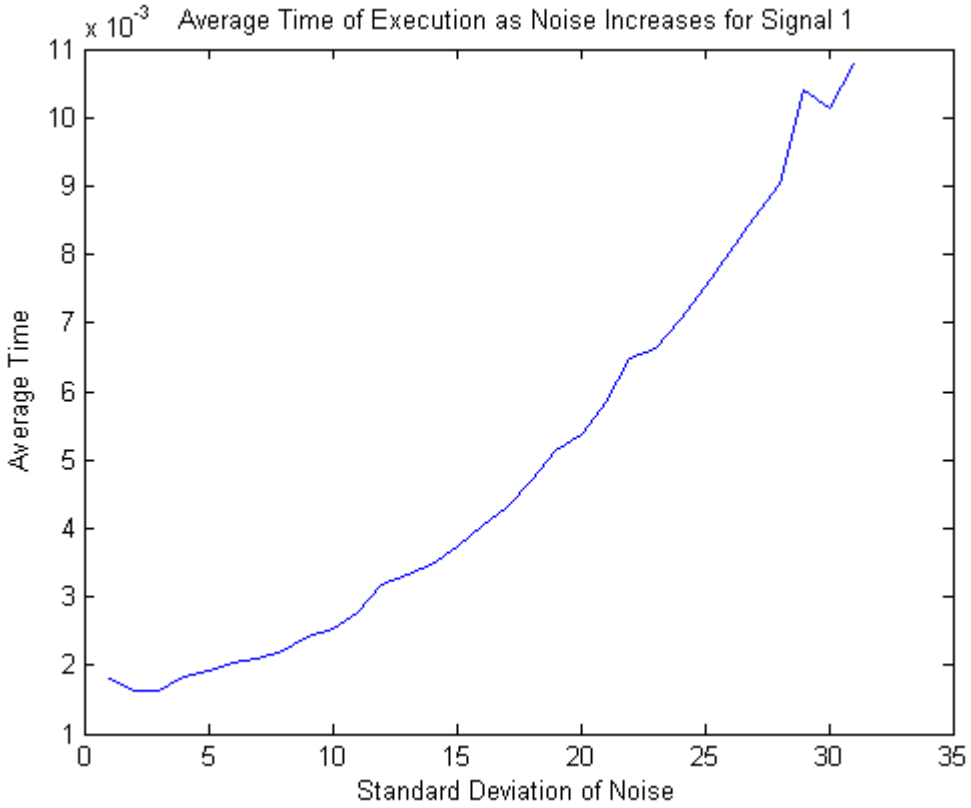

Figure 8.4

The average time of execution as a function of the standard deviation of the noise for a single cycle sinusoid (50 repetitions per point).

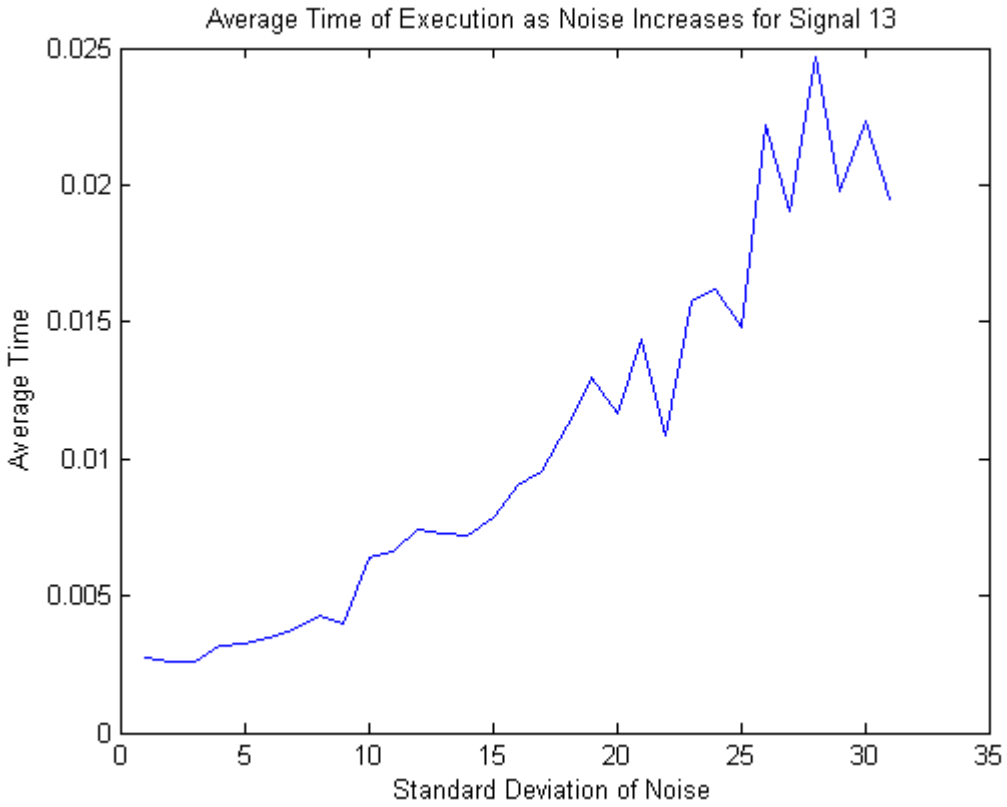

Figure 8.5

The average time of execution as a function of the standard deviation of the noise for the sum of a frequency 1, sine wave, a frequency 4 sine wave, and a frequency 20 cosine wave (50 repetitions per point).

For a real world application, it is also important to know not only the time it takes to execute the entire program, but also the number of samples that are required in order to reconstruct the signal. This is because the signal will only be transmitted for a limited time, so the hardware must be able to take the right number of samples in that time. From the processing perspective, even with very slow hardware the signal could eventually be reconstructed, but the same is not the case if the correct number of samples cannot be garnered. The number of samples required is always on O(sd^2) specifically sd^2/6.25+1 if sd<76, and sd^2/9+∼200 if sd>=76. The experimental values are shown in Figure 3 and Figure 4.

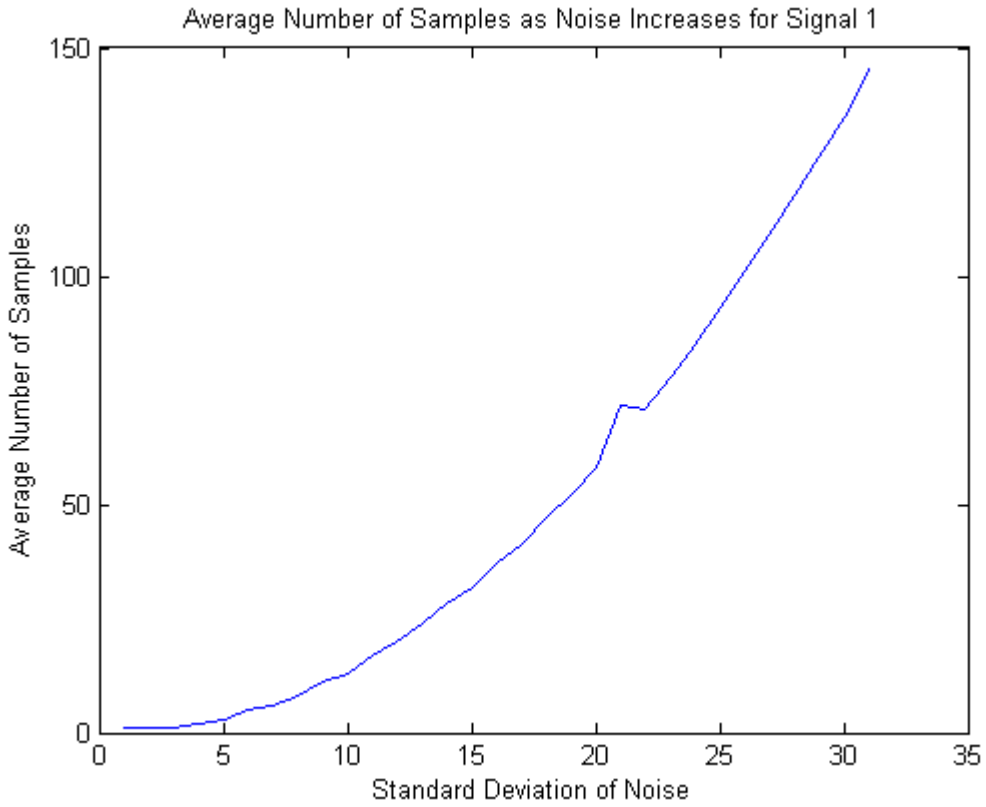

Figure 8.6

The average number of samples required to reconstruct the signal as standard deviation increases for a single cycle sine wave (50 repetitions at each point).

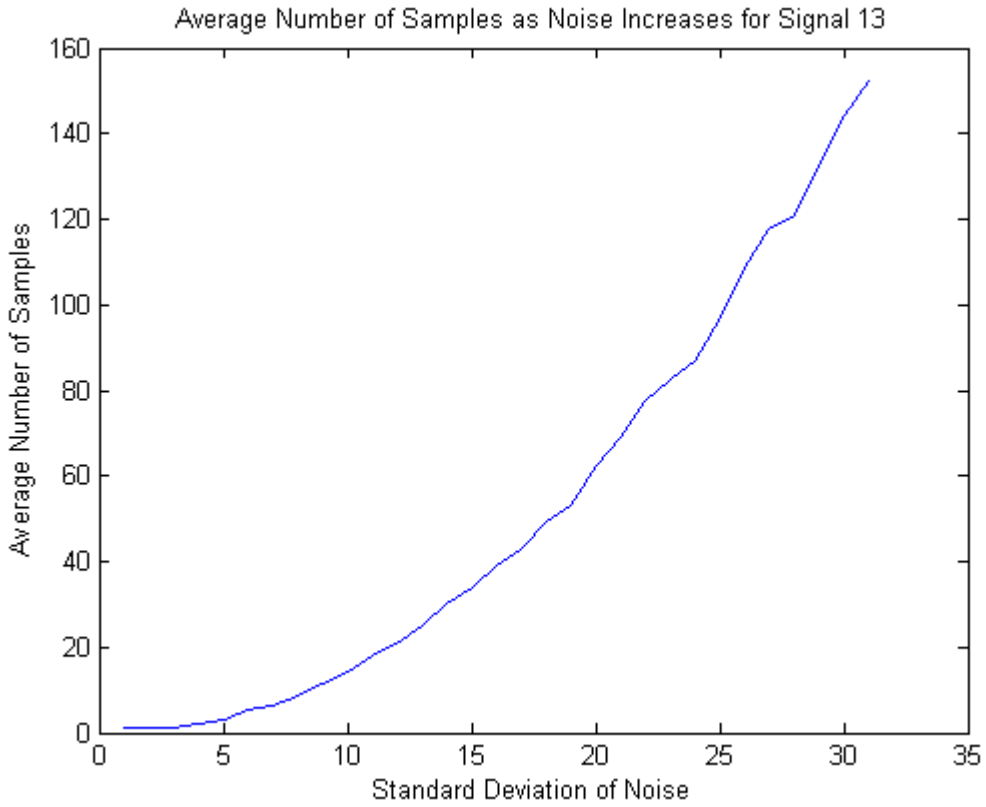

Figure 8.7

The average number of samples to reconstruct the signal as a function of the standard deviation of the noise for the sum of a frequency 1 sine wave, a frequency 4 sine wave, and a frequency 20 cosine wave (50 repetitions per point).

8.3.3 Examples of Execution

All of the following figures are comprised of a series of graphs. The first graph is the initial signal with noise, as well as the initial signal; the next four graphs are the reconstructed signal at consecutive iterations along with the initial signal; the final graph is the final reconstructed signal along with the initial signal.

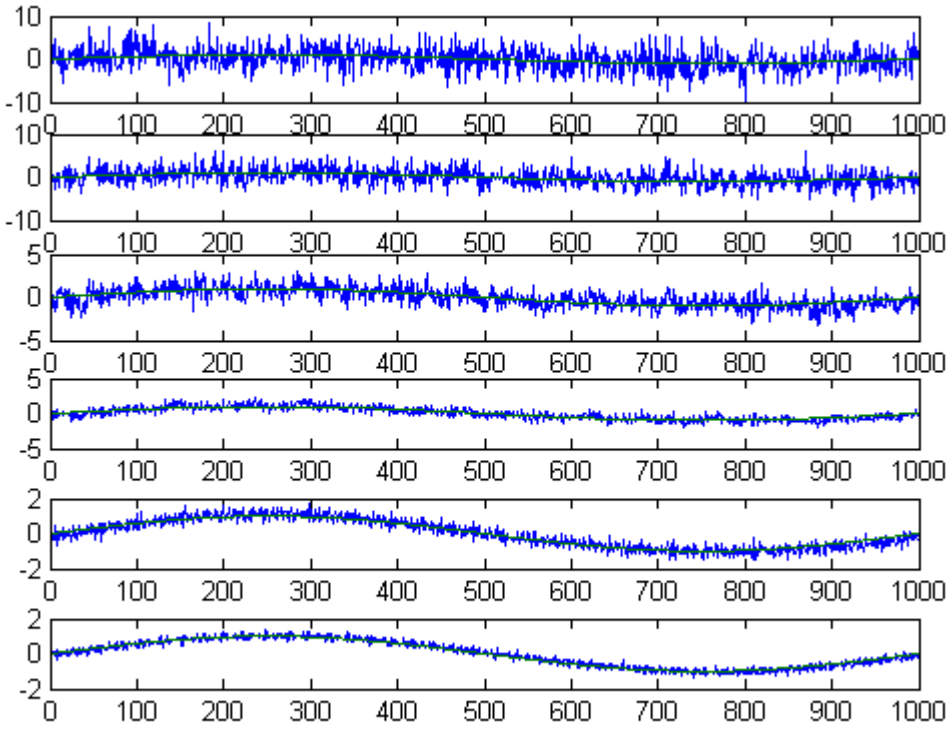

Figure 8.8

Execution from algorithm for signal 1, a frequency 1 sine wave with noise standard deviation of 5.

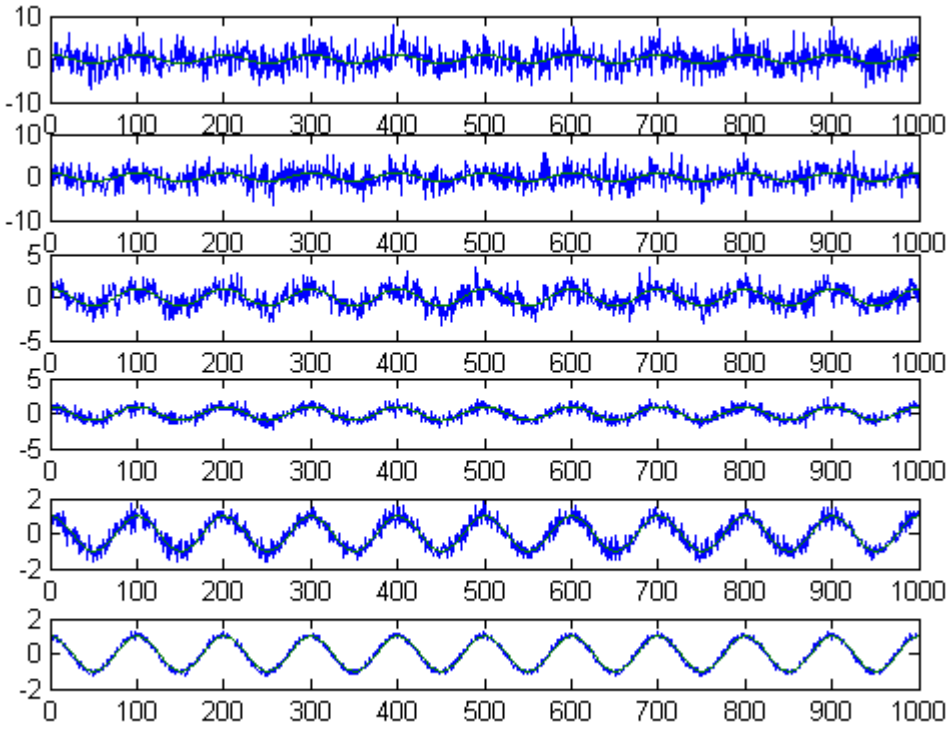

Figure 8.9

Execution from algorithm for signal 10, a frequency 10 cosine wave with noise standard deviation of 5.

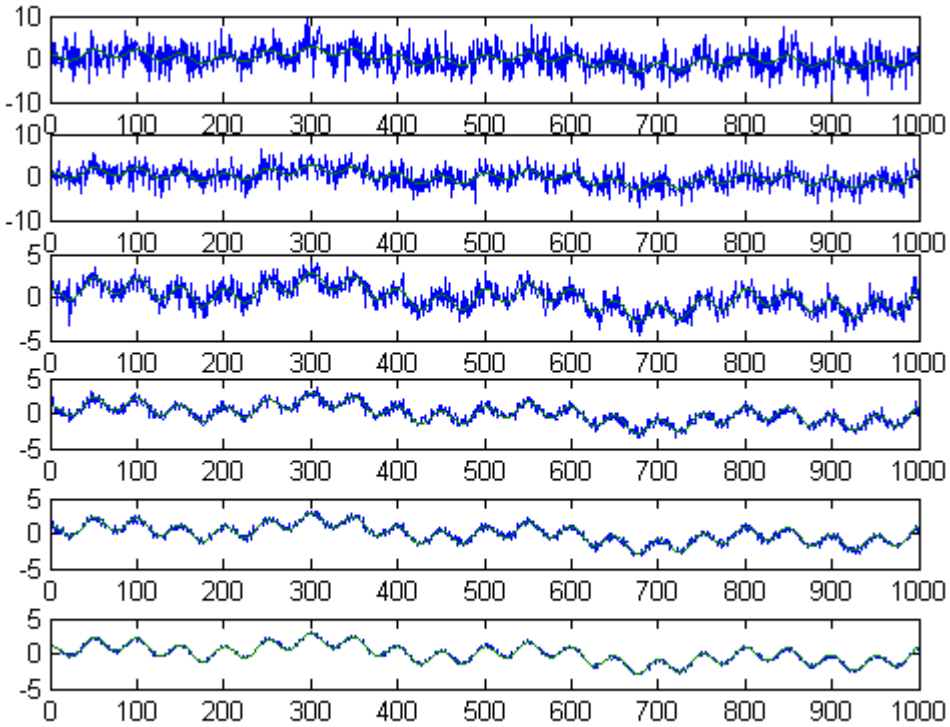

Figure 8.10

Execution from algorithm for signal 13, the sum of a frequency 1 sine wave, a frequency 4 sine wave, and a frequency 20 cosine wave with noise standard deviation of 5.

8.4 Conclusion[4]

8.4.1 Conclusion

With priming, the regression line correlating number of samples and standard deviation is roughly (sd^2)/6.5 + 1, which amounts to **O(N^2)** complexity. However, although this may seem slow, our method permits perfect recovery of complicated (albeit sparse) signals *with* **arbitrary levels of AWGN**. Thus, for reasonable data set sizes and values of standard deviation, the algorithm functions quite nicely for accurate signal reconstruction. Although if given infinite samples and time, it can recover any signal that is relatively sparse given infinite time.

Without priming the noise, and taking 50 samples, we can achieve **O(1)** complexity – extremely desirable, but the recovery percentage falls off rapidly with increase in noise standard deviation starting at standard deviation values around 3.5. Thus, this version of the algorithm could be desirable in non-critical

[4]This content is available online at <http://cnx.org/content/m33080/1.2/>.

applications where the strength of the noise is known to be low relative to that of the signal. We certainly would not recommend using the non-primed algorithm in data sensitive digital applications.

8.4.2 Further Avenues of Inquiry

Colored Noise
It would be interesting to extend the algorithm to accept **different types of noise** – pink, brown, purple, etc. Logically the exact same algorithm would work on these, but it would be nice to verify this experimentally.
Physical Prototype
A physical prototype of this system would allow a far better testing of the theory than simple simulation. Unfortunately, due to the cost of even moderate quality receivers and FPGAs, this was not feasible.
Dynamic Noise
One major benefit of a noise resistant system is ECCM, Electronic Counter Countermeasures (counter-jamming). It would be interesting to test whether a system using the described algorithm could resist noise from a transmitter moving towards the system (without simply taking a conservative estimate of worst-case noise during the signal reconstruction period).
Dynamic Priming
A useful addition to this algorithm, would be to be able to pick the optimal bound for priming to minimize the number of samples rather than simply choosing the best of two options.

8.5 Code[5]

8.5.1 Code

The following is the MATLAB source code for each of the components of our project.

8.5.1.1 addNoise.m

```
function out = addNoise(sig,mean,sd,Plot)
%addNoise
%adds noise with given mean and sd to the signal
    rand=randn(1,1000)*sd+mean;
    out=sig+rand;
    if(Plot==1)
        plot(1:1000,out,1:1000,sig);
    end
end
```

8.5.1.2 sample.m

```
function out = sample(sd,plot,sig)
%sample
%samples a manually constructed signal, and adds gaussian noise to it
%with a standard deviation that is provided
out=fft(addNoise(sig,0,sd,plot));
end
```

[5]This content is available online at <http://cnx.org/content/m33079/1.2/>.

8.5.1.3 init.m

```
    function [out,samp]=init(sig,sd)
    %averages the signal and the noise over a number of samples to make the
    %noise level manageable
    out=sig+randn(1,1000).*sd;
    %optimize number of samples
    if sd<76
        val=6.25;
    else
        val=9;
    end
    samp=floor((ceil(sd))^2/(val));
    for n=2:samp
        out=(out.*(n-1)+sig+randn(1,1000).*sd)/n;
    end
    out=fft(out);
end
```

8.5.1.4 simpleIterate.m

```
    function [mask, NSig,runT] = simpleIterate(sigMask,threshold,run,n,sd,sig)
%simpleIterate(sigMask,threshold,run,n)
%computes an iteration of the thresholding, with a running average of run,
%on iteration n, with the current signal mask of sigMask
%returns the new signal mask, the current signal(non-masked) NSig and the
%running average of the signal runT
    siz=size(sigMask);
    temp=zeros(1,siz(2));
    for i=1:4
        NSig=sample(sd,0,sig).*sigMask;
        if(n==1)
            runT=NSig;
        else
            runT=(run.*(n-1)+NSig)/n;
        end
        %temp=temp+(max(abs(real(NSig)),abs(imag(NSig)))>threshold);
        temp=temp+(max(abs(real(runT)),abs(imag(runT)))>threshold);
        %temp=temp+(abs(NSig)>threshold);
    end
    mask=zeros(1,siz(2));
    for l=1:siz(2)
        if(temp(l)<2)
            mask(l)=0;
        else
            mask(l)=sigMask(l);
        end
    end
end
```

8.5.1.5 testArbitary.m

```
    function [flag,samples,time]=testArbitrary(sig,sd)
%Simulates the transmission of a signal in the library, and tests whether
%or not it can be recovered.
    siglib=cat(1,sin(0:pi/500:(1000*pi-1)/500),sin(0:pi/250:(2000*pi-1)/500),sin(0:pi/125:(4000*pi-1)/5
    siglib=cat(1,siglib,sin(0:pi/500:(1000*pi-1)/500)+sin(0:pi/50:(10000*pi-1)/500),cos(0:pi/500:(1000*
    siglib=cat(1,siglib,cos(0:pi/25:(20000*pi-1)/500),cos(0:pi/25:(20000*pi-1)/500)+sin(0:pi/500:(1000*
    sigmax=max(abs(fft(siglib(sig,:))));
    threshhold=sigmax-3*max(abs(real(fft(randn(1,1000)))));
    tolerance=.5;
    A=ones(1,1000);
    flag=0;
    tic
    [C,samples]=init(siglib(sig,:),sd);
    for i=1:10000
        [A,B,C]=simpleIterate(A,threshhold,C,i+samples,sd,siglib(sig,:));
        for j=1:size(siglib)
            if(abs(ifft(A.*C)-siglib(j,:))<tolerance)
                flag=j;
                break;
            end
        end
        if(flag>0)
            break;
        end
    end
    samples=samples+i;
    time=toc;
end
```

8.5.1.6 Controller.m

```
    function accepted = Controller(enteredpassword,sd)
%Tests whether or not a transmission of a password will activate the system
%This simulates the noise and processing as well as the values
    actualpassword=cat(1,13,5,10,4,2,8);
    accepted=1;
    redundancy=3;
    for i=1:size(actualpassword);
        flag=0;
        %while flag==0
        for j=1:redundancy
            [flag,runs]=testArbitrary(enteredpassword(i),sd);
        end
        if(flag~=actualpassword(i))
            accepted=-i;
            break;
        end
    end
```

```
end
```

8.5.1.7 Controller2.m

```
    function Controller2()
%Helper function used to graph trends
    sig=1;
    for sd=0:30
        passed=0;
        for reps=1:50
            if(testArbitrary(sig,3+sd/10)==sig)
                passed=passed+1;
            end
        end
        temp(sd*10-29)=passed
    end
    subplot(1,1,1);
    plot(temp);
end
```

8.6 References and Acknowledgements[6]

8.6.1 References and Acknowledgements

We wish to thank our mentor, JP Slavinsky. Without your guidance and support, this project would not have been possible.

Many thanks also to Dr. Rich Baraniuk – for creating Connexions, and (arguably more importantly), for presenting inspiring signal processing lectures throughout the semester.

J D Haupt's presentation to the Electrical Engineering department on sparse signal reconstruction was integral to the development of our algorithm, although it concentrated on efficiency rather than arbitrary reconstruction.

The algorithms and techniques discussed in the following papers were used for comparison against our algorithm:

Haupt, J. and R. Nowak. "Signal Reconstruction From Noisy Random Projections." *IEEE Trans. Info. Theory*, vol.52, no.9, pp.4036-4048, 2006. http://ieeexplore.ieee.org/stamp/stamp.jsp?arnumber=1683924&isnumber=35459[7]

J. Tropp and A. Gilbert, "Signal Recovery from Partial Information via Orthogonal Matching Pursuit." *IEEE Trans. Info. Theory*, vol. 53, no. 12, pp. 4655–4666, 2007. http://www.math.lsa.umich.edu/∼annacg/papers/TG05-signal-recovery-rev-v2.pdf[8]

[6] This content is available online at <http://cnx.org/content/m33083/1.2/>.

[7] http://ieeexplore.ieee.org/stamp/stamp.jsp?arnumber=1683924&isnumber=35459

[8] http://www.math.lsa.umich.edu/∼annacg/papers/TG05-signal-recovery-rev-v2.pdf

8.7 Team[9]

8.7.1 Team

8.7.1.1 Grant Cathcart

Figure 8.11

Grant Cathcart was born in Cleveland Ohio, in 1989. Grant is currently a junior Electrical Engineering major at Rice University specializing in signals and systems. Grant is employed by the Navy as part of the Tactical Electronic Warfare Division. When not working on projects and cursing matlab, Grant likes to play chess and video games.

[9]This content is available online at <http://cnx.org/content/m33086/1.2/>.

8.7.1.2 Graham de Wit

Figure 8.12

Graham was born in Cincinnati, OH in 1989. However, he spent most of his life in Memphis, TN, the Home of the Blues. Graham is currently a junior Electrical Engineering major at Rice University specializing in Computer Engineering. Graham enjoys convolving signals, computing Fourier Transforms, and inducing capacitor explosions. When he is not buried in problem sets, Graham spends time eating, sleeping, hanging out with friends, and composing music via his synthesizers.

8.7.1.3 Nicholas "Re'Sean" Newton

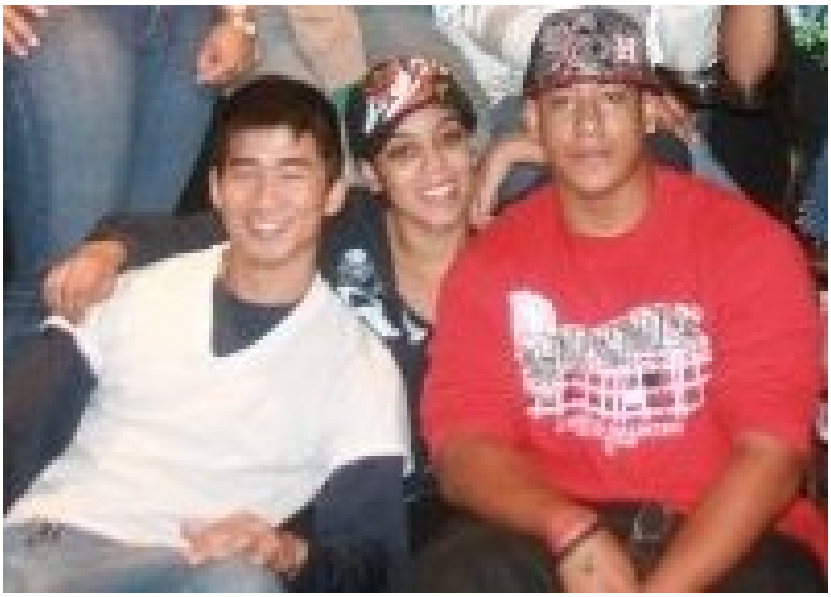

Figure 8.13

Nicholas Newton was born in Wichita Falls,TX in 1989. He is currently an junior Electrical Engineering major with a specialization in Computer Engineering at Rice University . He plans to attend Graduate School after he graduates from Rice. Nicholas has a deep passion for the Computer Engineering industry and computers in general. Outside of his academic career, Nicholas enjoys working out and a number of different sports.

Chapter 9

Video Stabilization

9.1 Introduction[1]

Introduction
A common problem in dealing with Unmanned Aerial Vehicles (UAVs) is image stabilization. If an operator wishes to control the craft in real-time, a camera mounted on the UAV is often a good solution. This video feed, if left in its original state, has varying amounts of jitter, which in turn makes operating the craft more difficult and makes the footage of the flight much less pleasant to watch. We decided that we could stabilize the video without using any additional hardware-based assistance (such as gyroscopes) with the digital signal processing techniques we've learned over the semester. Our first approach to solving this problem was to correlate each video frame with the previous one, but this proved to be less than optimal ; there exists a faster, more accurate technique. Enter KLT feature tracking and Serial Affine Transformation. We used a freely-available KLT feature tracker from Stan Birchfield, then prototyped our affine transformation techniques in MATLAB. We have started porting our work to C, and in the future we expect this sort of solution to be fully implemented on GPUs for real-time processing.

9.2 Background[2]

Background
Image stabilization can be done in many different ways. Kanade-Lucas-Tomasi (KLT) feature tracking[3] is one of the computationally inexpensive ways, in comparison to 2-D correlation and even SIFT. We chose Stan Birchfield's implementation because it is written in C and we found it easy to interface to in comparison with other open-source implementations.

When we have a set of common features between two images, we can 'undo' the transformation that makes the second image's features reside in a different location than the first, creating a new image whose features have similar locations to those in the first image.

In order to accomplish this, we use a series of least-squares affine transformations on the set of features to determine the 'best' values for the un-affine we perform to correct the later image. After this, we then filter the resulting affine transformation, keeping the low-frequency movement (such as panning) and removing the high-frequency jitter.

Pictorally, the process is as such:

[1] This content is available online at <http://cnx.org/content/m33246/1.1/>.
[2] This content is available online at <http://cnx.org/content/m33247/1.1/>.
[3] http://en.wikipedia.org/wiki/Kanade-Lucas-Tomasi_Feature_Tracker

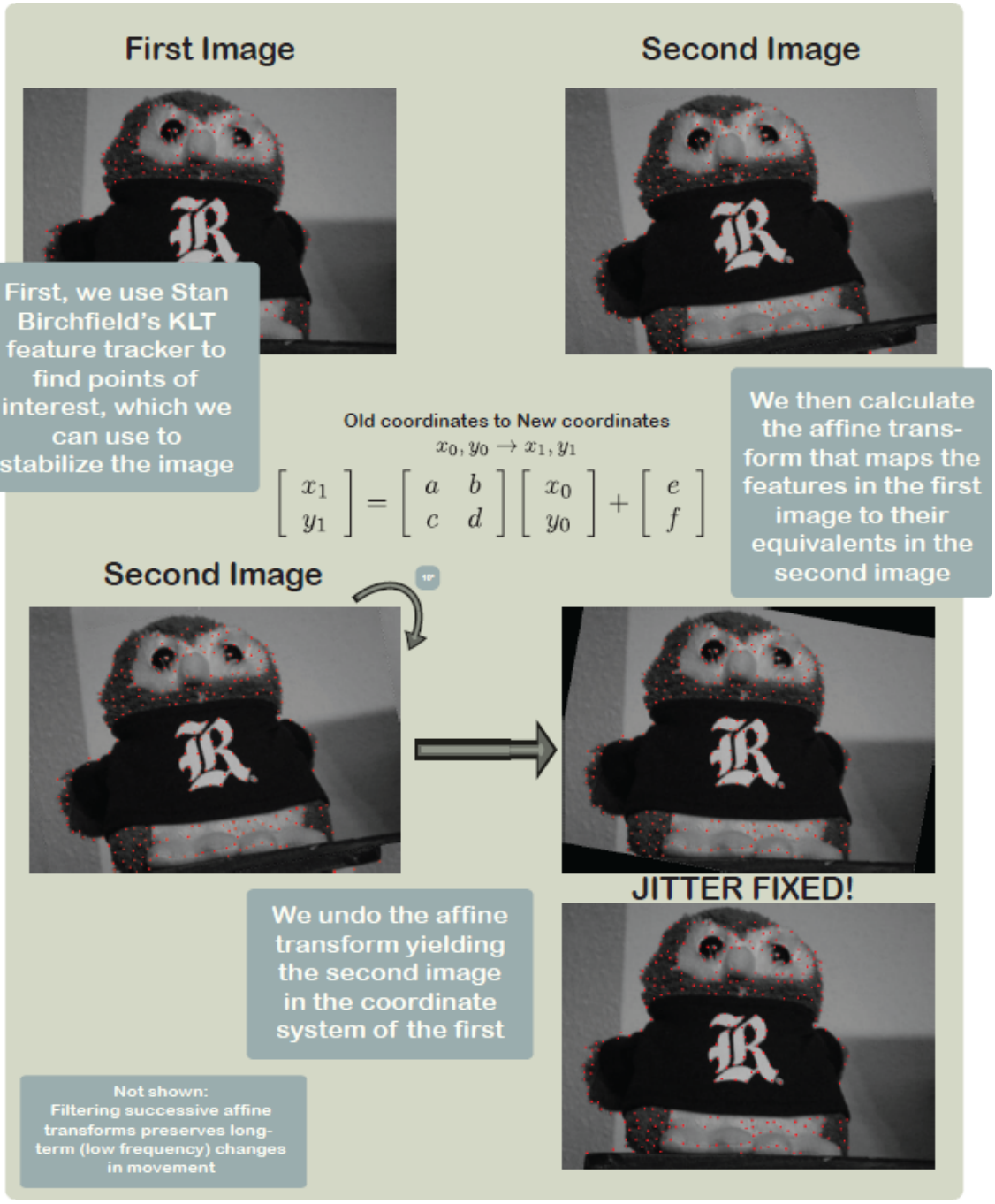

9.3 Procedures[4]

9.3.1 Affine Transform Estimation

We wish to approximate the movement of the feature points by an affine transform, because it can account for rotation, zooming, and panning, all of which are common features in videos. The coordinates of a feature

[4] This content is available online at <http://cnx.org/content/m33251/1.1/>.

in the old frame are written as (x_0, y_0) and in the new frame as (x_1, y_1). Then an affine transform can be written as:

$$\begin{bmatrix} x_1 \\ y_1 \end{bmatrix} = \begin{bmatrix} a & b \\ c & d \end{bmatrix} \begin{bmatrix} x_0 \\ y_0 \end{bmatrix} + \begin{bmatrix} e \\ f \end{bmatrix} \tag{9.1}$$

However, this form needs some modification to deal with multiple point pairs at once, and needs rearranging to find a, b, c, d, e, and f. It can be easily verified that the form below is equivalent to the one just given:

$$\begin{bmatrix} x_0 & y_0 & 0 & 0 & 1 & 0 \\ 0 & 0 & x_0 & y_0 & 0 & 1 \end{bmatrix} \begin{bmatrix} a \\ b \\ c \\ d \\ e \\ f \end{bmatrix} = \begin{bmatrix} x_1 \\ y_1 \end{bmatrix} \tag{9.2}$$

With this form, it is easy to add multiple feature points by stacking two additional rows on the left and on the right. Denoting the pairs of points as $\left(\left(x_0^{(1)}, y_0^{(1)}\right), \left(x_1^{(1)}, y_1^{(1)}\right)\right)$, $\left(\left(x_0^{(2)}, y_0^{(2)}\right), \left(x_1^{(2)}, y_1^{(2)}\right)\right)$, $\left(\left(x_0^{(3)}, y_0^{(3)}\right), \left(x_1^{(3)}, y_1^{(3)}\right)\right)$, etc, the matrices will now look like:

$$\begin{bmatrix} x_0^{(1)} & y_0^{(1)} & 0 & 0 & 1 & 0 \\ 0 & 0 & x_0^{(1)} & y_0^{(1)} & 0 & 1 \\ x_0^{(2)} & y_0^{(2)} & 0 & 0 & 1 & 0 \\ 0 & 0 & x_0^{(2)} & y_0^{(2)} & 0 & 1 \\ x_0^{(3)} & y_0^{(3)} & 0 & 0 & 1 & 0 \\ 0 & 0 & x_0^{(3)} & y_0^{(3)} & 0 & 1 \\ \vdots & \vdots & \vdots & \vdots & \vdots & \vdots \end{bmatrix} \begin{bmatrix} a \\ b \\ c \\ d \\ e \\ f \end{bmatrix} = \begin{bmatrix} x_1^{(1)} \\ y_1^{(1)} \\ x_1^{(2)} \\ y_1^{(2)} \\ x_1^{(3)} \\ y_1^{(3)} \\ \vdots \end{bmatrix} \tag{9.3}$$

So long as there are more than three points, the system of equations will be overdetermined. Therefore the objective is to find the solution $[a, b, c, d, e, f]$ in the least squares sense. This is done using the pseudoinverse of the matrix on the left.

9.3.2 Filtering

The affine transforms produced above only relate one video frame to the one immediately after it. The problem with this is that if the video is jerky, it will take several consecutive frames to have a good idea of what the average position of the camera is during this time. Then the difference between the current location and the moving-average location can be used to correct the current frame to be in this average position.

When the features are tracked frame-to-frame, it constitutes an implicit differentiation in terms of measuring the overall movement of the camera. In order to track changes across many frames, we sequentially accumulate the frame-to-frame differences. This is akin to an integral operator. Unfortunately, when integrating imperfect data, errors will build up linearly in time, and that is true here. However, since the stream of integrated affine transforms is not used directly, these errors are not as important.

Once the stream of integrated affine transforms is generated, the goal is to undo high-frequency motions, while leaving the low-frequency motions intact. This is done by treating the coefficients of the stream of integrated affine transforms as independent, and applying six high pass filters, one for each stream of

coefficients. Although this technique works, it is hoped that a more elegant way of handling the filtering may be developed in the future.

Since a high pass filter is being used, it is important to not have large phase offsets created by the filter. If the transform which ideally stabilized frame #5 was instead applied to frame #10, and so forth, the delay would wholly invalidate the offsets, and the resulting video would be more jerky than before, instead of less. Therefore, we decided to use the zero phase filtering technique of applying a filter in both the forward and reverse time directions sequentially. This is handled by the Matlab function filtfilt.

Initially, we tried various order-4 to order-8 IIR filters with cutoff frequencies around 0.1 pi. However, the unit step response of nearly all IIR filters involves a significant amount of overshoot and ringing. Since our signal is best viewed as a time-domain signal instead of a frequency-domain signal, we sought to avoid this overshoot. Therefore, we switched to a truncated Gaussian FIR filter, which averages across a bit more than one second worth of video at a time. This removed the overshoot and ringing which had been visible with the IIR filters.

In the algorithm we used, the high pass filter is implicitly generated by using a low pass filter, then subtracting the low-pass version from the original. It would be mathematically equivalent to simply change the impulse response of the filter and skip the subtraction step.

The last wrinkle is that for affine transforms, the identity transform has the a and d coefficients equal to one, instead of zero. The high pass filter will create a stream of transforms which are centered around having all the coefficients zero. Therefore, after the high pass filter, we added 1 back to the a and d coefficients of the stream of affine transforms, so they would be centered on the identity transform.

9.4 Results[5]

Results: Output Quality
We successfully used Stan Birchfeld's KLT tracker with our implementation of affine transforms in MATLAB to stabilize the sample UAV video that Aswin provided us. The video is of six cars at the end of a runway with the plane slowly circling them. There is some jitter, and evidence of a couple of dropped frames. Our filter completely removes these, but it also eliminates the perspective change caused by the movement of the plane. This introduces considerable distortion after more than about 10 seconds. High pass filtering of the affine transformation series does remove the jitter while preserving the overall motion.

UAV Footage Stabilized with KLT + Affine Transforms

This media object is a video file. Please view or download it at<uav_source.avi>
(a)

This media object is a video file. Please view or download it at<uav_stable.avi>
(b)

Figure 9.1: Source footage provided by Aswin Sankaranarayanan.

We wanted a more serious test of the jitter reduction, with more sudden motion. To do this we wrote some MATLAB code that takes an individual frame and generates a sequence of frames based on it, each with a random displacement from the original. The effect is that of a VERY jerky camera. The KLT-affine transform combination undoes this severe jitter quite nicely. We then superimposed a circular motion on top of the jitter to see if the filtered affine transformation series would preserve it while still removing the jitter. It does an acceptable job at this, although there are a few visible kinks.

[5]This content is available online at <http://cnx.org/content/m33248/1.1/>.

Shifted Image Sequence Stabilized with KLT + Filtered Affine Transforms

This media object is a video file. Please view or download it at<owl_source.avi>
(a)
This media object is a video file. Please view or download it at<owl_stable.avi>
(b)

Figure 9.2

Additional testing revealed that although the KLT tracker we used does a good job on tracking features through sudden translations, it cannot effectively deal with large sudden rotations. It loses track of all features in these cases. Hopefully this will not be an issue for our ultimate application, or we will be able to compensate for the rotation using additional input from gyros.

We also experimented with stabilizing jerky footage from movies, such as the opening scene to Saving Private Ryan. This works quite well! We invite you to test out our code on DVD-quality video and see what you think of the results. (At some point we plan to "stabilize" The Blair Witch Project so those of us prone to motion sickness can watch it without becoming ill.) Of course the output needs to be cropped somewhat to eliminate the black border caused by shifting the image: we cannot create data from nothing!

Results: Speed

Our code is not nearly fast enough for real-time use. Greyscale output at 640x480 resolution runs at about one-third of realtime, whereas color output at the same resolution is about one-tenth real time, on the 2GHz Intel Core2 Duo laptop used for testing. The biggest bottleneck right now seems to be in the interpolation used to assign pixel intensity values for the corrected frames. The KLT tracker itself is the next slowest component. Hopefully converting the code to C and/or offloading some of the work to the GPU will improve performance.

9.5 Sources[6]

We'd like to thank Aswin Sankaranarayanan at Rice DSP for pointing us in the correct direction early in our work and steering us away from trouble. Also, a key piece of the project required using Stan Birchfeld's KLT feature tracker[7] and the interface code he wrote to easily move the table of features into MATLAB.

9.6 The Team[8]

Jeffrey A. Bridge
Studying for a BS Electrical Engineering at Rice University in 2011. I am interested in spaceflight and hope to do more aerospace related research in the future.

Robert T. Brockman II
Rice University Computer Science, Lovett '11. I'm interested in artificial intelligence and neuroscience and hope to do graduate work in one of those fields.

Stamatios Mastrogiannis
Rice University ECE, Brown '11. I'm interested in bionics, cybernetics, and anything that brings man and machine closer together. I plan on going into medical research to further these fields.

[6] This content is available online at <http://cnx.org/content/m33249/1.1/>.
[7] http://www.ces.clemson.edu/~stb/klt/
[8] This content is available online at <http://cnx.org/content/m33250/1.1/>.

9.7 Code[9]

The main pieces of code used to accomplish the stabilization are shown below. There are several addition files needed for the complete program, which are available for download instead of being shown inline:

- tracker.c[10]
- im2_jpeg.c[11]
- imload_bw.m[12]
- write_jpeg_bw.m[13]
- write_jpeg_col.m[14]

l2aff.m

```
    % Least Squares Affine Transformation
% ELEC 301 Group Project
% 11/29/2009
% Jeffrey Bridge, Robert Brockman II, Stamatios Mastrogiannis
%
% Calculate the least squares affine transformation for two corresponding
% sets of pixel locations.
% px inputs are of the form:
%[ x_1 y_1
%  x_2 y_2
%  :   :
%  x_N y_N ]
%
% [x'] = [a, b] * [x] + [e]
% [y']   [c, d]   [y]   [f]

function Aff = l2aff(pxold, pxnew)
    b = reshape(pxnew.', [], 1);
    A = makenice(pxold);
    x = pinv(A) * b; % Was psinv, our version of computing the pseudoinv
    Aff = [x(1), x(2), x(5); ...
          x(3), x(4), x(6)];
return

function A = makenice(pxold)
    [r, c] = size(pxold);
    A = zeros(2*r, 6);
    for k=1:r
        x = pxold(k,1);
        y = pxold(k,2);
        %correspond to a, b, c, d, e, f
        A(2*k-1, :) = [x, y, 0, 0, 1, 0];
        A(2*k  , :) = [0, 0, x, y, 0, 1];
    end
return
```

[9] This content is available online at <http://cnx.org/content/m33253/1.1/>.
[10] See the file at <http://cnx.org/content/m33253/latest/tracker.c>
[11] See the file at <http://cnx.org/content/m33253/latest/im2_jpeg.c>
[12] See the file at <http://cnx.org/content/m33253/latest/imload_bw.m>
[13] See the file at <http://cnx.org/content/m33253/latest/write_jpeg_bw.m>
[14] See the file at <http://cnx.org/content/m33253/latest/write_jpeg_col.m>

aff_mul.m

```
    % ELEC 301 Group Project
% 2009 December 12
% Jeffrey Bridge, Robert Brockman II, Stamatios Mastrogiannis
%
% Combine two affine transforms into one
%
% Aff = [a b e
%        c d f]
%
% [x'] = [a, b] * [x] + [e]
% [y']   [c, d]   [y]   [f]

function Aff = aff_mul(Aff2, Aff1)
a1 = Aff1(1,1);
b1 = Aff1(1,2);
c1 = Aff1(2,1);
d1 = Aff1(2,2);
e1 = Aff1(1,3);
f1 = Aff1(2,3);

a2 = Aff2(1,1);
b2 = Aff2(1,2);
c2 = Aff2(2,1);
d2 = Aff2(2,2);
e2 = Aff2(1,3);
f2 = Aff2(2,3);

Aff = [...
    a2*a1 + b2*c1, ...
    a2*b1 + b2*d1, ...
    a2*e1 + e2; ...
    c2*d1 + c2*a1, ...
    c2*b1 + d1*d2, ...
    d2*f1 + f2];
return
```

stabilize.m

```
    % Perform video stabilization on a set of jpeg images
% ELEC 301 Group Project
% 11/29/2009
% Jeffrey Bridge, Robert Brockman II, Stamatios Mastrogiannis
%
% Uses KLT features generated via track_destabilize.sh
%  or track_movie.sh
% Reads destabilized stream of jpegs from stabilize_input
% Outputs stabilized stream of jpegs to stabilize_output
%
% Use view_stabilize.sh to play back results
%
function stabilize()
```

```
% Read feature table.  x and y contain coordinates of each feature
% for each frame.  val is used to determine whether a feature has been
% replaced.
[x,y,val] = klt_read_featuretable('stabilize_input/features.txt');
% x, y are sets of column vectors, which we like.

% Extract number of features and frames from feature table.
[nFeatures, nFrames] = size(x);

invalid_inds = [];

% Each frame will have an affine transformation which allows it
% to be transformed back into the coordinates of the original frame.
% (These transforms will then be filtered to keep low-speed drift.)
Affs = zeros(nFrames,6);

% Affine transformation starts out as the identity transformation.
myAff = [1 0 0; 0 1 0];

% Iterate over all input frames
for n = 2:nFrames
    fprintf('processing features for frame %d...', n);

    % Position of features in previous frame.
    pxold = [ x(:,n-1) y(:,n-1) ];
    % Position of features in new frame.
    pxnew = [ x(:,n) y(:,n)];

    % Features which have replaced those that have left the scene
    % have non-zero values in the feature table.  These must be excluded
    % from computing our affine transformation
    ind = find(val(:,n) ~= 0);
    invalid_inds = ind;

    % These are the indices of valid rows in our feature table
    valid_inds = setdiff([1:nFeatures].', invalid_inds);
    fprintf(' only %d features left\n', length(valid_inds));

    % Extract valid features.
    valid_pxold = pxold(valid_inds,:);
    valid_pxnew = pxnew(valid_inds,:);

    % Compute affine transformation which minimizes least squares
    % difference in distances between features in the previous frame
    % vs. the new frame transformed back to the original coordinates.
    aff = l2aff(valid_pxold, valid_pxnew);

    % Combine this "frame-by-frame" transformation with those from
    % all previous frames to get an affine transformation that will
    % transform the current frame into the coordinate system of the
```

```
    % FIRST frame.

    myAff = aff_mul(aff, myAff);

    % Make the resulting transform into a vector for ease of filtering
    % and add it to the array of transforms for each frame.
    Affs(n,:) = reshape(myAff,1,[]);
end

% High-pass filter the series of affine transformations to allow low
% frequency movement (panning, etc.) to show up in the final output.
%
% We do this by first low-pass filtering the series and then subtracting
% the result from the original.
%%{
switch 2 % Choose a filter
    case 1 % Butterworth filter
        [b, a] = butter(4,.05);
    case 2 % Gaussian filter
        b = exp(-linspace(-3,3,41).^2/2);
        b = b / sum(b);
        a = [1];
    otherwise
        error('Bad filter number');
end
filter_a = a;
filter_b = b;

% Pad beginning of transformation series with identity transforms
% to eliminate startup distortion.
eyeAff = [1 0 0 1 0 0];
prepCount = 1;
filtinAffs = [eyeAff(ones(prepCount,1),:); Affs(2:end,:)];

% LFP the affine transforms TWICE, the second time in time-reversed
% sequence.  This eliminates phase distortion caused by the filter.
LpAffs = filtfilt(filter_b, filter_a, filtinAffs);
LpAffs = LpAffs(prepCount:end,:); % Remove padding

% HPF by subtracting LPF'd series from original.
Affs = Affs - LpAffs;

% Add back 1's in corners of rotation matrix component of transform
% removed by LPF. (Add back in identity transform)
Affs(:,1) = Affs(:,1) + 1;
Affs(:,4) = Affs(:,4) + 1;
%}

% Apply affine transforms to each frame to provide video stabilization.
%%{
for n = 2:nFrames
```

```
    % Get transform back into matrix form.
    aff = reshape(Affs(n,:),2,3);

    fprintf('interpolating image %d...\n', n);
    disp(aff);

    filename = sprintf('stabilize_input/D%08d.jpg', n);

    % Black and white output is 3x faster to compute.
    if 1
        A = imread(filename);

        Ar = single(A(:,:,1));
        Ag = single(A(:,:,2));
        Ab = single(A(:,:,3));

        %B is image in coordinate system of first frame.
        Br = im_unaff(Ar, aff);
        Bg = im_unaff(Ag, aff);
        Bb = im_unaff(Ab, aff);
        B = cat(3,Br,Bg,Bb);
        write_jpeg_col(B,sprintf('stabilize_output/S%08d.jpg',n));
    else
        A = imload_bw(filename);
        B = im_unaff(A, aff);
        write_jpeg_bw(B,sprintf('stabilize_output/S%08d.jpg',n));
    end
end
%}
return
```

destabilize.m

```
    % Generate Synthetic unstable test data
% ELEC 301 Group Project
% 11/29/2009
% Jeffrey Bridge, Robert Brockman II, Stamatios Mastrogiannis

function destabilize()

% Load a big source image, and split it into colors
filename = 'destabilize_input.jpg';
A = imread(filename);
Ar = single(A(:,:,1));
Ag = single(A(:,:,2));
Ab = single(A(:,:,3));

% Size of output image to generate, a subset of the source image
output_w = 560;
output_h = 400;

% Center of source image
[r,c] = size(Ar);
```

```
center_row = r/2;% - 50;
center_col = c/2;

% Number of output frames to generate
N = 300;

% Standard deviation of jerky movement in pixels
dev = 5;

% Parameters controlling slow drift
drift_radius = 10;
drift_period = 100;

for n = 1:N
    fprintf('Generating destabilized image %d...\n', n);

    % Add in slow drift of the image center
    drift_rows = drift_radius * sin(n*2*pi/drift_period);
    drift_cols = drift_radius * cos(n*2*pi/drift_period);

    % Add in fast random jerky movements
    offset_rows = floor(randn(1) * dev);
    offset_cols = floor(randn(1) * dev);

    % Calculate current image boundaries
    left = floor(center_col + drift_cols - output_w/2 + offset_cols);
    right = left + output_w - 1;
    top = floor(center_row + drift_rows - output_h/2 + offset_rows);
    bottom = top + output_h - 1;

    % Grab an offset portion of the larger image
    Br = Ar(top:bottom, left:right);
    Bg = Ag(top:bottom, left:right);
    Bb = Ab(top:bottom, left:right);

    % Save it to its own file
    B = cat(3,Br,Bg,Bb);
    write_jpeg_col(B,sprintf('destabilize_output/D%08d.jpg',n));
    % Play back with view_destabilize.sh
end

return
```

im_unaff.m

```
    % IMage UNdo an AFFine transformation
% ELEC 301 Group Project
% 11/29/2009
% Jeffrey Bridge, Robert Brockman II, Stamatios Mastrogiannis
%
% --- INPUTS ---
% Z = image matrix (2D grid of intensities)
% Aff = affine transformation
```

```
%   [a b  e
%    c d  f]
% [x'] = [a b]*[x] + [e]
% [y']   [c d] [y]   [f]
%
% --- OUTPUTS ---
% ZI = output image matrix

function ZI = im_unaff(Z, Aff)
% Extract size of image.
[r,c] = size(Z);

% Extract affine transformation coefficients.
Aa = Aff(1,1);
Ab = Aff(1,2);
Ac = Aff(2,1);
Ad = Aff(2,2);
Ae = Aff(1,3);
Af = Aff(2,3);

% generate new sets of grid points
[X0,Y0] = meshgrid(1:c, 1:r);
% XI(c,r) and YI(c,r) contain where to look in Z for the correct
% intensity value to place in the new image ZI at coordinates (r,c).
XI = Aa*X0 + Ab*Y0 + Ae;
YI = Ac*X0 + Ad*Y0 + Af;

% Since XI and YI contain non-integer values, a simple lookup will not
% suffice.  We must perform interpolation.
ZI = interp2(Z, XI, YI);

return
```

9.8 Future Work[15]

Future Work
Now that we basic algorithms down, the focus should be on improving the speed so we can get real-time stabilized video feed while operating our UAV. This means converting the code to C. It may also be necessary to use KLT trackers that use the video card GPU, as well as writing an equivalent of the MATLAB interp2 that does the same.

While taking the first steps towards this conversion, we realized that our video stabilizer would make a pretty cool GStreamer plugin. GStreamer[16] is a media framework for the open-sourse Gnome desktop environment. With it, we will be able route video sources of many kinds through our stabilizer and then on to our choice of video sinks. We have already figured out how to implement a "null" plugin that just copies frames from the source to the sink already, so once our algorithms are in C using GStreamer should be easy.

If these improvements can be made, the next step will be to test the code out with live footage from our own UAV.

[15] This content is available online at <http://cnx.org/content/m33254/1.1/>.
[16] http://gstreamer.freedesktop.org/

Chapter 10

Facial Recognition using Eigenfaces

10.1 Facial Recognition using Eigenfaces: Introduction[1]

10.1.1 Introduction

10.1.1.1 Facial Recognition Preface

Although humans have an amazing ability to distinguish and recognize faces, facial recognition on computers is an advanced field of study yet to be perfected. Only within the past decade have people seen the rise of face tracking in digital cameras and public security systems. Unlike humans, computers are easily confused by changes in illumination, variation in face angles, and accessories such as hair, glasses, and hats. However, computer face recognition is worth pursuing, because of the wealth of applications in security, digital photography, social networking, and other fields. This project uses the eigenface method to identify faces from still images.

[1] This content is available online at <http://cnx.org/content/m33173/1.3/>.

Figure 10.1: A potential face recognition/X-Ray technology application.

10.1.1.2 Facial Recognition Approach

When considering the proper approach for identifying faces, it was decided that the approach to be able to deal with imperfect settings such as different relative positions, sizes, and shapes of facial features such as the eyes, nose, cheekbones, and jaw. While facial features are a major component of some facial recognition algorithms, the extraction of landmarks were determined to be insufficiently robust for this project without a powerful normalization algorithm capable of features such as keeping a constant light intensity, correction of angles and pose variations, and accounting for accessories like glasses.

10.2 Facial Recognition using Eigenfaces: Background[2]

10.2.1 Background

10.2.1.1 Computational Implementations

Current facial recognition algorithms can be separated into two groups: geometric and statistical. The geometric approach looks into the distinguishing features of the face. The other algorithms are photometric, a statistical approach that distills an image into values and compares those values with those from a template or training set to eliminate variances. Some popular recognition algorithms include Principal Component Analysis (eigenfaces), Linear Discriminate Analysis, Elastic Bunch Graph Matching (fisherfaces), the Hidden Markov model, and dynamic link matching.

10.2.1.2 Eigenfaces

We decided to use eigenfaces for this project. Eigenfaces are created using a statistical tool called **Principal Component Analysis (PCA)**. Eigenfaces are useful because they focus on the differences between the

[2]This content is available online at <http://cnx.org/content/m33174/1.5/>.

data points (i.e., the small variations in eye shape, nose size, and skin color that humans unconsciously and effectively use to tell each other apart). Eigenfaces can be speedily extracted from large data sets, so this method is very applicable to our project.

However, the eigenface method has one major drawback: it is greatly affected by non-homogenous conditions. For example, Matthew Turk and Alex Pentland of MIT found that the eigenface approach identified a face correctly 96% of the time with lighting variation, 85% with orientation variation, and only 64% with size variation (1). Therefore, we decided to focus on one variable: lighting, background, face angle, position, or expression, and keep all the others constant. Our pictures were taken in a well-lit room against a white background, with the subject directly facing the camera, without accessories such as hats and glasses. We found that facial expressions were the most fun variable and decided to focus on that.

We worked with two databases: Rice University, which we created, and JAFFE (Japanese Female Facial Expression) from http://face-rec.org/[3] . The JAFFE database consists of 10 Japanese women, each expressing each of seven emotions. For the Rice database, we chose students of both genders and diverse ethnicities. Each subject was told to express each of six emotions: neutral, happy, sad, surprised, angry, and disgusted. We had sixteen subjects, each with six emotions, and we took two pictures per emotion, resulting in a database of 192 images. We used Matlab to process the images and create eigenfaces.

10.3 Facial Recognition using Eigenfaces: Obtaining Eigenfaces[4]

10.3.1 Obtaining Eigenfaces

10.3.1.1 Eigenface Concept

Each image is loaded into a computer as a matrix of different intensities. All the images were converted to gray scale so that we only need to operate on one layer of image (instead of three layers for a RBG image). A vector whose direction is unchanged when multiplied by the matrix is referred to as an eigenvector of that matrix. The eigenvectors of the covariance matrix associated with a large set of faces are called eigenfaces. The eigenfaces can be thought of as a basis for the set of faces. Just as any vector in a vector space is composed of a linear combination of the basis vectors, each face in the set can be expressed as a linear combination of the eigenfaces.

10.3.1.2 Format Input Data

To compute the eigenfaces, a portion of a given dataset is first chosen randomly to be the training set. The images in the training set are used to construct the image matrix A (Note: All images in the dataset must have the same dimensions). The training set can be chosen by selecting a given percentage of the dataset or by selecting a given number of images per person from the database. Once the images are selected, each image Ii is vectorized into a column vector Pi such that its length equals to the total number of pixels in the image. This process brings the mathematics of all the computations down to a lower-dimensionality space.

$$I = N \times M \quad \Rightarrow \quad P_i = 1 \times \mathrm{NM} \tag{10.1}$$

[3] http://face-rec.org/

[4] This content is available online at <http://cnx.org/content/m33183/1.6/>.

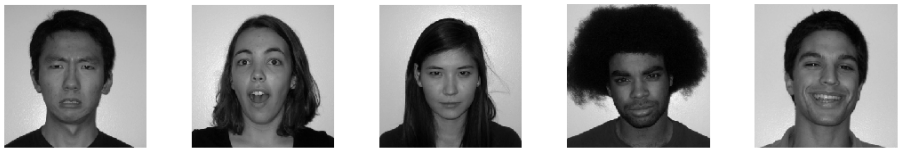

Figure 10.2: Sample training images

The mean face of the training set is computed and subtracted from all the images within the training set (given W images in the training set).

$$\mu = \frac{1}{W} \sum_{i=0}^{W} P_i \tag{10.2}$$

$$V_i = P_i - \mu \tag{10.3}$$

Figure 10.3: Mean face of HFH dataset

Finally, the mean subtracted training images are put into a single matrix of dimension NM x W, forming the image matrix A.

$$A = \begin{bmatrix} V_1 & V_2 & V_3 & \dots & V_W \end{bmatrix} \tag{10.4}$$

10.3.1.3 Compute Eigenfaces

Typical PCA calculation would first retrieve the covariance matrix C. Covariance measures the relation of how much two random variables vary together such that if the covariance is positive when both dimensions

increase together and negative when they are inversely proportional. The eigenfaces were then obtained by computing the eigenvectors of the covariance matrix C. This computation will yield NM unique eigenvectors.

$$C = \mathrm{A}\mathrm{A}^T \tag{10.5}$$

$$\mathrm{cov}\,(X,Y) = \frac{\sum (x_i - \overline{x})\,(y_i - \overline{y})}{n-1} \tag{10.6}$$

But in the case of this project, these resulting matrix of dimension NM x NM was way too large for MATLAB to process. Furthermore, even if MATLAB had the ability to process such a large matrix it would still later be too computationally intensive. Instead of computing the covariance matrix C directly, this project utilizes a smaller matrix S with dimensions W x W that can still be able to compute the eigenfaces efficiently. This simplification stems from the fact that the *rank* of the covariance matrix C is limited by the number of images in the training set. Since there are at most W-1 non-trivial eigenfaces for C, there is no need to compute all of the eigenfaces for the dataset. This simplification will prove to be useful as long as $NM \gg W$.

$$S = A^T A \tag{10.7}$$

The smaller matrix dimensions will be computationally effective later when large databases will be sorted through since only W eigenvalues and eigenfaces will be used.

Now, using some linear algebra tricks, we could show that the eigenvalues of C and S are the same and that the top W eigenvectors of C (ui) can be obtained from the eigenvectors of S (vi).

$$\begin{aligned}
\mathrm{S}\mathrm{v}_i &= \lambda_i v_i \\
\mathrm{A}^T\mathrm{A}\mathrm{v}_i &= \lambda_i v_i \\
\mathrm{A}\mathrm{A}^T\mathrm{A}\mathrm{v}_i &= \lambda_i \mathrm{A}\mathrm{v}_i \\
\mathrm{C}\mathrm{A}\mathrm{v}_i &= \lambda_i \mathrm{A}\mathrm{v}_i \\
\mathrm{C}\mathrm{u}_i &= \lambda_i u_i
\end{aligned} \tag{10.8}$$

In this manner, we can see that the eigenvectors of C can be derived from

$$\mathrm{A}\mathrm{v}_i = u_i \tag{10.9}$$

where the computation of vi's were much less computationally extensive than the direct computation of ui's.

These *ui* vectors will constitute the columns of the eigenfaces.

Eigenface = $[u_1 \quad u_2 \quad u_3 \quad \ldots \quad u_W$

10.3.1.4 Top K Eigenfaces

Even with this complexity reduction, it is still redundant to use all W eigenfaces for the reconstruction process. We could reduce the number of eigenfaces used even more by indentifying the eigenfaces that contain more content than the others. To determine this property, we bring our attentions to the eigenvalues that correspond to the individual eigenfaces. We immediately see that there are some eigenfaces that have higher eigenvalues than the others.

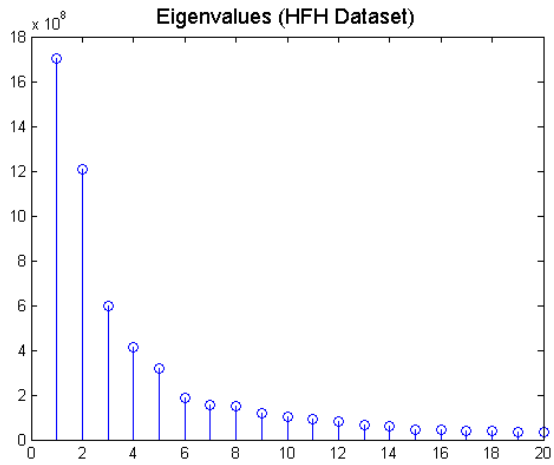

Figure 10.4: Eigenvalues of the corresponding eigenfaces of HFH dataset

After arranging the eigenvalues in descending order, the result becomes clearer. We conclude that the eigenfaces corresponding to high eigenvalues contain more content. In other words, the higher the eigenvalue, the more characteristic features of the face the particular eigenvector describes. Therefore, we simplify the reconstruction process by only using the top K eigenfaces. This completes the training process of our implementation.

Figure 10.5: Top 5 eigenfaces of HFH dataset

Figure 10.6: Last 5 eigenfaces of HFH dataset

In terms of the eigenfaces themselves, we found that the more important eigenfaces (those with higher eigenvalues) had lower spatial frequency than the less important eigenfaces (those with lower eigenvalues). This is apparent in the figure above, where the first eigenfaces look blurry and indistinct, and the later eigenfaces have sharp edges and look more like individual people. This suggests that faces can be identified based on their low-frequency components alone.

10.3.2 Eigenface Recognition Face Datasets

10.3.2.1 Test 1 (JAFFE database)

For the first test of this project's eigenface generation algorithm, the Japanese Female Facial Expression (JAFFE) Database was used. The JAFFE database fit our ideal conditions of similar lighting conditions, solid white backgrounds, and normalization of facial features such as the nose, eyes, and lips. The database is a set of 180 images of seven facial expressions (six basic facial expressions and one neutral).

10.3.2.2 Test 2 (Rice University)

For the Rice database, we chose students of both genders and diverse ethnicities. Each subject was told to express each of six emotions: neutral, happy, sad, surprised, angry, and disgusted. We had sixteen subjects, each with six emotions, and we took two pictures per emotion, resulting in a database of 192 images. We also created a special database of two emotions: closed eyes and expression of choice, to be used for demonstration at the poster session.

10.3.2.3 Algorithm Concept

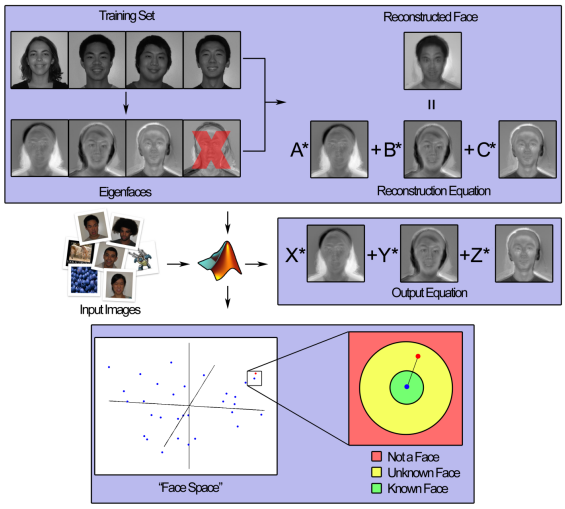

Figure 10.7: Diagram of eigenface computation and input with our algorithm. Also, a visual representation of K-dimensional "face space" and threshold setting between test image reconstruction (red dot) and closest match image reconstruction (blue dot)

10.4 Facial Recognition using Eigenfaces: Projection onto Face Space[5]

10.4.1 Projection onto Face Space

10.4.1.1 Compute Weight Matrix

Now that we have the eigenfaces, we could proceed to projecting the training images onto the face space. The K-dimension face space is spanned with the top K eigenfaces. An interesting thing to note here is that each axis of the face space is weighted with respect to the eigenvalue associated with it. So the first few axes will contain more weight than the later axes.

To project the mean-subtracted training images Vi's onto the face space, we first take each image and compute its weight wi on each of the axis by taking the dot product between the image and an eigenface. This process is repeated for each eigenface with each training image. The resulting weights are put into a weight matrix WM with a dimension of K x W.

$$V_j = w_1 u_1 + w_2 u_2 + ... + w_k u_k \tag{10.10}$$

[5]This content is available online at <http://cnx.org/content/m33182/1.6/>.

$$\text{WM} = \begin{bmatrix} (w_1)_{V_1} & (w_1)_{V_2} & \dots & (w_1)_{V_W} \\ (w_2)_{V_1} & (w_2)_{V_2} & \dots & (w_2)_{V_W} \\ (w_3)_{V_1} & (w_3)_{V_2} & \dots & (w_3)_{V_W} \\ \dots & \dots & \dots & \dots \\ (w_k)_{V_1} & (w_k)_{V_2} & \dots & (w_k)_{V_W} \end{bmatrix} \tag{10.11}$$

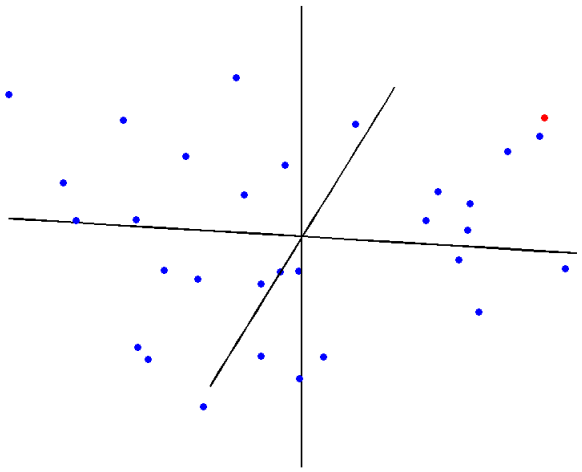

Figure 10.8: Projection of training images (blue dots) and test image (red dot) onto the 3-dimensional face space

10.4.1.2 Compute Threshold Values

When given a test image (red dot), it is first projected onto the face space using the same method as before and then categorized using some threshold values. By testing these and graphing the minimum distance between each test image and the closest image in the training set, we were able to experimentally come up with the thresholds. The following graph shows the result of a particular run on the HFH dataset.

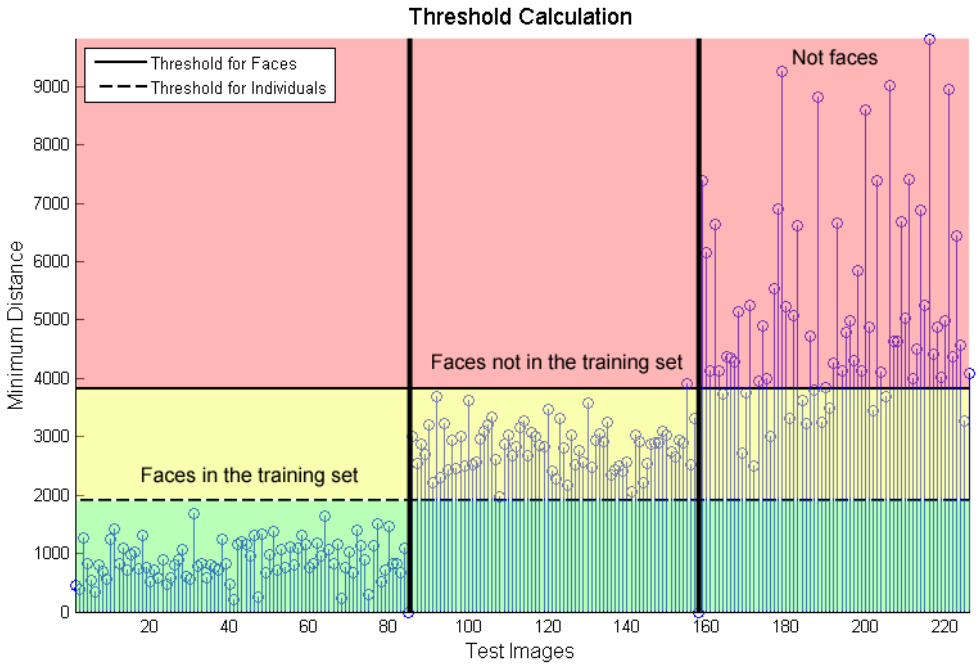

Figure 10.9: Minimum distances of various test images to determine thresholds

This graph shows the minimum distance between each test image and the closest image in the training set. Images 0-91 represent faces in the training set, images 92-160 are faces not in the training set, and images 161-225 are images that are not faces. Because the training set is randomly selected from our databases, the thresholds vary each time the code is run. The thresholds are dynamic values that change with respect to the furthest distance d between any two training images. However, a trend emerged after looking at the data, and we determined that the thresholds were to be set at 10% $(0.1d)$ and 20%$(0.2d)$ of the maximum distance between two faces in the training set for determining if it was a match and whether or not the image was a face at all, respectively. These thresholds are used when determining the success or failure of recognition for both the JAFFE and Rice University datasets.

As the figure shows, in this particular run, our algorithm successfully identified all faces in the training set as known faces. Similarly, all but one of the unknown faces fell within the correct threshold. However, our algorithm had some trouble identifying images that were not faces: about $\frac{1}{4}$ of them were identified as unknown faces. We think this occurred because some non-face images had the same round shape as a face (fruit, for example), or had features (animals). Despite this weakness, our algorithm was successful overall.

10.5 Facial Recognition using Eigenfaces: Results[6]

10.5.1 Results

10.5.1.1 JAFFE Results

For the JAFFE database, our algorithm recognized a new photo of the person 65% to 75% of the time. We defined recognition as successfully matching a test image to a picture of the same person from the training

[6] This content is available online at <http://cnx.org/content/m33181/1.6/>.

set, even though the two images had different expressions. Recognition rate increased dramatically as we increased the number of eigenfaces, but stabilized after four eigenfaces (that is, our recognition rate did not increase by using more than four eigenfaces). The recognition rate also increased when we used more test images per person in the training set. Similarly, the recognition rate increased when we used a greater percentage of the dataset in the training set (with pictures chosen randomly from the dataset).

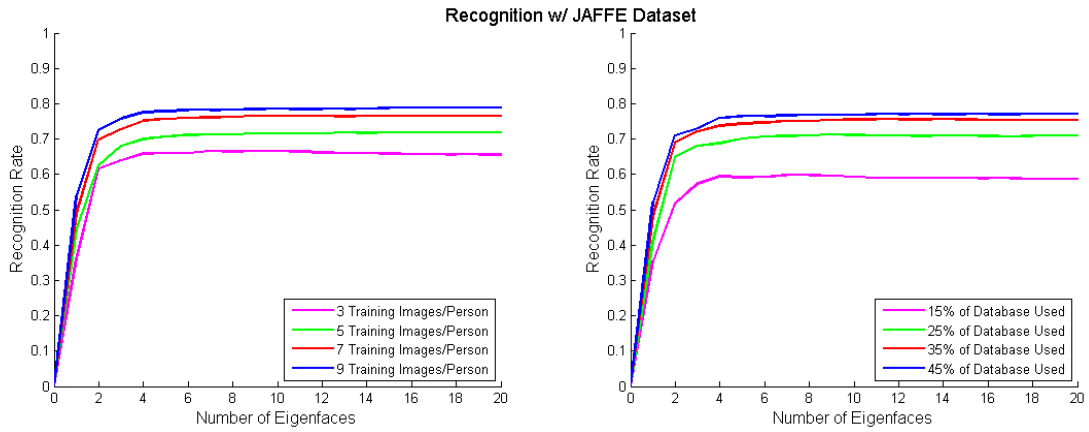

Figure 10.10: Results when varying the number of training images per person & the percent of database used to as input images

10.5.1.2 Rice University Field Test Results

For the Rice University database, our algorithm recognized a new photo of the person 65% to 75% of the time. Again, recognition rate increased dramatically as we increased the number of eigenfaces. In this case, the recognition rate stabilized after six eigenfaces. The recognition rate required more eigenfaces to stabilize because the Rice database was more diverse, including people of both genders and many different ethnicities. Therefore, more eigenfaces are needed for an accurate representation of the Rice population. Again, the recognition rate increased when we used more test images per person in the training set. The recognition rate also increased when we used a greater percentage of the dataset in the training set.

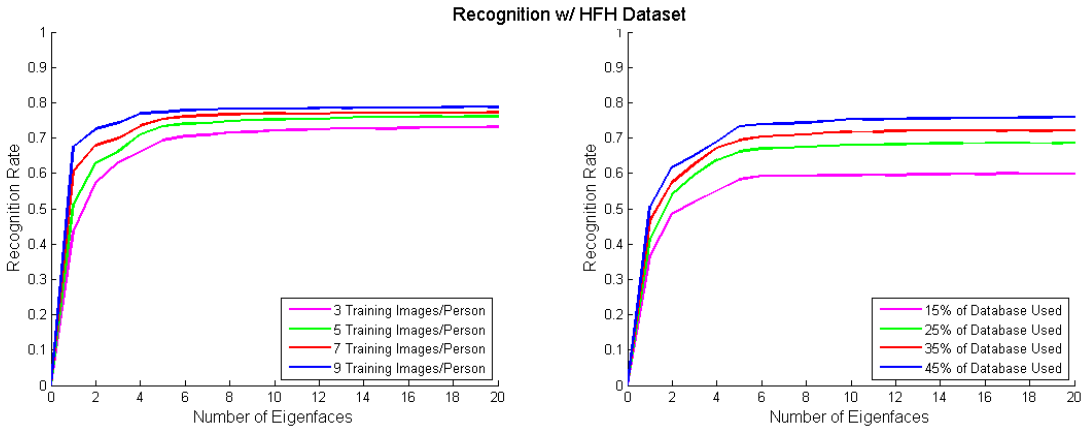

Figure 10.11: Results when varying the number of training images per person & the percent of database used to as input images

The resulting final algorithm was able to determine, at the four rates shown in the previous two figures, whether a test image was a non-face or face and also a match to known face, finding the closest match to a known face (as shown below).

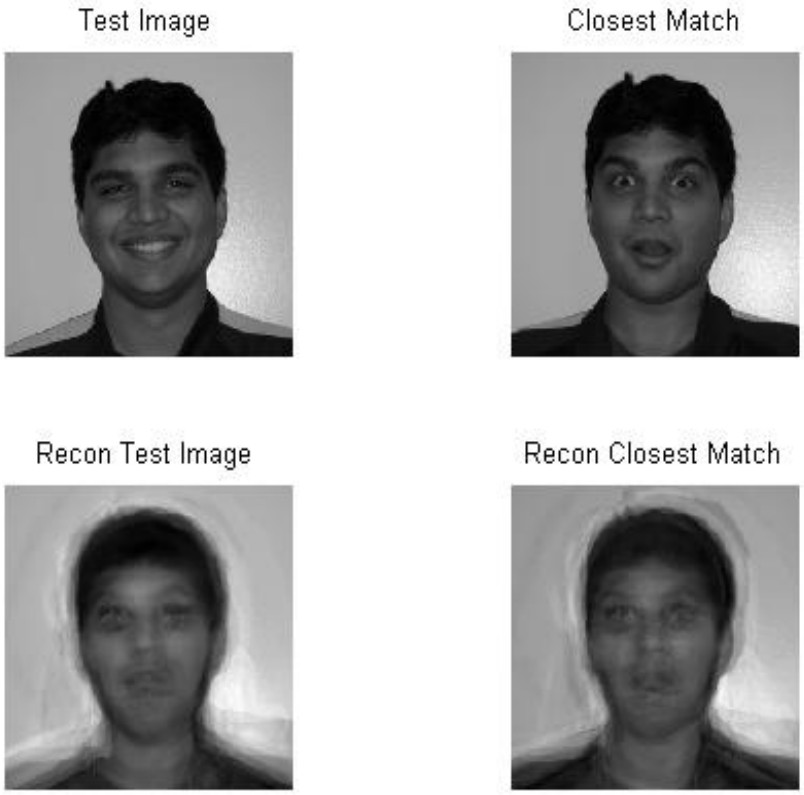

Figure 10.12: Counterclockwise from top left: Sample test image taken as input; test image reconstructed using eigenfaces; closest reconstructed image match; corresponding closest match image.

10.6 Facial Recognition using Eigenfaces: Conclusion[7]

10.6.1 Conclusion

This project yielded fairly accurate face detection results using the eigenface method. Interestingly, we found that a database of some 200 images can be accurately represented with only about 6 eigenfaces. This demonstrates that the eigenface method is useful for its ability to compress large datasets into a small number of eigenfaces and weights. We predict that our results will scale, that is, the number of eigenfaces needed to represent a database of 1,000 or 1,000,000 images will be far fewer than the number of images. Based on our results, we hypothesize that more diverse datasets require slightly more eigenfaces for accurate representation. Our project demonstrates that the eigenface method is an efficient and accurate technique for facial recognition.

[7] This content is available online at <http://cnx.org/content/m33177/1.4/>.

10.6.1.1 Further work

To improve the results of the eigenface method implemented, a normalization program could be developed to determine the facial metrics and normalize the photos such that facial features are held in constant positions and contrast and light intensities between photos are balanced. Localizing of the features would keep head positions fairly consistent and yield better eigenfaces.

Creating a program to extract faces from their environment (for example, by using a matched filter) would expand the possible applications of this project. Individual faces could be extracted from security cameras or group pictures.

A larger and more diverse dataset would also increase face identification and recognition. We would like to include people of diverse ages, since everyone in both the JAFFE and Rice datasets was in their teens or twenties. Increasing the size and quality of the dataset would boost the recognition rate. We would like to see how many eigenfaces are needed to represent a dataset of 1,000 or 1,000,000 images.

Because both our datasets have emotions as a variable, it would be interesting to create an "emotion detector", as was done with the JAFFE data. Despite the fact that emotions look different on every person (fear was found to be an especially problematic emotion), emotion recognition rates of over 67% were attainedusing Gabor wavelets[2] . It would be interesting to see how the eigenface method compares.

10.6.2 Facial Recognition Source Codes

- If you would like to try out out our facial recognition code for yourself, you can download them here[8]. This code allows you to input one test image and matches it to the closest image in the given dataset. The JAFFE dataset is included for testing.
- If you would like to test with our full code or to obtain the HFH dataset, please contact Aron Yu (aron.yu@rice.edu[9])
- GUI version of the code coming soon...

10.7 Facial Recognition using Eigenfaces: References and Acknowledgements[10]

10.7.1 References and Acknowledgements

Team members:

- Catherine Elder (cje1@rice.edu)
- Norman Pai (nlp1@rice.edu)
- Jeffrey Yeh (jwy1@rice.edu)
- Yingbo "Aron" Yu (yy4@rice.edu)

We would like to thank Manjari Narayan, our advisor for this project, for all her help. Finally, we would like to thank professor Richard Baraniuk and Matthew Moravec for the opportunity to work on this project.

10.7.1.1 References

1. Zhao, W. et al. "Face Recognition: A Literature Survey." ACM Computing Surveys, Vol. 35, No. 4, December 2003, pp. 399–458
2. M. Turk and A. Pentland (1991). "Face recognition using eigenfaces[11] ". Proc. IEEE Conference on Computer Vision and Pattern Recognition. pp. 586–591

[8] See the file at <http://cnx.org/content/m33177/latest/SingleRun.rar>
[9] aron.yu@rice.edu
[10] This content is available online at <http://cnx.org/content/m33180/1.3/>.
[11] http://www.cs.ucsb.edu/~mturk/Papers/mturk-CVPR91.pdf

3. JAFFE image database – "Coding Facial Expressions with Gabor Wavelets", Michael J. Lyons, Shigeru Akamatsu, Miyuki Kamachi, Jiro Gyoba < http://www.kasrl.org/jaffe.html[12] >.
4. "Introduction to Fourier Transforms for Image Processing." <http://www.cs.unm.edu/∼brayer/vision/fourier.html[13] >.
5. "Face Recognition Using Eigenfaces." <http://www.cs.princeton.edu/∼cdecoro/eigenfaces/[14] >.
6. Pissarenko, Dimitri. "Eigenface-based facial recognition." <http://openbio.sourceforge.net/resources/eigenfaces/eigenfa html/facesOptions.html[15] >.

[12] http://www.kasrl.org/jaffe.html
[13] http://www.cs.unm.edu/∼brayer/vision/fourier.html
[14] http://www.cs.princeton.edu/∼cdecoro/eigenfaces/
[15] http://openbio.sourceforge.net/resources/eigenfaces/eigenfaces-html/facesOptions.html

Chapter 11

Speak and Sing

11.1 Speak and Sing - Introduction[1]

11.1.1 Speech Scaling and Pitch Correction

The speech scaling and pitch correction program, or "Speak & Sing", generates a properly-timed and pitch-accurate sample of a known song from recorded spoken words.

A voice modulation application which detects the timing and pitch of the recorded input and automatically performs time scaling and pitch correction to match the speech to a pre-selected song, producing a musical output.

11.1.1.1 Making a Smarter Autotuner

Pitch correction is used by musicians to improve the sound of song vocals by fixing off-key singing or adding distortion. It can be applied real-time using a synthesizer keyboard or added after recording. However, these "autotuners" can't fix off-tempo singing, and automatic autotuners depend on the singer to be relatively close to the right pitch.

Goals for the Speak and Sing:

- Proof-of-concept of automated syllable detection, time scaling, and pitch correction in one robust application
- Provides open-ended, customizable options for audio processing
- Demonstrates time and frequency DSP applications using MatLab

11.1.1.2 Implementation: An Overview

Recording:

Input voice samples are recorded in mono-channel audio at a sampling frequency of 16,000 (although any sampling frequency can be used). It is then imported into MatLab and the following functions are run in sequence:

Song Interpretation and Retrieval:

Contains data for selected songs based on sheet music. It returns a vector of fundamental note frequencies and note lengths depending on the song selected and the desired tempo.

Available Songs:

1. Christina Aguilera - *Genie in a Bottle*
2. *Mary Had a Little Lamb*

[1] This content is available online at <http://cnx.org/content/m33229/1.1/>.

3. *Row, Row, Row Your Boat*

Syllable Detection

Analyzes the input speech data and determines the locations and lengths of each syllable. After dividing the signal up into several short windowed pieces, it detects the periodicity and energy of each window to determine the type of sound (vowel, consonant, or noise). The locations of the syllables is then determined based on the pattern of sounds.

Time scaling

Interprets the detected syllable locations and stretches or shrinks the syllable to match the length of the word in the song. The time scaling is performed using a time-domain Waveform Similarity Overlap Add (WSOLA) algorithm, which breaks up the signal into overlapping windows and copies each window to a new location, either closer together or further apart. This stretches or compresses the length of the speech without losing quality or information.

Pitch correction

Detects the pitch of the signal, compares it to the desired pitch of the song, and makes pitch corrections. Pitch detection is done using FAST-autocorrelation, in which small windows of the signal are offset and autocorrelated to find the period, and thus frequency, of the signal for that interval. Pitch correction is performed with Pitch Synchronous Overlap Add (PSOLA), which moves windowed segments closer or further apart and overlap-added to alter the frequency without loss of sound.

11.1.1.3 The Result

The resulting audio file sounds like the input speech or singing, but the words will now line up with those of the original song and the pitch will be adjusted. The resulting impact on sound is that the recorded input will now sound more like the song, without compromising the original voice or speech.

11.2 Speak and Sing - Recording Procedure[2]

11.2.1 Recording

Input voice samples are recorded in mono-channel audio with a sampling frequency of 16,000 Hz. The sampling rate chosen allows for a balance of processing efficiency and sound quality – the computation time of the program generally scales linearly with increase in sampling rate. The selected sampling frequency is also convenient for computation, as the MatLab program's wave audio operations perform best with sampling frequencies in increments of 8,000 Hz. The program allows for the use of any sampling frequency and will perform adequately for sampling frequencies up to and beyond the audio standard 44.1 kHz, but processing time and program durability become an issue.

When recording, the best results are produced for input speech or song which is delivered slowly and clearly, with either brief pauses or strongly-enunciated consonants between syllables and words.

The recorded sound is processed in Audacity, a freeware recording software, to trim out excess electrical and environmental noise and remove existing DC offsets. It is then ready for handling in the MatLab environment.

11.3 Speak and Sing - Song Interpretation[3]

11.3.1 Song Interpretation

The songs to be used by the Speak and Sing were predetermined and preprogrammed. For simplicity, the songs feature a one-to-one format. That means every syllable of the lyrics is associated with one duration and one pitch, there are no rests and no slurs. The song interpretation is done in two vectors, one contains

[2]This content is available online at <http://cnx.org/content/m33233/1.1/>.

[3]This content is available online at <http://cnx.org/content/m33237/1.1/>.

all of the durations (in seconds) to be used by the duration matching, and the other contains all of the note frequencies (in hertz) to be used by the pitch matching.

Here is an example of a measure of sheet music that has been turned into a useable vector.

Mary Had a Little Lamb

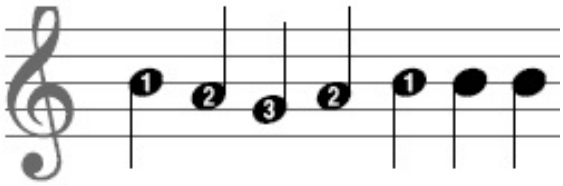

Figure 11.1

```
notes = ([246.94; 220;196; 220; 246.94; 246.94; 246.94;]);
duration = ([.5; .5; .5; .5; .5; .5; .5;]);
```

Three songs were made available for use:

1. Christina Aguilera - *Genie in a Bottle*
2. *Mary Had a Little Lamb*
3. *Row, Row, Row Your Boat*

11.4 Speak and Sing - Syllable Detection[4]

11.4.1 Syllable Detection

The syllable detection algorithm takes as its input recorded speech and produces an output matrix denoting the start and end times of each syllable in the recording. There are two main parts to the algorithm. First, each sound in the input file must be classified as a vowel, consonant, or noise. Second, the algorithm must determine which sequences of sounds correspond to valid syllables.

11.4.1.1 Sound Classification

The sound classification step splits the input signal into many small windows to be analyzed separately. The classification of these windows as vowels, consonants, or noise relies on two core characteristics of the signal: energy and periodicity. Vowels stand out as having the highest energy and periodicity values, noise ideally has extremely low energy, and consonants are everything that falls between these two extremes.

The energy of a window of the input vector W is calculated as

```
E = |W|^2.
```

However it is necessary to set general energy thresholds that are valid for speech samples of varying volume. In order to accomplish this, after the energies of all the windows have been calculated, they are converted into decibels relative to the maximum energy value.

[4]This content is available online at <http://cnx.org/content/m33241/1.1/>.

```
E' = 10*log10(E/max(E)).
```

The energy thresholds are then defined in terms of a percent of the total energy range. For example, if an energy threshold was 25 percent and the energies ranged from -100 to 0 dB, then everything from -25 to 0 dB would be above the threshold.

In some cases, energy alone is enough to determine whether a certain sound is a vowel, consonant, or noise. For instance, here is a plot of the energy vs. time of a recording of the spoken word "cat." It is easy to tell which portions of the figure correspond to vowels, consonants, and noise by inspection:

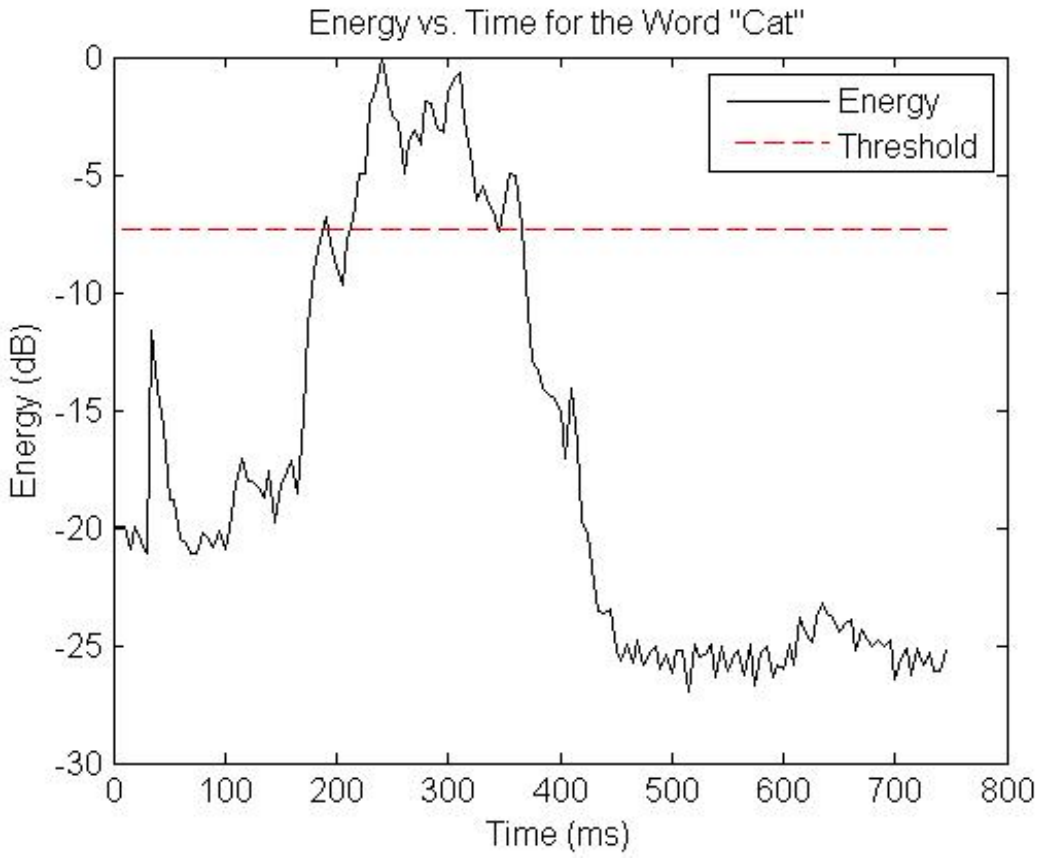

Figure 11.2: The energy threshold clearly divides the high-energy vowel portion of the signal from the consonants.

However, energy cannot always separate vowels and consonants so dramatically. For example, the word "zoo."

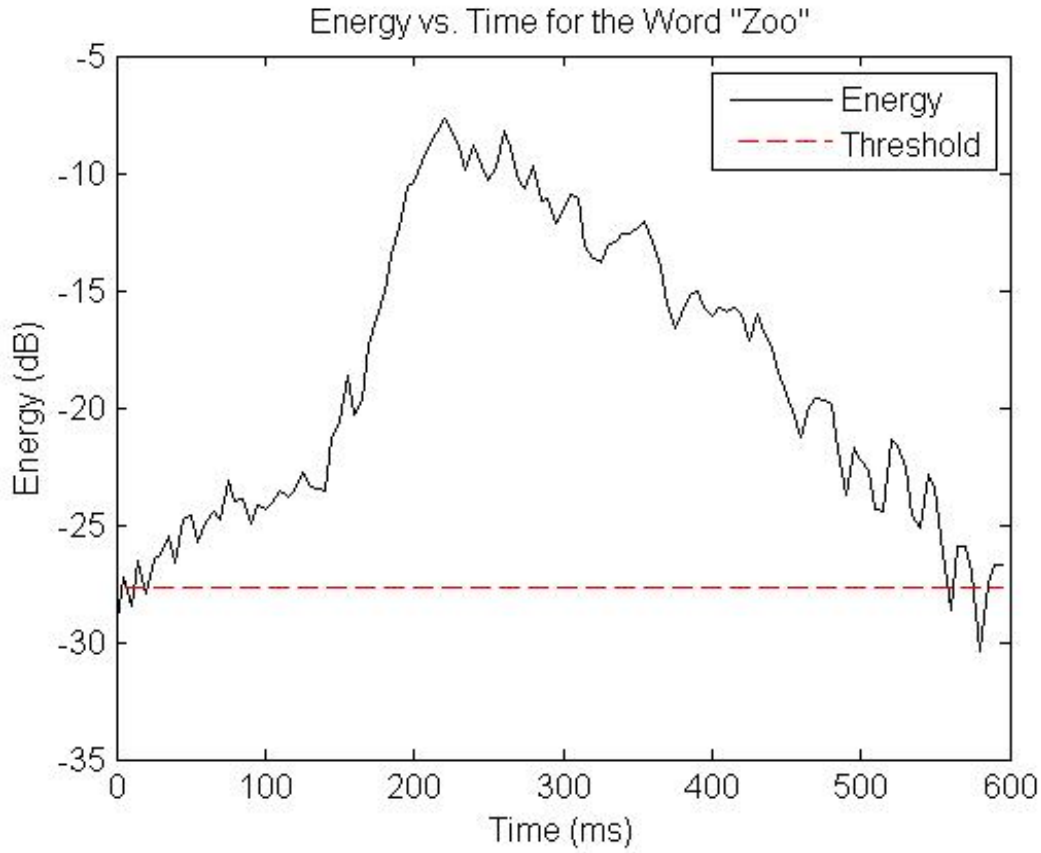

Figure 11.3: The ending vowel sound drops too close to the threshold.

Although a portion of the vowel still has significantly higher energy than the consonant, the ending portion of the vowel drops in energy to the point where it is dangerously close to the threshold. Raising the threshold so that the "z" sound is certain not to be counted as a vowel only makes it more likely that portions of the "oo" sound will be mistakenly classified as consonants. Clearly, additional steps are necessary to more accurately differentiate between consonants and vowels.

11.4.1.2 Periodicity Analysis

The algorithm uses the periodicity of the signal to accomplish this task. The periodicity is obtained using the autocovariance of the window being analyzed. This is calculated as:

```
C(m) = E[(W(n+m)-mu)*conj(W(n)-mu)]
```

Mu is the mean of the window W. It measures how similar the signal is to itself at shifts of m samples and can therefore distinguish periodic signals from aperiodic ones due to their repetitive nature. The autocovariance vector is most stable and therefore most meaningful for values of m relatively close to 0, since for larger m, fewer samples are considered, causing the results to become more random and unreliable. Therefore, the

sound classification algorithm only considers autocovariance values with m less than 1/5 the total window size. These autocovariance values are normalized so that the value at m = 0 is 1, the largest possible value. The maximum autocovariance in this stable region is considered the periodicity of the window.

The periodicity values for vowels are extremely high, while most unvoiced, and some voiced, consonants exhibit very low periodicity. Periodicity is especially useful in detecting fricative or affricate consonants which are both characterized by a great deal of random, possibly high-energy, noise due to their method of articulation. Examples of these consonants include "s," "z," "j," and "ch." The contrast between the periodicity of a fricative consonant and a vowel can be clearly seen in this plot.

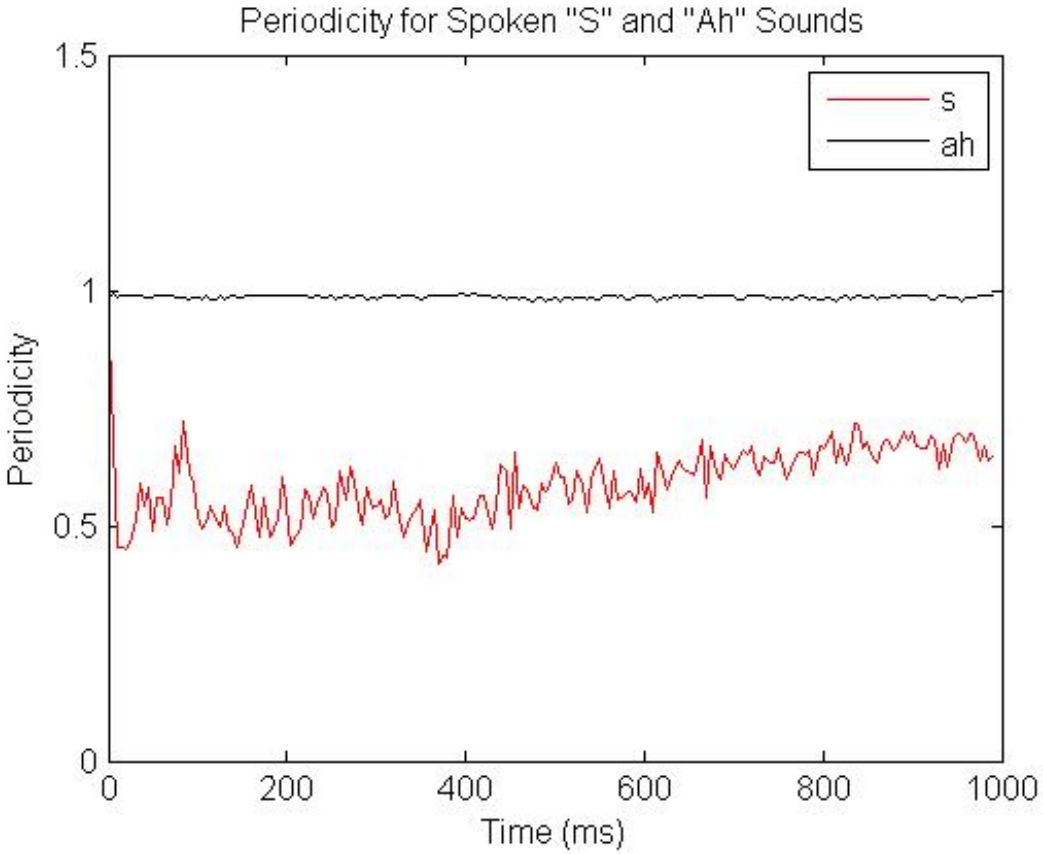

Figure 11.4

Putting it all together, the sound classification portion of the algorithm first calculates the energy and periodicity of each window of the input signal. If both the energy and periodicity are higher than certain thresholds, the window is classified as a vowel. If the energy is smaller than a very low threshold, the window is counted as noise, and everything in between is considered a consonant. Let's take another look at the energy characteristics of the word "zoo" (refer to figure 2). Using this alone, we could not easily distinguish the high-energy "z" from the lower-energy portion of the "oo." However, here is a plot of the periodicity vs. time for the same recording.

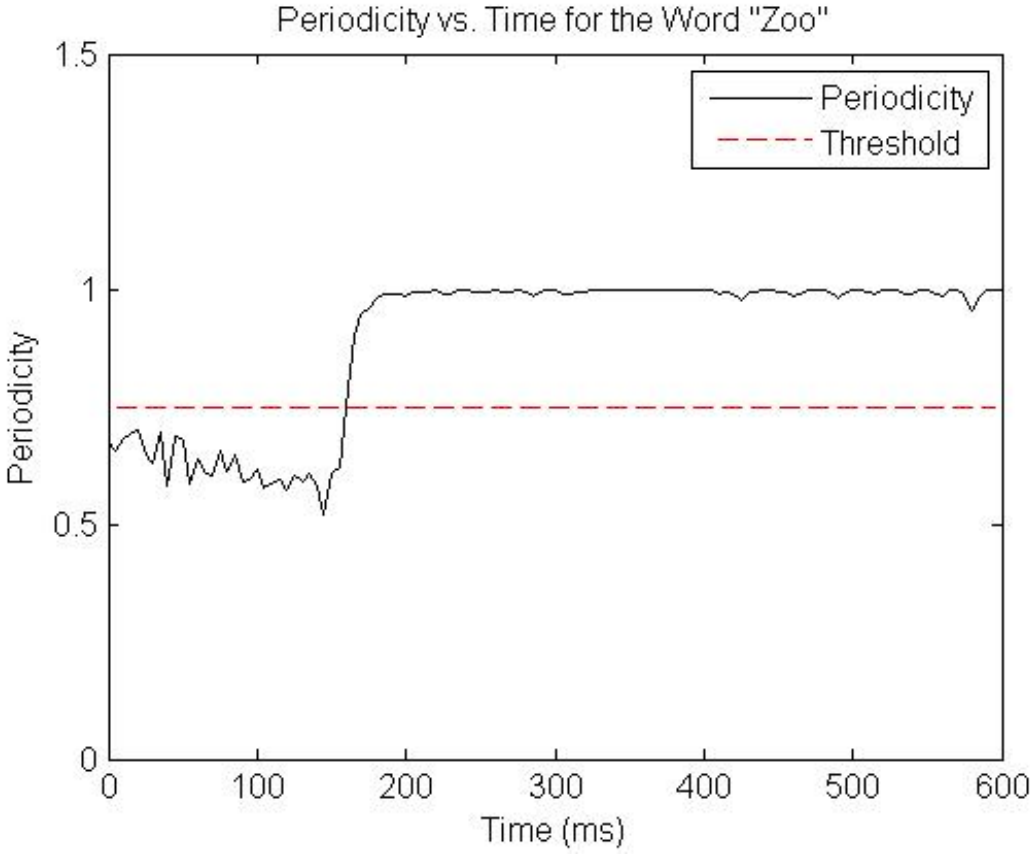

Figure 11.5: The difference between the "z" and the "oo" is now much more pronounced.

This plot shows a clear contrast between the aperiodic fricative "z" and the periodic vowel. Taken together, these data now provide sufficient information for the sound classification algorithm to correctly identify each sound in this recording.

This method works with a reasonable degree of accuracy, but there are a few challenges that must be considered. The greatest among these is the handling of liquid consonants like "l," "y," or "m." In certain cases, these sounds are used as consonants at syllable boundaries, while in other circumstances, they act as a vowel usually would in making up the majority of the syllable. For example, in the word "little," the first "l" is acting as a consonant, but the "l" sound is also used as the central portion of the second syllable. Therefore, these sounds are not always accurately classified, and they must be annunciated strongly in the input recording if they are acting as syllable boundaries.

Another issue with this method is that sometimes it detects short bursts of one sound type in the middle of another. For instance, there may be 1 or 2 consonant windows surrounded by a large number of noise windows or a small number of vowel windows in the middle of a large section of consonant windows. Several situations can lead to errors like this. For example, the background noise in a recording might boost the energy of a window high enough to be classified as a consonant, or random spikes in the periodicity of an otherwise aperiodic signal could cause part of a consonant to be classified as a vowel. These errors can be minimized by imposing a length constraint on sounds. In order for a group of windows to be classified as a particular sound, they must represent a long enough chunk of time to be considered meaningful. If the group of windows is too small, they are reclassified to match the sound immediately preceding them.

11.4.1.3 Syllable Interpretation

After each sound in the input has been classified, it is necessary to determine which sound sequences should be interpreted as syllables. This is accomplished using a tree-like decision structure which examines consecutive elements of the sound classification vector, comparing them to all possible sequences. Once a known sequence is identified, it is added to the list of syllables, and the algorithm moves on to the next ungrouped sounds. The decision structure is depicted in the following figure.

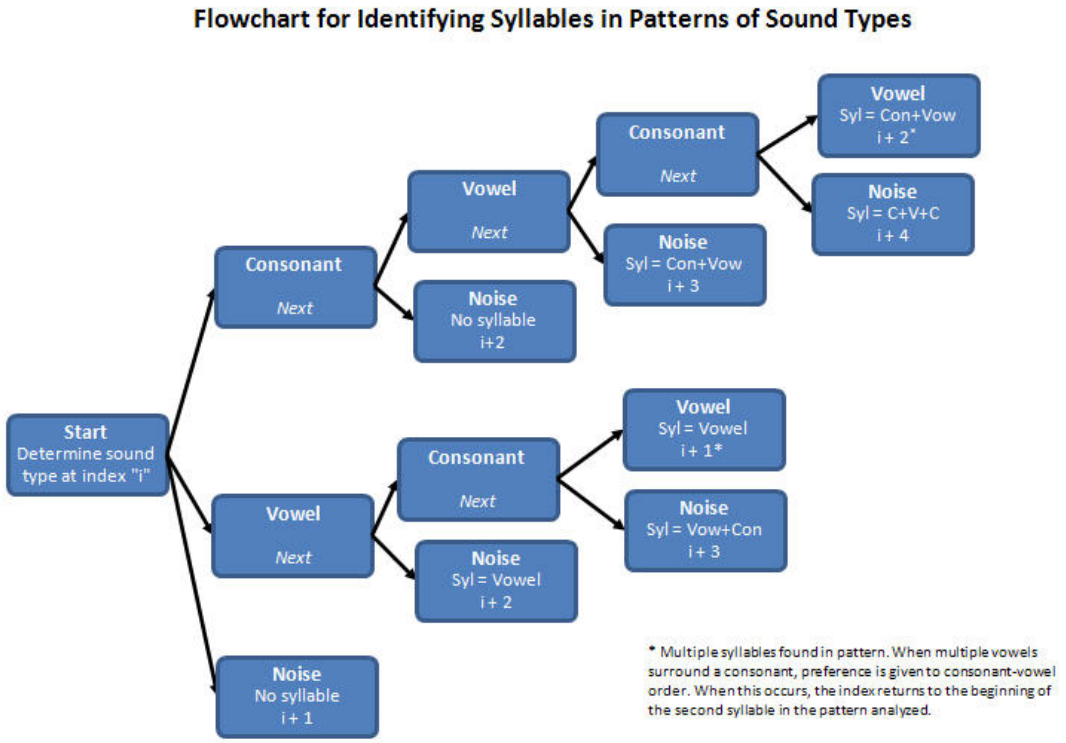

Figure 11.6

After this step, some syllables were occasionally much too short. For instance, the word "good" had a small probability of being split up into two syllables ("goo"" and "d") depending on how much the speaker emphasizes the voicing of the d. Further increasing the minimum allowable sound duration caused too much information to be lost or misinterpreted, so a minimum syllable duration parameter was also added. If a syllable is too short, it is combined with an adjacent syllable based on its surrounding sounds. If one of the sounds adjacent to the short syllable is noise and the other is not, the short syllable is added to the side without noise to preserve continuity of the signal. If neither sound adjacent to the syllable is noise, the duration of each adjacent sound is calculated, and the syllable is tacked onto the side with the shortest neighboring sound as this one is more likely to have been cut off in error.

The following table lists the values for the various thresholds and parameters we found worked best for relatively clean, noise-free, input signals. These parameters must be adjusted if a great deal of periodic or energetic background noise, such as might be caused by a microphone picking up the sound of a computer

fan, is expected to corrupt the input recording.

Parameter	Value
Window length	5 ms
Vowel periodicity threshold	.75
Vowel energy threshold	27% of total energy range
Noise energy threshold	55% of total energy range
Minimum sound duration	40 ms
Minimum syllable length	80 ms

Table 11.1

11.5 Speak and Sing - Time Scaling with WSOLA[5]

11.5.1 Introduction

There are many applications for time-scale modification ranging from post production of audio video synchronization in film to voicemail playback. Time-scale modification essentially is the process of either speeding up or slowing down the apparent rate of speech without corrupting other characteristics of the signal such as pitch and voice quality. Resampling is out of the question because is directly modifies pitch and very often voice quality loss is significant. To maintain these characteristics, the short-time Fourier transform of corresponding regions of the original (input) and scaled (output) signals should be very similar. Overlap add algorithms achieve this by simply cutting out smoothly windowed chunks of the input signal, repositioning them to corresponding time indexes in the output signal, overlapping the windows to achieve continuity, and adding. WSOLA is unique among overlap add algorithms in that it maintains local Fourier similarity in a time-scaled fashion but more importantly, the excised segment is similar to the segment adjacent to the previously excised segment. This makes WSOLA a very robust time-scaling algorithm being able to time scale even in the presence of noise and even competing voices in the input speech signal.

11.5.2 The Algorithm

The first step is to window the input signal with a smooth window such as a hanning window. Let w(n) be the window. Then establish a time warp function τ(n) such that for n an index in the input signal τ(n) equals the time scaled index in the output signal.

The input signal should then be windowed such that each segment overlaps with half of the previous segment. Then copy the first windowed segment to the output signal. The first segment of the input should be copied to the first segment in the output without consideration for the time warp function. Call the location of the last copied segment in the input S_1. Now the algorithm needs to find the next segment which it will copy, overlap and add with the current output signal.

There are quite a few ways to find this next segment. The most obvious method is to simply copy the segment at $\tau^{-1}(S_2)$ to the segment at S_2 in the output. However, this would wreak havoc on the phase synchronicity of the signal. The second method is to copy phase synchronous segment such that overlapping and adding will not cause huge phase differences between the two segments. This would maintain Fourier characteristics but would sound very choppy at syllable change edges in the speech. The WSOLA algorithm looks for a segment near $\tau^{-1}(S_2)$ that is most similar to the segment at $\tau^{-1}(S_2)$ + length(w). The next signal must be near (within a threshold) of the index given by the time warp function but also similar in Fourier

[5]This content is available online at <http://cnx.org/content/m33240/1.1/>.

characteristics to the next segment in the input signal. In other words, it finds a segment near the time scaled index such that it is very similar to the next naturally occurring segment in the input signal.

There are many ways to define most similar. The easiest way is Euclidian distance between the two signals. But computing the distance between the segments is computationally very expensive $O(N^2)$. The cross-correlation between the next adjacent segment and the region of interest seems to be the next alternative. The normalized cross-correlation if computed in the time domain is equally expensive. However, in the frequency domain, the computation is rather fast O(NlogN). The peak of the normalized cross-correlation occurs at the point of highest similarity. The segment corresponding to this point is then taken as the next segment and copied over to the output signal, overlapped with the existing signal and added. This is done iteratively until the entire output signal is created.

This algorithm can take arbitrary time-warp functions and can time-scale a signal while reliably maintaining Fourier characteristics. It is also less computationally expensive than simple up sampling or down sampling for non-integer scaling factors. In fact, sampling rate modification cannot be easily done for irrational scaling factors but this algorithm will even handle that.

11.5.3 Implementation

This algorithm was implemented in matlab and achieved good results even with arbitrary constant time warp functions. Constants ranging from .1 to 10 were tested with satisfactory results.

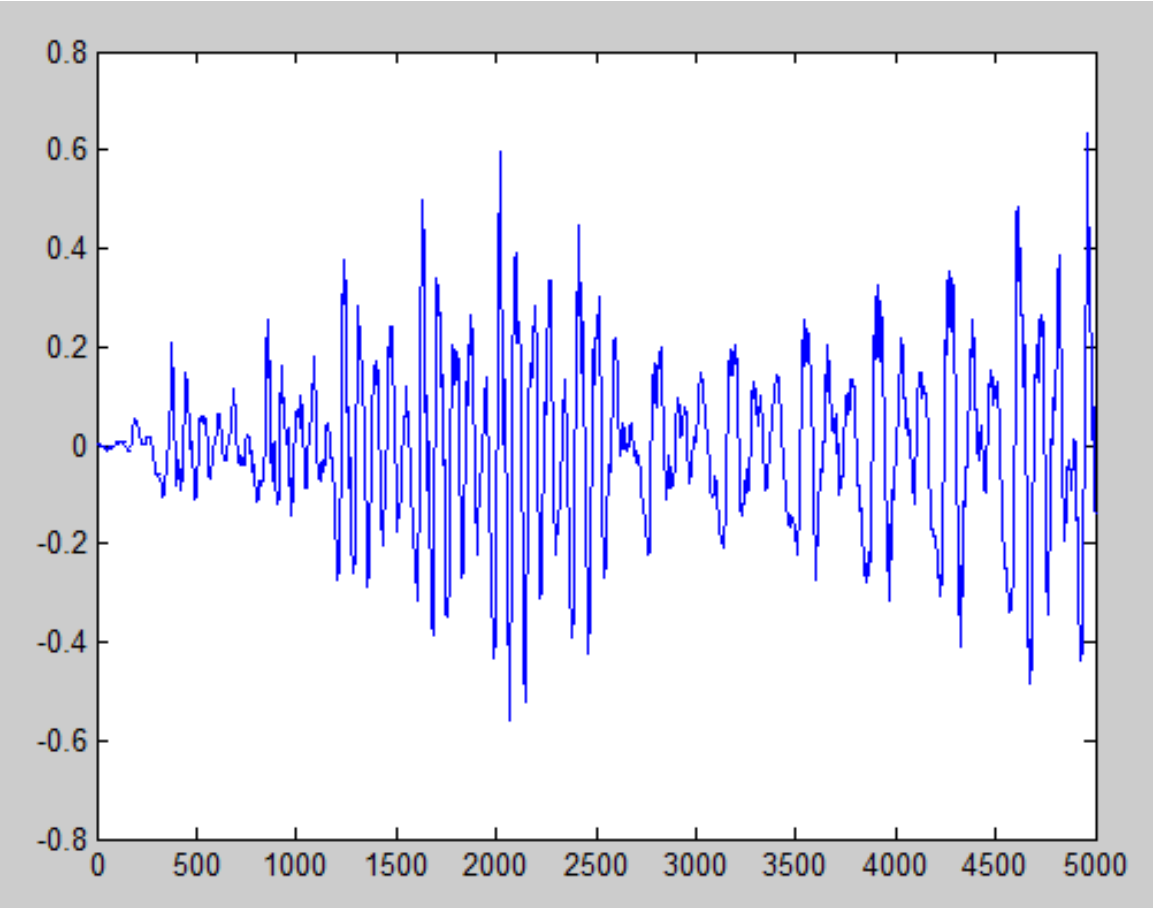

Figure 11.7: Short sample of a speech signal

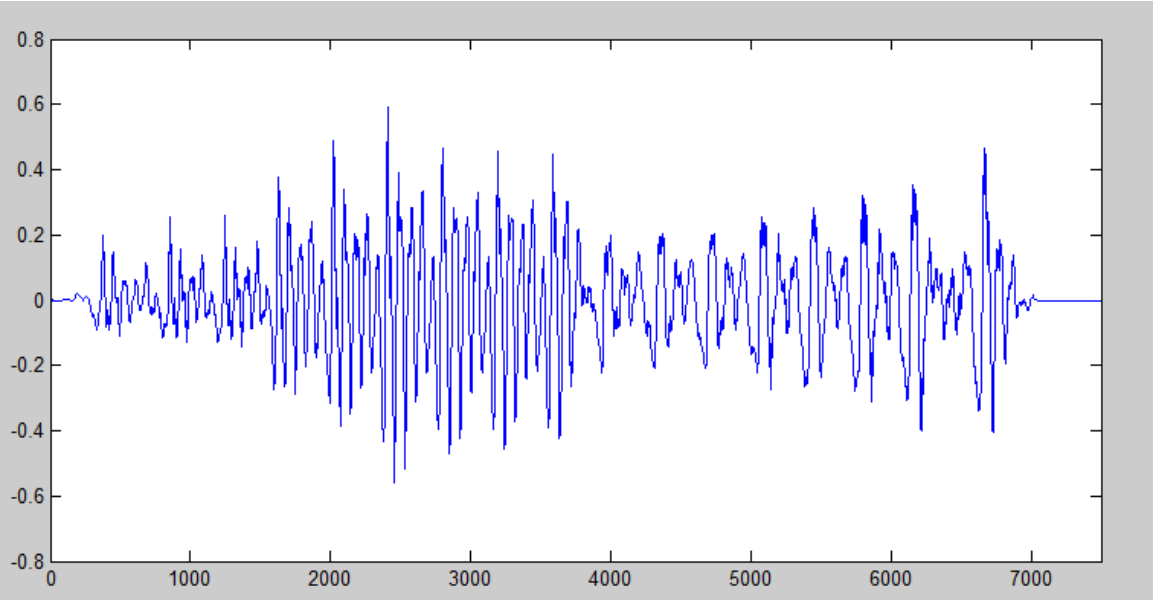

Figure 11.8: Time scaled version of previous speech signal

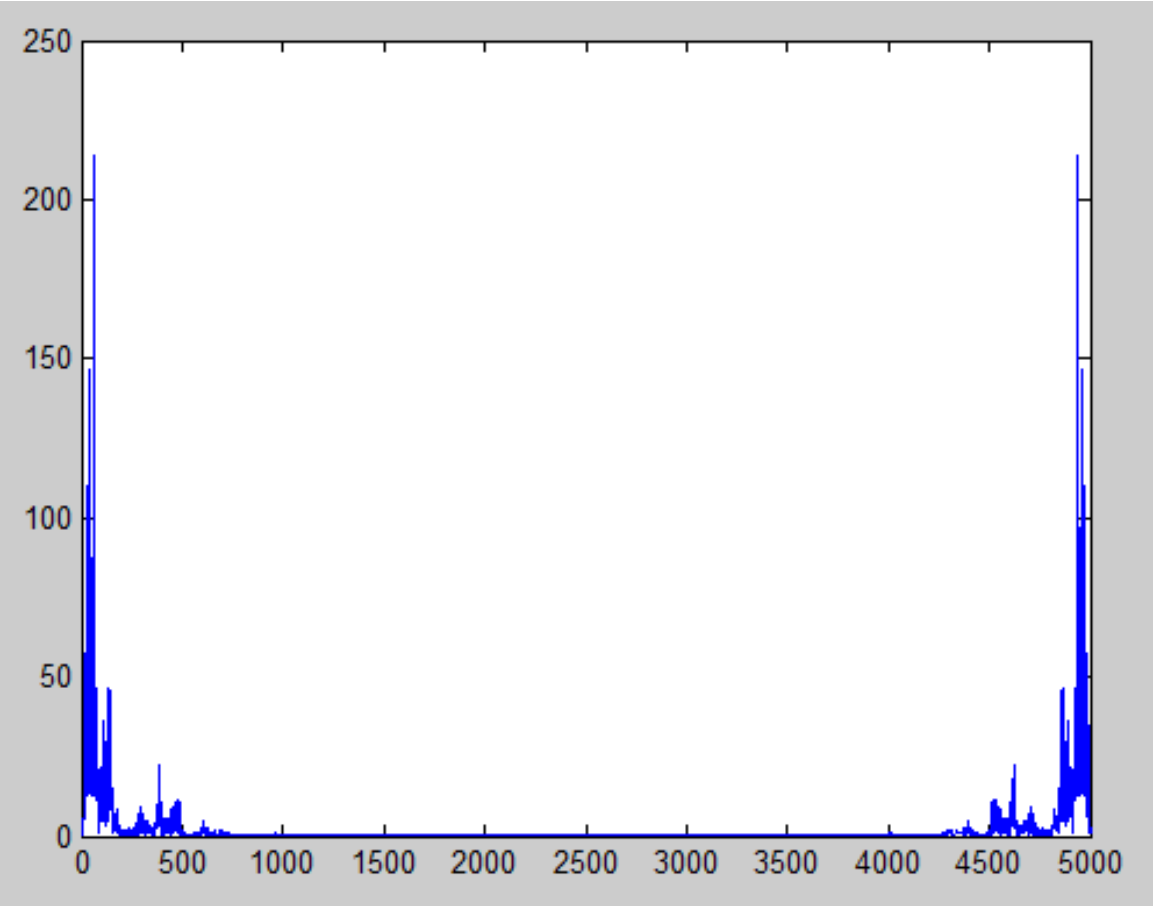

Figure 11.9: Fourier Transform of speech signal

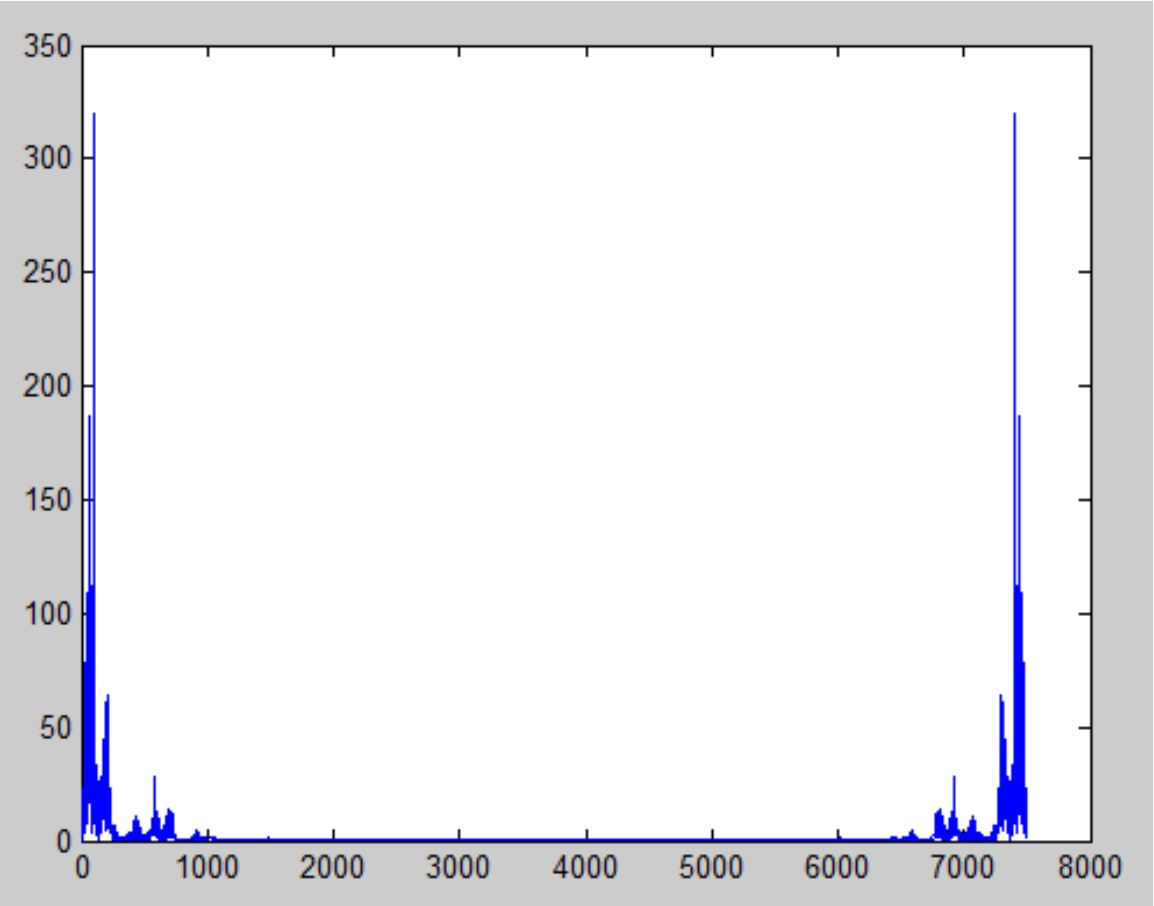

Figure 11.10: Fourier Transform of time scaled speech signal

11.6 Speak and Sing - Pitch Correction with PSOLA[6]

11.6.1 Introduction

Pitch correction of the human voice is a common activity, with applications in music, entertainment, and law. It can be used to alter pitch to produce a more accurate or more pleasing tone in music, as well as add distortion effects. Several programs for entertainment use a form of pitch correction to modulate and distort a user's voice, allowing one to sound like a different gender or emulate a celebrity or other well-known voice. Voice distortion is also often required to protect the anonymity of individuals in the criminal justice system. However, it is the first of these applications that we are most interested in - producing a pleasing, tone-accurate song from a human voice.

Implementation

Pitch adjustment of a digitally-sampled audio file can be implemented simply using resampling. However, this completely alters the time scaling and cannot account for changes in the pitch and inflection of a voice over time, and thus cannot be considered. Instead, we shall use the more sophisticated Pitch-Synchronous

[6] This content is available online at <http://cnx.org/content/m33242/1.1/>.

Overlap Add algorithm, which allows us to modify pitch without compromised information or modifying the time scaling.

The pitch correction method involves the following basic steps:

- Detection of original pitch
- Parsing of desired pitch frequencies
- Correction of pitch

11.6.2 Pitch Detection

First, the pitch of the original signal is determined. This is done using the FAST-Autocorrelation algorithm. This algorithm makes use of the fact that for a signal to have pitch, it must have a somewhat periodic nature, even if it is not a strictly periodic wave. The signal is divided into several small windows, each only a few milliseconds long and containing thousands of samples - enough to detect at least two periods and thus to determine the window's frequency.

Finding periods

Each windowed segment is autocorrelated with itself to identify the length of the period. This is done by convolving the signal with itself with an increasing offset τ to obtain the autocorrelation function:

$R(\tau) = f(-\tau) * f(\tau)$

For discrete, finite-length signals, it can be found as a sum of the product of the signal and its offset, in this form:

$R(s) = Sum(x(n)x(n-s))$

This autocorrelation acts as a match filter: the signal and its offset form will be the most alike when offset s is equal to one period. Thus, the autocorrelation function is at a minimum when the offset corresponds to the length of one period, in samples.

Making it FAST

Autocorrelation in this fashion is very computationally expensive - one can expect that the algorithm will have to convolve two length-1000 signals several hundred times for each window to obtain the frequency from within the full possible range of frequencies for a human voice. To speed this up, we can make two assumptions:

1. The frequency of a window should be relatively close to that of the window before it
2. The first minimum corresponds to the period, so no further minima are needed

By starting at an offset relatively close to the previously found period length (perhaps 20 samples before where the period was found), we can eliminate a few hundred calculations per window. If a minimum is not found in this area, we simply broaden our range and try again. To reduce the computation time further, we also calculate the derivative dR(s)/ds to determine where the minimum occurs. Once we find the first minimum, we are finished with obtaining the frequency for this window, having shaved off up to 70% of our computation time.

When we're done...

Once a frequency has been found for every window, a vector of frequencies (one for each window) is compiled and returned to the pitch correction handler function.

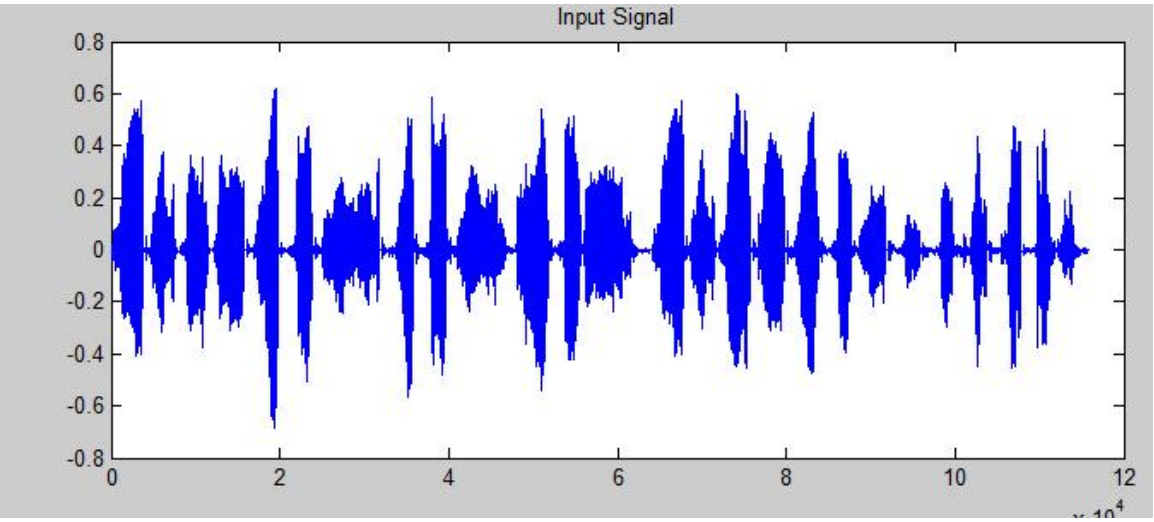

Figure 11.11: Waveform of an input audio signal (speech: "Mary had a little lamb...")

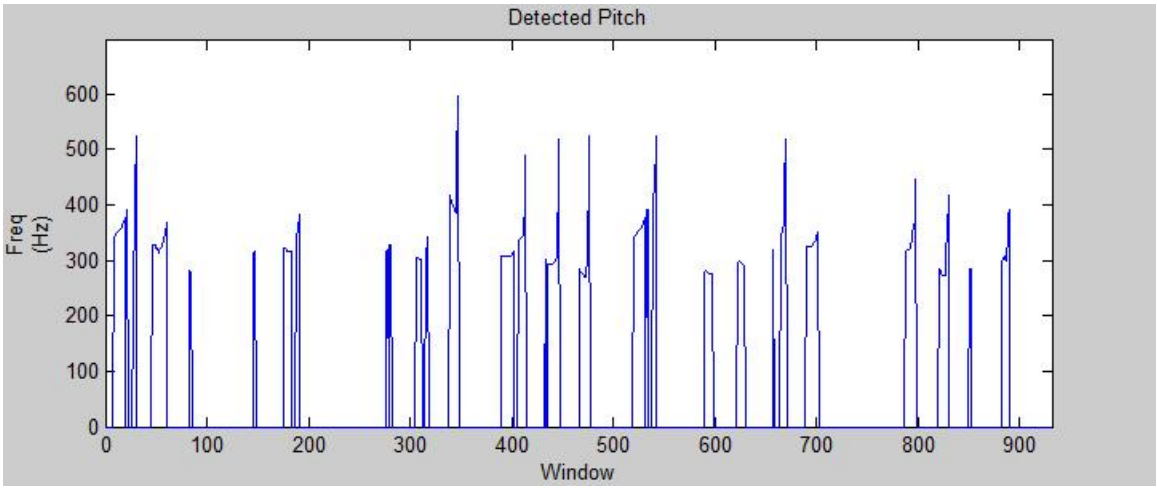

Figure 11.12: Detected frequencies of the signal above, one per window. Here it is easier to observe the spikes in frequency for parts of speech that may be spoken higher in pitch. If this input was sung rather than spoken, this plot would be much smoother and look closer to the desired frequency.

11.6.3 Desired pitch

The PSOLA pitch correction algorithm requires both an original pitch and a "target" pitch to achieve. If this were a fully-automated pitch-smoothing autotuner, the target pitch would be whatever "note" frequency was closest to the one observed. We on the other hand would like to bend the pitch to the specific frequency of the song, regardless of our starting point. To this end, we must generate a vector of desired frequencies.

Fortunately, thanks to our song interpretation earlier, we already have vectors of the pitch and length of each note in the song at hand. These vectors assume the following format:

- Frequencies: fundamental frequency in Hz (one per note)
- Durations: length in seconds independent of sampling frequency (one per note)

First, we generate a vector of frequencies for each sample at our defined sampling rate. This is as simple as producing a vector with a length equal to the total length of the song in seconds times the sampling frequency (thus, lengthN = sum(durations)*Fs). Then, for each note, we copy the frequency of that note over every sample in the vector for a range of the note's duration. This is most easily done using MatLab's "cumsum" function on the durations vector to make each note indexed by the cumulative time passed, and then multiply these by the sampling frequency to produce the index of each note in samples.

Now that we have the frequency for every sample, we can chop up this full-length signal into windows just as we did to the input signal. For each window's range, we simply take the mode of the frequencies in that range (given their short length, a window will never span more than two notes) and let that be the desired frequency for that window.

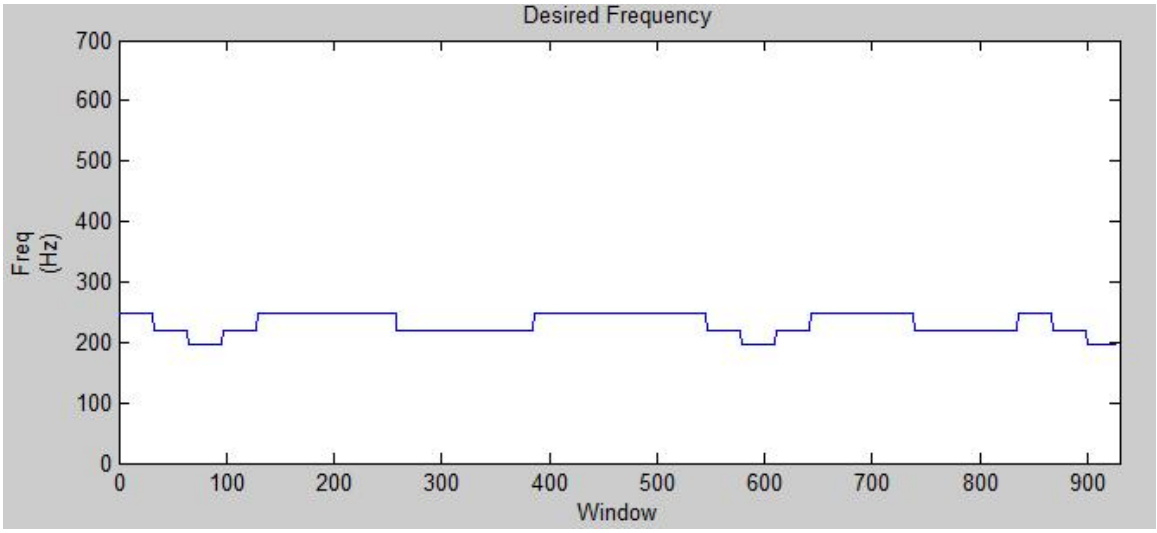

Figure 11.13: A plot of the desired frequency-per-window of "Mary Had a Little Lamb". The high and low notes are very clearly distinguishable.

11.6.4 PSOLA

Now that we have our original and target frequencies, we can exercise the Pitch-Synchronous Overlap Add algorithm to attempt to correct the frequencies. Like autocorrelation, the PSOLA begins with a windowed, segmented signal. Because we have already determined pitches for a specific number of segments, the PSOLA computations will use the same segment length. This is easy to remember, but introduces some issues. For example, the PSOLA algorithm can make the finest pitch corrections with a greater number of smaller segments, allowing for smoother correction across the signal. But what would happen to the autocorrelation pitch detector if the segment was so small that a full period could not be obtained? A compromise must be made on a segment length which allows for optimal pitch detection and pitch correction, with guesswork as the only means of finding the "happy medium".

Modifying pitch with Hanning windows
The signal we input to the PSOLA algorithm is already "windowed" into several overlapping segments. For each segment, the PSOLA creates Hanning windows (windows with a centralized hump-shaped distribution) centralized around the pitch-marks, or spikes in the amplitude. Once the segment is divided into overlapping windows, these windowed areas can be artificially pushed closer together for a shorter, higher-pitched signal, or farther apart for a longer, lower-pitched signal. The jumps between the beginning of each window is shortened or lengthened, and segments are duplicated or omitted where necessary. Unlike resampling, this change of pitch and duration does not compromise the underlying information.
Smoothing it out with Overlap and Add
Once the pitch and duration of the signal have been adjusted, the segments are then recombined by overlapping and adding. This Overlap-Add method exploits the knowledge that a long discrete convolution can be simplified as the sum of several short convolutions, which is convenient for us since we already have a number of short segments. The Overlap-Add produces a signal which is the same duration as its input and has roughly the same spectrum as the input, but now contains bands of frequency close to our desired frequency and, when played back, shows the result of our desired pitch correction effect.

The PSOLA algorithm described here is the Time-Domain PSOLA. Alternative PSOLA methods exist which depend on linear predictor coefficients rather than segmented waves. The TD-PSOLA is used for its simplicity in programming versus marginal increase in computational cost.

11.6.5 References

Gareth Middleton, "Pitch Detection Algorithms," Connexions, December 17, 2003, http://cnx.org/content/m11714/1.2/[7]

Lemmetty, Sami. Review of Speech Synthesis Technology. (Master's Thesis: Helsinki University of Technology) March 1999. http://www.acoustics.hut.fi/∼slemmett/dippa/thesis.pdf[8]

Upperman, Gina. "Changing Pitch with PSOLA for Voice Conversion." Connexions. December 17, 2004. http://cnx.org/content/m12474/1.3/[9]

11.7 Speak and Sing - Conclusion[10]

11.7.1 Results

After the signal has been processed by the various functions, we obtain a resultant signal (in the form of a data vector) which has been time-scaled and pitch-corrected. The resulting audio playback is (presumably) on-beat, in time with the song, and of the correct pitch. The individual results of each step's implementation are described individually below.
Syllable Detection
The method of detecting sound types by energy and periodicity proved highly effective, with a decent rate of accuracy. The syllable identification by patterns seems to cover all cases effectively (assuming sound type detection worked). The input signal may need to be "doctored" a bit to remove the DC offset, amplify the signal, and remove excessive noise caused by noisy environments or electronic interference.
Time Scaling
The WSOLA algorithm works very well for duration scaling. It is able to shorten or expand syllables dramatically without any discernible loss of information. Tests indicate that the signal could be stretched to ten times its original length without audio artifacting occurring. Assuming the syllable detection function was accurate, the time scaling function produces a signal timed exactly to the song.

[7] "Pitch Detection Algorithms" <http://cnx.org/content/m11714/1.2/>
[8] http://www.acoustics.hut.fi/∼slemmett/dippa/thesis.pdf
[9] "Changing Pitch with PSOLA for Voice Conversion" <http://cnx.org/content/m12474/1.3/>
[10] This content is available online at <http://cnx.org/content/m33243/1.1/>.

Pitch Correction
The PSOLA algorithm works as designed and introduces pitch correction. Given a relatively pitch-accurate input signal (such as a song or a sine wave), it will correct the input to the desired frequency. However, attempting to correct a dramatically different pitch (such as correcting the low timbre of a male voice speaking to a middle true C-note) causes a discernible gap between frequencies when listening to the signal. The result does not truly bend the pitch of the signal, but rather introduces harmonized distortion (hereafter dubbed "the T-Pain effect[11] ").

11.7.2 Limitations and areas for improvement

Song Interpretation

- No allowance is made for note slurs or variations within a syllable. Sustained words which vary in pitch are not currently supported. This would be relatively simple to implement by modifying the song vectors so that each syllable can contain multiple notes and durations.
- Songs must currently be coded by hand by examining sheet music or "playing by ear". For this reason, song selection is limited to how many man-hours are put into song coding. In the future, a MIDI file decoder could automate this task. A more advanced approach would be to develop a pitch detector which identifies the vocal component of the song and then detects pitch.

Syllable Detection

- A relatively "clean" pre-processed signal produces best results. It would be possible to include DC offset removal, amplification, and finer noise detection in the MatLab function itself rather than rely on an outside program.
- Soft consonants (L, R, Y, and others) do not produce the same contrasting energy and periodicity as hard consonants. Multiple syllables which are separated by a soft consonant which is not clearly enunciated or emphasized may be grouped together as one. Further research and a more robust understanding of this sound type should allow for changes which will improve detection.

Pitch Correction

- The PSOLA algorithm is well-suited for minor pitch corrections but cannot produce major pitch bends; attempts to do so result in the T-Pain effect. A more aggressive pitch correction method could produce tonal sound from any input but would compromise the sound information, leaving very little of the original speech intact.
- The FAST-autocorrelation and PSOLA algorithms must use the same length and number of windowed segments. This creates a trade-off: autocorrelation can catch higher pitches and detect more accurately when using a longer window length, while PSOLA is able to make finer adjustments when given a larger number of smaller windows. If the window length is too small, autocorrelation may not detect any periods and would return zero frequency for that window. If the window length is too large, shorter sounds would not be pitch-corrected.
- The repeated convolutions of the autocorrelation and PSOLA algorithms make this the most computationally expensive step in the process. Methods such as the FAST method of reducing the number of test cases have dramatically improved this time, but there is still room for improvement.

11.7.3 Potential Applications

The Speak and Sing is a robust package which offers functionality and techniques not found in conventional autotuners. This all-in-one program and derivatives thereof show potential for applications in:

[11] http://www.youtube.com/watch?v=R7yfISlGLNU

- **Music:** the Speak and Sing could provide a multi-functional alternative in situations where pitch correction and autotuner distortion are desired. It can also provide tempo and timing corrections on a dynamic scale.
- **Entertainment:** the Speak and Sing would, at the very least, make for an interesting iPhone app of the same name.
- **Communication:** pitch correction and timescaling are important facets of voice synthesis and could be used to augment human-interface and accessibility programs.
- **Speech analysis:** the syllable detection algorithm can be used to parse recordings and perhaps find use in speech-to-text applications.

11.7.4 In conclusion...

The Speak and Sing has served as an excellent demonstration of core digital signal processing techniques. Its development has served as a great learning experience for the team and has allowed each of us to flex our creative muscle.

While the "spoken words to full song" concept was not fully realized within this limited framework, the Speak and Sing is nonethelesss a functional, robust, and impressive program. It executes its syllable detection, time scaling, and pitch correction components correctly and produces an audible, tangible result from the input speech.

Chapter 12

Musical Instrument Recognition Through Fourier Analysis

12.1 Musical Instrument Recognition Through Fourier Analysis[1]

Introduction
Different instruments produce distinct sounds that are easily distinguishable by a human ear. Our goal was to create a digital system that can accomplish the same thing. This has potential future application in helping to decode: Old recordings Multiple instruments overlapping (orchestras, bands, etc.) With a computer system that can automatically detect what is being played, confusion caused by our human ability to distinguish sounds can be avoided by looking at the physics behind sounds and how these are formed. All instruments make distinct sounds by producing vibrations in different ways. This leads to the signals they produce having different properties that can be distinguished by a computer system. By analyzing the harmonic frequencies from a sound file, and by looking at the different energy levels on each and how they relate to each other, one can determine what the source of this sound is. A system such as this could potentially be applied to things such as converting audio to formats to MIDI or determining what instruments were used in a big band recording.
Theory
When a note is played on a musical instrument, we associate it with a certain frequency. However it is really a combination of the frequency we hear (the note played) and a series of less powerful harmonic frequencies. The combination of these creates the tone, or timbre, we associate with each instrument. Our job was to write a program that looks at these harmonics and how they relate to the strongest pitch and judge what type of instrument was most likely to have made the sound. We did this by coming up with a point system that gives points to each family based on what qualities are displayed in the sample we took.
Method
Our system for determining which instrument family a .wav file comes from: 1. Take a .05 second sample of the wav file 2. Take the FFT of the sample 3. Figure out how many harmonics there are (i.e. spikes at least 1/10 as powerful as the main tone) 4. Assign points to each family based on the order and power of harmonics 5. Repeat for the next sample 6. When one family has enough points over the other families, stop the system and declare that family the winner For instance, string instruments have fewer and less powerful overtones than brass instruments, while woodwinds fall somewhere between the two. The ratio of an overtone to the previous overtone is also much more likely to be below one in string instruments.
Results
We tested our system with multiple samples of instruments playing individual notes in Propellerhead's Reason software, as well as with recordings of live solo performances. Because our program takes many

[1] This content is available online at <http://cnx.org/content/m33260/1.1/>.

samples from different points in each track, it does a good job of identifying which instrument is being used in which song. Our biggest problem was not with the live performances, but with computer samples playing notes that are out of some instruments' standard ranges. For instance, the FFT of a bassoon playing in its upper ranges looks extremely similar to that of a violin. However, our system can accurately place the following instruments: Violin (3 Reason samples, 2 live performances), Trumpet (2 Reason samples, 2 live performance), English Horn (1 Reason sample), Oboe (2 Reason samples, 2 live performances), Cello (1 Reason sample, 1 live performance), Tuba (1 Reason Sample), low range Bassoon (2 Reason Samples)

Conclusion

We were able to create a system that is capable of classifying instruments in separate families. By analyzing the different composition of the sound waves created by different instruments, we were able to find traits common to multiple instruments in each category. These were present in many instruments under each family since they produce sound in similar ways, allowing us to successfully separate them into strings, woodwinds or brass.

Bibliography

[1] J. Cai, E. J. Cand[U+FFFD] and Z. Shen. A singular value thresholding algorithm for matrix completion. *arXiv:0810.3286v1*, October 2008.

[2] E. J. Cand[U+FFFD]nd Y. Plan. Matrix completion with noise. *arXiv:0903.3131v1*, March 2009.

[3] E. J. Cand[U+FFFD]nd B. Recht. Exact matrix completion via convex optimization. *arXiv:0805.4471v1*, May 2008.

[4] J. Hofmueller, A. Bachmann, and I. O. zmoelnig. The transmission of ip datagrams over the semaphore flag signaling system (sfss). http://tools.ietf.org/html/rfc4824, April 2007.

[5] C. Hornig. A standard for the transmission of ip datagrams over ethernet networks. http://tools.ietf.org/html/rfc894, April 1984.

[6] R. H. Keshavan, A. Montanari, and S. Oh. Matrix completion from a few entries. *arXiv:0901.3150v4*, September 2009.

[7] R. H. Keshavan and S. Oh. Optspace: A gradient descent algorithm on the grassman manifold for matrix completion. *arXiv:0910.5260v2*, November 2009.

[8] Audun Larsen. The highly unofficial cpip wg. http://www.blug.linux.no/rfc1149/, April 2001.

[9] Netflix. Netflix prize. http://www.netflixprize.com//index.

[10] A. Singer. A remark on global positioning from local distances. *Proc. Natl. Acad. Sci. USA*, 105:9507–9511, July 2008.

[11] L. Zhang, L. Liu, C. Gotsman, and S.J. Gortler. An as-rigid-as-possible approach to sensor network localization. *Harvard Computer Science Technical Report: TR-01-09*, January 2009.

Index of Keywords and Terms

Keywords are listed by the section with that keyword (page numbers are in parentheses). Keywords do not necessarily appear in the text of the page. They are merely associated with that section. *Ex.* apples, § 1.1 (1) **Terms** are referenced by the page they appear on. *Ex.* apples, 1

Attributions

Collection: *ELEC 301 Projects Fall 2009*
Edited by: Rice University ELEC 301
URL: http://cnx.org/content/col11153/1.3/
License: http://creativecommons.org/licenses/by/3.0/

Module: "Introduction"
By: Yilong Yao
URL: http://cnx.org/content/m33185/1.2/
Page: 1
Copyright: Yilong Yao
License: http://creativecommons.org/licenses/by/3.0/

Module: "The Fingerprint of a Song"
By: Yilong Yao
URL: http://cnx.org/content/m33186/1.2/
Page: 1
Copyright: Yilong Yao
License: http://creativecommons.org/licenses/by/3.0/

Module: "The Fingerprint Finding Algorithm"
By: Yilong Yao
URL: http://cnx.org/content/m33188/1.4/
Pages: 2-4
Copyright: Yilong Yao
License: http://creativecommons.org/licenses/by/3.0/

Module: "The Resulting Fingerprint"
By: Yilong Yao
URL: http://cnx.org/content/m33189/1.4/
Pages: 4-5
Copyright: Yilong Yao
License: http://creativecommons.org/licenses/by/3.0/

Module: "Matched Filter for Spectrogram Peaks"
By: Yilong Yao
URL: http://cnx.org/content/m33191/1.1/
Page: 6
Copyright: Yilong Yao
License: http://creativecommons.org/licenses/by/3.0/

Module: "The Matched Filter Algorithm"
By: Yilong Yao
URL: http://cnx.org/content/m33193/1.3/
Pages: 6-9
Copyright: Yilong Yao
License: http://creativecommons.org/licenses/by/3.0/

Module: "Results"
By: Yilong Yao
URL: http://cnx.org/content/m33194/1.3/
Pages: 9-11
Copyright: Yilong Yao
License: http://creativecommons.org/licenses/by/3.0/

Module: "About the Team"
By: Yilong Yao
URL: http://cnx.org/content/m33196/1.2/
Page: 12
Copyright: Yilong Yao
License: http://creativecommons.org/licenses/by/3.0/

Module: "Introduction"
By: Anthony Austin, Gilberto Hernandez, Jose Garcia, Stephen Jong
URL: http://cnx.org/content/m33135/1.1/
Page: 13
Copyright: Anthony Austin, Gilberto Hernandez, Jose Garcia, Stephen Jong
License: http://creativecommons.org/licenses/by/3.0/

Module: "Matrix Completion: An Overview"
By: Anthony Austin, Jose Garcia, Stephen Jong, Gilberto Hernandez
URL: http://cnx.org/content/m33136/1.1/
Pages: 13-14
Copyright: Anthony Austin, Jose Garcia, Stephen Jong, Gilberto Hernandez
License: http://creativecommons.org/licenses/by/3.0/

Module: "Simulation Procedure"
By: Anthony Austin, Gilberto Hernandez, Jose Garcia, Stephen Jong
URL: http://cnx.org/content/m33138/1.1/
Pages: 14-15
Copyright: Anthony Austin, Gilberto Hernandez, Jose Garcia, Stephen Jong
License: http://creativecommons.org/licenses/by/3.0/

Module: "Results, Conclusions, and Future Work"
By: Anthony Austin, Jose Garcia, Stephen Jong, Gilberto Hernandez
URL: http://cnx.org/content/m33141/1.1/
Pages: 16-25
Copyright: Anthony Austin, Jose Garcia, Stephen Jong, Gilberto Hernandez
License: http://creativecommons.org/licenses/by/3.0/

Module: "Acknowledgments"
By: Anthony Austin, Gilberto Hernandez, Jose Garcia, Stephen Jong
URL: http://cnx.org/content/m33142/1.1/
Page: 25
Copyright: Anthony Austin, Gilberto Hernandez, Jose Garcia, Stephen Jong
License: http://creativecommons.org/licenses/by/3.0/

Module: "References"
By: Anthony Austin, Jose Garcia, Stephen Jong, Gilberto Hernandez
URL: http://cnx.org/content/m33146/1.1/
Page: 25
Copyright: Anthony Austin, Jose Garcia, Stephen Jong, Gilberto Hernandez
License: http://creativecommons.org/licenses/by/3.0/

Module: "Introduction"
By: Brian Viel
URL: http://cnx.org/content/m33147/1.1/
Page: 27
Copyright: Brian Viel
License: http://creativecommons.org/licenses/by/3.0/

Module: "The Problem"
By: Brian Viel
URL: http://cnx.org/content/m33155/1.1/
Pages: 27-28
Copyright: Brian Viel
License: http://creativecommons.org/licenses/by/3.0/

Module: "Transmitter"
By: Brian Viel
URL: http://cnx.org/content/m33148/1.1/
Pages: 28-30
Copyright: Brian Viel
License: http://creativecommons.org/licenses/by/3.0/

Module: "The Channel"
By: Brian Viel
URL: http://cnx.org/content/m33144/1.1/
Pages: 31-32
Copyright: Brian Viel
License: http://creativecommons.org/licenses/by/3.0/

Module: "Receiver"
By: Brian Viel
URL: http://cnx.org/content/m33151/1.1/
Pages: 33-34
Copyright: Brian Viel
License: http://creativecommons.org/licenses/by/3.0/

Module: "Results and Conclusions"
By: Brian Viel
URL: http://cnx.org/content/m33152/1.1/
Pages: 34-36
Copyright: Brian Viel
License: http://creativecommons.org/licenses/by/3.0/

Module: "Our Gang"
By: Brian Viel
URL: http://cnx.org/content/m33153/1.1/
Page: 37
Copyright: Brian Viel
License: http://creativecommons.org/licenses/by/3.0/

Module: "Acknowledgements"
By: Brian Viel
URL: http://cnx.org/content/m33140/1.1/
Page: 37
Copyright: Brian Viel
License: http://creativecommons.org/licenses/by/3.0/

Module: "Meet the Team"
By: Haiying Lu
URL: http://cnx.org/content/m33133/1.2/
Pages: 39-40
Copyright: Haiying Lu
License: http://creativecommons.org/licenses/by/3.0/

Module: "Introduction and some Background Information"
By: Haiying Lu
URL: http://cnx.org/content/m33121/1.2/
Pages: 40-41
Copyright: Haiying Lu
License: http://creativecommons.org/licenses/by/3.0/

Module: "Our System Setup"
By: Haiying Lu
URL: http://cnx.org/content/m33115/1.1/
Pages: 41-43
Copyright: Haiying Lu
License: http://creativecommons.org/licenses/by/3.0/

Module: "Behind the Scene: From Formants to PMFs"
By: Haiying Lu
URL: http://cnx.org/content/m33134/1.3/
Pages: 43-49
Copyright: Haiying Lu
License: http://creativecommons.org/licenses/by/3.0/

Module: "Results"
By: Haiying Lu
URL: http://cnx.org/content/m33113/1.2/
Pages: 49-50
Copyright: Haiying Lu
License: http://creativecommons.org/licenses/by/3.0/

Module: "Conclusions"
By: Haiying Lu
URL: http://cnx.org/content/m33127/1.3/
Page: 51
Copyright: Haiying Lu
License: http://creativecommons.org/licenses/by/3.0/

Module: "A Flag Semaphore Computer Vision System: Introduction"
By: Stephen Kruzick, Peter Hokanson, Seoyeon(Tara) Hong
URL: http://cnx.org/content/m33092/1.2/
Pages: 53-54
Copyright: Stephen Kruzick, Peter Hokanson, Seoyeon(Tara) Hong
License: http://creativecommons.org/licenses/by/3.0/

Module: "A Flag Semaphore Computer Vision System: Program Flow"
By: Stephen Kruzick, Peter Hokanson, Seoyeon(Tara) Hong
URL: http://cnx.org/content/m33095/1.2/
Pages: 54-56
Copyright: Stephen Kruzick, Peter Hokanson, Seoyeon(Tara) Hong
License: http://creativecommons.org/licenses/by/3.0/

Module: "A Flag Semaphore Computer Vision System: Program Assessment"
By: Stephen Kruzick, Peter Hokanson, Seoyeon(Tara) Hong
URL: http://cnx.org/content/m33098/1.2/
Pages: 56-57
Copyright: Stephen Kruzick, Peter Hokanson, Seoyeon(Tara) Hong
License: http://creativecommons.org/licenses/by/3.0/

Module: "A Flag Semaphore Computer Vision System: Demonstration"
By: Stephen Kruzick, Peter Hokanson, Seoyeon(Tara) Hong
URL: http://cnx.org/content/m33100/1.2/
Pages: 57-59
Copyright: Stephen Kruzick, Peter Hokanson, Seoyeon(Tara) Hong
License: http://creativecommons.org/licenses/by/3.0/

Module: "A Flag Semaphore Computer Vision System: TCP/IP"
By: Stephen Kruzick, Peter Hokanson, Seoyeon(Tara) Hong
URL: http://cnx.org/content/m33094/1.2/
Pages: 59-60
Copyright: Stephen Kruzick, Peter Hokanson, Seoyeon(Tara) Hong
License: http://creativecommons.org/licenses/by/3.0/

Module: "A Flag Semaphore Computer Vision System: Future Work"
By: Stephen Kruzick, Peter Hokanson, Seoyeon(Tara) Hong
URL: http://cnx.org/content/m33103/1.2/
Pages: 60-61
Copyright: Stephen Kruzick, Peter Hokanson, Seoyeon(Tara) Hong
License: http://creativecommons.org/licenses/by/3.0/

Module: "A Flag Semaphore Computer Vision System: Acknowledgements"
By: Stephen Kruzick, Peter Hokanson, Seoyeon(Tara) Hong
URL: http://cnx.org/content/m33106/1.2/
Page: 61
Copyright: Stephen Kruzick, Peter Hokanson, Seoyeon(Tara) Hong
License: http://creativecommons.org/licenses/by/3.0/

Module: "A Flag Semaphore Computer Vision System: Additional Resources"
By: Stephen Kruzick, Peter Hokanson, Seoyeon(Tara) Hong
URL: http://cnx.org/content/m33107/1.2/
Pages: 61-62
Copyright: Stephen Kruzick, Peter Hokanson, Seoyeon(Tara) Hong
License: http://creativecommons.org/licenses/by/3.0/

Module: "A Flag Semaphore Computer Vision System: Conclusions"
By: Stephen Kruzick, Peter Hokanson, Seoyeon(Tara) Hong
URL: http://cnx.org/content/m33109/1.2/
Page: 62
Copyright: Stephen Kruzick, Peter Hokanson, Seoyeon(Tara) Hong
License: http://creativecommons.org/licenses/by/3.0/

Module: "Prelude"
By: Chinwei Hu, Kyle Li, Cynthia Sung, Lei Cao
URL: http://cnx.org/content/m33154/1.2/
Page: 63

Module: "Image Processing - License Plate Localization and Letters Extraction"
By: Cynthia Sung, Chinwei Hu, Kyle Li, Lei Cao
URL: http://cnx.org/content/m33156/1.2/
Pages: 63-67

Module: "SVM Train"
By: Chinwei Hu, Kyle Li, Cynthia Sung, Lei Cao
URL: http://cnx.org/content/m33159/1.2/
Pages: 67-69

Module: "Conclusions"
By: Chinwei Hu, Cynthia Sung, Kyle Li, Lei Cao
URL: http://cnx.org/content/m33160/1.3/
Page: 70

Module: "Introduction"
By: Sharon Du, Dan Calderon
URL: http://cnx.org/content/m33167/1.3/
Pages: 71-72

Module: "How ECG Signals Are Analyzed"
By: Sharon Du, Dan Calderon
URL: http://cnx.org/content/m33166/1.2/
Pages: 72-74

Module: "Algorithms"
By: Sharon Du, Dan Calderon
URL: http://cnx.org/content/m33164/1.2/
Pages: 74-77

Module: "Testing"
By: Sharon Du, Dan Calderon
URL: http://cnx.org/content/m33168/1.2/
Pages: 77-78

Module: "Conclusion"
By: Sharon Du, Dan Calderon
URL: http://cnx.org/content/m33165/1.2/
Pages: 78-79
Copyright: Sharon Du, Dan Calderon
License: http://creativecommons.org/licenses/by/3.0/

Module: "Introduction"
By: Graham de Wit, Nicholas Newton, Grant Cathcart
URL: http://cnx.org/content/m33082/1.2/
Page: 81
Copyright: Graham de Wit, Nicholas Newton, Grant Cathcart
License: http://creativecommons.org/licenses/by/3.0/

Module: "Theory"
By: Graham de Wit, Nicholas Newton, Grant Cathcart
URL: http://cnx.org/content/m33087/1.2/
Pages: 81-83
Copyright: Graham de Wit, Nicholas Newton, Grant Cathcart
License: http://creativecommons.org/licenses/by/3.0/

Module: "Implementation"
By: Grant Cathcart, Graham de Wit, Nicholas Newton
URL: http://cnx.org/content/m33081/1.2/
Pages: 83-92
Copyright: Grant Cathcart, Graham de Wit, Nicholas Newton
License: http://creativecommons.org/licenses/by/3.0/

Module: "Conclusion"
By: Graham de Wit, Nicholas Newton, Grant Cathcart
URL: http://cnx.org/content/m33080/1.2/
Pages: 92-93
Copyright: Graham de Wit, Nicholas Newton, Grant Cathcart
License: http://creativecommons.org/licenses/by/3.0/

Module: "Code"
By: Graham de Wit, Nicholas Newton, Grant Cathcart
URL: http://cnx.org/content/m33079/1.2/
Pages: 93-96
Copyright: Graham de Wit, Nicholas Newton, Grant Cathcart
License: http://creativecommons.org/licenses/by/3.0/

Module: "References and Acknowledgements"
By: Graham de Wit, Nicholas Newton, Grant Cathcart
URL: http://cnx.org/content/m33083/1.2/
Page: 96
Copyright: Graham de Wit, Nicholas Newton, Grant Cathcart
License: http://creativecommons.org/licenses/by/3.0/

Module: "Team"
By: Graham de Wit, Nicholas Newton, Grant Cathcart
URL: http://cnx.org/content/m33086/1.2/
Pages: 97-99
Copyright: Graham de Wit, Nicholas Newton, Grant Cathcart
License: http://creativecommons.org/licenses/by/3.0/

Module: "Introduction"
By: Robert Brockman
URL: http://cnx.org/content/m33246/1.1/
Page: 101
Copyright: Robert Brockman
License: http://creativecommons.org/licenses/by/3.0/

Module: "Background"
By: Stamatios Mastrogiannis
URL: http://cnx.org/content/m33247/1.1/
Pages: 101-102
Copyright: Stamatios Mastrogiannis
License: http://creativecommons.org/licenses/by/3.0/

Module: "Procedures"
By: Jeffrey Bridge
URL: http://cnx.org/content/m33251/1.1/
Pages: 102-104
Copyright: Jeffrey Bridge
License: http://creativecommons.org/licenses/by/3.0/

Module: "Results"
By: Robert Brockman, Jeffrey Bridge, Stamatios Mastrogiannis
URL: http://cnx.org/content/m33248/1.1/
Pages: 104-105
Copyright: Robert Brockman, Jeffrey Bridge, Stamatios Mastrogiannis
License: http://creativecommons.org/licenses/by/3.0/

Module: "Sources"
By: Robert Brockman
URL: http://cnx.org/content/m33249/1.1/
Page: 105
Copyright: Robert Brockman
License: http://creativecommons.org/licenses/by/3.0/

Module: "The Team"
By: Stamatios Mastrogiannis
URL: http://cnx.org/content/m33250/1.1/
Page: 105
Copyright: Stamatios Mastrogiannis
License: http://creativecommons.org/licenses/by/3.0/

Module: "Code"
By: Jeffrey Bridge
URL: http://cnx.org/content/m33253/1.1/
Pages: 106-112
Copyright: Jeffrey Bridge
License: http://creativecommons.org/licenses/by/3.0/

Module: "Future Work"
By: Robert Brockman
URL: http://cnx.org/content/m33254/1.1/
Page: 112
Copyright: Robert Brockman
License: http://creativecommons.org/licenses/by/3.0/

Module: "Facial Recognition using Eigenfaces: Introduction"
By: Aron Yu, Catherine Elder, Jeff Yeh, Norman Pai
URL: http://cnx.org/content/m33173/1.3/
Pages: 113-114
Copyright: Aron Yu, Catherine Elder, Jeff Yeh, Norman Pai
License: http://creativecommons.org/licenses/by/3.0/

Module: "Facial Recognition using Eigenfaces: Background"
By: Aron Yu, Catherine Elder, Jeff Yeh, Norman Pai
URL: http://cnx.org/content/m33174/1.5/
Pages: 114-115
Copyright: Aron Yu, Catherine Elder, Jeff Yeh, Norman Pai
License: http://creativecommons.org/licenses/by/3.0/

Module: "Facial Recognition using Eigenfaces: Obtaining Eigenfaces"
By: Aron Yu, Catherine Elder, Jeff Yeh, Norman Pai
URL: http://cnx.org/content/m33183/1.6/
Pages: 115-120
Copyright: Aron Yu, Catherine Elder, Jeff Yeh, Norman Pai
License: http://creativecommons.org/licenses/by/3.0/

Module: "Facial Recognition using Eigenfaces: Projection onto Face Space"
By: Aron Yu, Catherine Elder, Jeff Yeh, Norman Pai
URL: http://cnx.org/content/m33182/1.6/
Pages: 120-122
Copyright: Aron Yu, Catherine Elder, Jeff Yeh, Norman Pai
License: http://creativecommons.org/licenses/by/3.0/

Module: "Facial Recognition using Eigenfaces: Results"
By: Aron Yu, Catherine Elder, Jeff Yeh, Norman Pai
URL: http://cnx.org/content/m33181/1.6/
Pages: 122-125
Copyright: Aron Yu, Catherine Elder, Jeff Yeh, Norman Pai
License: http://creativecommons.org/licenses/by/3.0/

Module: "Facial Recognition using Eigenfaces: Conclusion"
By: Aron Yu, Catherine Elder, Jeff Yeh, Norman Pai
URL: http://cnx.org/content/m33177/1.4/
Pages: 125-126
Copyright: Aron Yu, Catherine Elder, Jeff Yeh, Norman Pai
License: http://creativecommons.org/licenses/by/3.0/

Module: "Facial Recognition using Eigenfaces: References and Acknowledgements"
By: Aron Yu, Catherine Elder, Jeff Yeh, Norman Pai
URL: http://cnx.org/content/m33180/1.3/
Pages: 126-127
Copyright: Aron Yu, Catherine Elder, Jeff Yeh, Norman Pai
License: http://creativecommons.org/licenses/by/3.0/

Module: "Speak and Sing - Introduction"
By: Graham Houser, Alysha Jeans, Sam Soundar, Matt Szalkowski
URL: http://cnx.org/content/m33229/1.1/
Pages: 129-130
Copyright: Graham Houser, Alysha Jeans, Sam Soundar, Matt Szalkowski
License: http://creativecommons.org/licenses/by/3.0/

Module: "Speak and Sing - Recording Procedure"
By: Graham Houser, Alysha Jeans, Sam Soundar, Matt Szalkowski
URL: http://cnx.org/content/m33233/1.1/
Page: 130
Copyright: Graham Houser, Alysha Jeans, Sam Soundar, Matt Szalkowski
License: http://creativecommons.org/licenses/by/3.0/

Module: "Speak and Sing - Song Interpretation"
By: Graham Houser, Matt Szalkowski, Alysha Jeans, Sam Soundar
URL: http://cnx.org/content/m33237/1.1/
Pages: 130-131
Copyright: Graham Houser, Matt Szalkowski, Alysha Jeans, Sam Soundar
License: http://creativecommons.org/licenses/by/3.0/

Module: "Speak and Sing - Syllable Detection"
By: Graham Houser, Alysha Jeans, Sam Soundar, Matt Szalkowski
URL: http://cnx.org/content/m33241/1.1/
Pages: 131-137
Copyright: Graham Houser, Alysha Jeans, Sam Soundar, Matt Szalkowski
License: http://creativecommons.org/licenses/by/3.0/

Module: "Speak and Sing - Time Scaling with WSOLA"
By: Sam Soundar, Alysha Jeans, Graham Houser, Matt Szalkowski
URL: http://cnx.org/content/m33240/1.1/
Pages: 137-142
Copyright: Sam Soundar, Alysha Jeans, Graham Houser, Matt Szalkowski
License: http://creativecommons.org/licenses/by/3.0/

Module: "Speak and Sing - Pitch Correction with PSOLA"
By: Graham Houser, Alysha Jeans, Sam Soundar, Matt Szalkowski
URL: http://cnx.org/content/m33242/1.1/
Pages: 142-146
Copyright: Graham Houser, Alysha Jeans, Sam Soundar, Matt Szalkowski
License: http://creativecommons.org/licenses/by/3.0/

Module: "Speak and Sing - Conclusion"
By: Graham Houser, Alysha Jeans, Sam Soundar, Matt Szalkowski
URL: http://cnx.org/content/m33243/1.1/
Pages: 146-148
Copyright: Graham Houser, Alysha Jeans, Sam Soundar, Matt Szalkowski
License: http://creativecommons.org/licenses/by/3.0/

Module: "Musical Instrument Recognition Through Fourier Analysis"
By: James Kohli
URL: http://cnx.org/content/m33260/1.1/
Pages: 149-150
Copyright: James Kohli
License: http://creativecommons.org/licenses/by/3.0/

ELEC 301 Projects Fall 2009
A collection of the class projects of Rice University's Fall 2009 ELEC 301 Signals and Systems course.

About Connexions
Since 1999, Connexions has been pioneering a global system where anyone can create course materials and make them fully accessible and easily reusable free of charge. We are a Web-based authoring, teaching and learning environment open to anyone interested in education, including students, teachers, professors and lifelong learners. We connect ideas and facilitate educational communities.

Connexions's modular, interactive courses are in use worldwide by universities, community colleges, K-12 schools, distance learners, and lifelong learners. Connexions materials are in many languages, including English, Spanish, Chinese, Japanese, Italian, Vietnamese, French, Portuguese, and Thai. Connexions is part of an exciting new information distribution system that allows for **Print on Demand Books**. Connexions has partnered with innovative on-demand publisher QOOP to accelerate the delivery of printed course materials and textbooks into classrooms worldwide at lower prices than traditional academic publishers.